University of Alberta

Silencing immunoglobulin gene enhancers as a potential treatment strategy for multiple myeloma

by

Inka Toman

A thesis submitted to the Faculty of Graduate Studies and Research
in partial fulfillment of the requirements for the degree of

Master of Science
in
Experimental Oncology

Department of Oncology

Fall 2009
Edmonton, Alberta

Examining Committee

Dr. Tony Reiman, Oncology

Dr. Mary Hitt, Oncology

Dr. Heather McDermid, Biological Sciences

Abstract

Multiple myeloma is a bone marrow malignancy characterized by the presence of monoclonal plasma cells. In 50-75% of myeloma patients, chromosome translocations at the IgH locus are observed, which result in overexpression of oncogenes from the translocated chromosome due to linkage with the IgH enhancers. IgH enhancer activity is mediated by the B cell-specific transcription factors Bob1 and Oct2. We hypothesized that inhibiting the IgH enhancer, through inhibition of Bob1 and Oct2, is a potential therapeutic strategy for translocation-positive myeloma. The expression and prognostic value of Bob1 and Oct2 in myeloma patient samples were assayed. High Bob1 expression was associated with increased survival, whereas high Oct2 expression was associated with reduced survival. In a t(4;14) myeloma cell line, Bob1 inhibition led to decreased expression of the translocated oncogene, FGFR3; however, this did not lead to decreased proliferation or increased apoptosis. To fully understand the roles of Bob1 and Oct2 in myeloma, further research is required.

Acknowledgements

Many individuals contributed to this project, and these contributions are greatly appreciated. CD138 sorting of patient samples was performed by Dr. Pilarski's lab. Jim Wan constructed the multiple myeloma tissue microarray, and Dr. Lai and Dr. Berendt lent their pathology expertise to this project. Rick Linford provided guidance with tissue staining, and Sarah Mitchell performed IHC staining on the tissue slides. Tissue microarray slides were kindly provided by Dr. Magliocco and Dr. Bahlis from the Tom Baker Cancer Center in Calgary. Also, the assistance with tissue staining and HistoRx software usage provided by Dr. Alex Klimowicz at the University of Calgary is greatly appreciated. I would also like to acknowledge the efforts of Jon Loree, who compiled the patient database and scored patient samples. Ann Berg from flow cytometry and Gerry Barron from cell imaging were always very willing to provide technical assistance. Dr. Sunita Ghosh provided statistical assistance. The support over the past two years from members of Dr. Reiman's lab, including Dr. Robert Evans, Tara Steffler, Kim Duerksen and Tamara Checkland, has been greatly valued. I want to acknowledge the support and guidance of my committee members: Dr. Mary Hitt, Dr. Heather McDermid and Dr. Tony Reiman. I greatly appreciated Mary stepping in as my co-supervisor when needed, and for welcoming me into her lab group. I want to thank Tony for being a great supervisor with a positive attitude, always providing constructive feedback and for always acting with my best interests and future goals in mind. Finally, I want to thank Mom, Dad and Auntie Margie for always taking great care of me and supporting me through my educational endeavours.

Table of Contents

List of Tables

List of Figures

List of Abbreviations

AQUA	Automated quantitative analysis
ASCT	Autologous stem cell transplant
BCR	B cell receptor
β_2-AR	β_2-adrenergic receptor
CCI	Cross Cancer Institute
CML	Chronic myeloid leukaemia
CSR	Class switch recombination
Ct	Cycle threshold
DAB	Diaminobenzidine
DSB	Double-strand break
ES	Embryonic stem cell
FGF	Fibroblast growth factor
FGFR3	Fibroblast growth factor receptor 3
FISH	Fluorescent *in situ* hybridization
GC	Germinal center
H&E	Hematoxylin and eosin
HRP	Horseradish peroxidase
IgH	Immunoglobulin heavy chain
IgL	Immunoglobulin light chain
IHC	Immunohistochemistry
IMWG	International Myeloma Working Group

ISS	International Staging System
LDH	Lactate dehydrogenase
LPF	Lipofectamine
LPS	Lipopolysaccharide
MACS	Automated magnetic cell sorting
MAPK	Mitogen activated protein kinase
MAR	Matrix attachment region
MGUS	Monoclonal gammopathy of undetermined significance
M-protein	Monoclonal immunoglobulin protein
NS	Non-specific
OS	Overall survival
PFS	Progression-free survival
PKA	Protein kinase A
PKC	Protein kinase C
PLACE	Pixel-based locale assignment for compartmentalization of expression
PR	Partial response
qRT-PCR	Quantitative real-time polymerase chain reaction
RESA	Rapid exponential subtraction algorithm
RISC	RNA-induced silencing complex
SD	Stable disease
SHM	Somatic hypermutation
shRNA	short hairpin RNA
siRNA	small interfering RNA

TBCC	Tom Baker Cancer Centre
TD	T cell-dependent
TI	T cell-independent
TMA	Tissue microarray
VSV-G	Vesicular stomatitis virus glycoprotein

1 Introduction

1.1 Multiple myeloma

1.1.1 Clinical features and prevalence

Multiple myeloma is a hematological malignancy characterized by the proliferation of monoclonal plasma cells. These malignant plasma cells infiltrate the bone marrow and secrete monoclonal immunoglobulin protein (M-protein), which can cause many clinical symptoms, including hypercalcaemia, renal insufficiency, anemia, recurrent infections and lytic bone lesions (1). The median age of diagnosis is 66 years, and the disease is slightly more prevalent in males than females (2, 3). It was estimated that 2100 people in Canada would be diagnosed with multiple myeloma in 2008, accounting for 1.3% of all cancer diagnoses, and that 1350 people would die from this disease (4). Multiple myeloma currently remains incurable; however, recent advancements in the understanding of myeloma pathology and novel treatment regimens have led to increased survival rates within the past decade (3).

1.1.2 Etiology and progression

The cause of multiple myeloma is not well understood. There is an increased incidence of myeloma in males compared to females (59% vs. 41%, respectively) (2), and in African Americans compared to Caucasians (2:1) (5). The risk of developing myeloma is increased in relatives of affected individuals (6), and families with multiple cases of myeloma have been identified (7). These

data suggest that there is an underlying genetic component; however, no genes have been conclusively linked to inheritance of myeloma.

Similarly, the cell of origin of myeloma has not been confirmed. The malignant cells in this cancer are plasma cells, which are terminally differentiated B cells. However, there is evidence to suggest that myeloma arises from an early stage B cell. Since B cells undergo V(D)J rearrangement of their DNA to generate unique antibodies, this rearranged sequence can be used to identify clonal B cells, which originated from the same cell. Different studies have identified early stage B cells that share the same antibody sequence as the malignant plasma cells in patients with myeloma (8, 9). These data suggest that the cell of origin in myeloma is not the plasma cell, but rather an early stage B cell. These studies also support the fact that although many patients with myeloma respond to initial treatment, they eventually relapse, likely due to the persistence of myeloma precursor B cells. However, there are also data that suggest myeloma arises from a post-germinal center (GC) B cell. When B cells are activated by antigen, they undergo somatic hypermutation (SHM) in the GC to increase the antibody affinity to the antigen. This process mutates nucleotides in the antigen-binding region of the antibody gene. Studies have shown that all malignant plasma cells in a myeloma patient share the same pattern of SHM in their antibody genes (10). These data suggest that malignant plasma cells arise from a late-stage, post-GC B cell.

Although the cause and cell of origin in myeloma remain elusive, the progression of this disease is better understood. A premalignant condition to

myeloma, known as monoclonal gammopathy of undetermined significance (MGUS), is well documented. MGUS is characterized by the presence of monoclonal plasma cells in the bone marrow (<10%) and M-protein in the serum (<30 g/L), but an absence of the organ damage or tissue impairment observed in myeloma (1). Approximately 2% of people over the age of 50 years have MGUS, and 1% of these will progress to myeloma each year (11). Recently, a prospective study of 77469 healthy individuals in the U.S., studied from 1992-2001, identified 71 individuals who went on to develop multiple myeloma. The study participants had provided annual blood samples to be used for research purposes. These samples were analyzed for the presence of M-protein to identify MGUS, which led to the discovery that MGUS preceded myeloma in 100% of patients studied (12). These results clearly demonstrate that myeloma begins as a benign growth of clonal plasma cells, which can progress to overt myeloma over time.

1.1.3 Novel treatment strategies

From 1971 to 1996, the median overall survival (OS) from the time of diagnosis of patients with myeloma was 30 months (3). However, with the introduction of novel therapeutic agents, such as thalidomide, lenalidomide and bortezomib, the median OS has increased to approximately 45 months over the past decade (3). High-dose chemotherapy followed by autologous stem cell transplant (ASCT) has also led to increased OS in patients below the age of 65 years (13, 14). In fact, the recent improvement in OS is most pronounced in younger patients. Patients diagnosed with myeloma in the past decade below the

age of 65 years had a median OS of 60 months, compared to only 33 months in older patients (3). As many clinical trials comparing the use of novel therapeutics with standard treatments, and in new combinations, are continuously being evaluated, treatment strategies that improve survival should continue to emerge.

Several studies have shown that high-dose chemotherapy with ASCT leads to increased response rates, OS and progression-free survival (PFS) in myeloma patients under the age of 65 years. Briefly, this procedure is performed by collecting $CD34^+$ hematopoietic stem cells from the patient, treating the patient with high-dose chemotherapy to rid the bone marrow of malignant cells, then transplanting the stem cells back into the patient. $CD34^+$ stem cells are the precursors for all cells in the hematopoietic lineage, so are able to regenerate the bone marrow cells that were destroyed during high-dose therapy. A randomized trial comparing high-dose chemotherapy and ASCT to conventional chemotherapy showed that 81% of the transplant patients responded to therapy, compared with only 22% in the conventional treatment group. This study also showed that transplant patients had a higher probability of five-year PFS (28% vs. 10%) and five-year OS (52% vs. 12%) compared with the conventional treatment group (13). A more recent trial confirmed that patients who received ASCT had a longer median OS (54.1 vs. 42.3 months) and PFS (31.6 vs. 19.6 months) than patients receiving conventional treatment (14). Based on the superiority of ASCT over conventional therapy, further studies have evaluated the use of tandem transplants compared to single transplants. Patients who received tandem transplants were shown to have significantly higher seven-year OS rates and PFS

rates compared to patients receiving only a single transplant (15). These studies clearly demonstrate the benefits of ASCT in patients with myeloma. However, only patients who are young (<65 years) and healthy enough to undergo this procedure are eligible.

The novel therapeutic agents thalidomide, lenalidomide and bortezomib have all shown promising results in myeloma treatment; additionally, these drugs are useful in older patients with myeloma, unlike ASCT. Thalidomide is an inhibitor of angiogenesis that is efficacious as a primary therapy and as salvage therapy in myeloma. This drug was initially tested in relapsed patients who were refractory to high-dose chemotherapy regimens. Thirty-two percent of these patients responded to thalidomide therapy, as measured by a reduction in M-protein (16). These results prompted trials testing thalidomide as a primary therapy for patients ineligible for ASCT. Elderly patients who received the standard frontline therapy of melphalan-prednisone, in combination with thalidomide, had significantly higher response rates, survival rates (17) and OS than patients who received melphalan-prednisone alone (18). In a randomized clinical trial comparing thalidomide-dexamethasone with dexamethasone alone as a primary therapy for myeloma, patients who received thalidomide showed a 63% response rate compared with 41% in the dexamethasone-only group (19). However, it is important to point out that significantly higher toxicity was observed when thalidomide was added to either the melphalan-prednisone or dexamethasone regimens.

Lenalidomide is a derivate of thalidomide that is also an effective myeloma treatment. An initial study that administered lenalidomide to relapsed and/or refractory myeloma patients demonstrated a response rate of 71% (20). Importantly, this treatment regimen was well tolerated by patients. A randomized trial comparing lenalidomide-dexamethasone with dexamethasone alone showed significantly higher OS, PFS and response rates in the patients that received lenalidomide (21). In addition to thalidomide and lenalidomide, the proteasome inhibitor bortezomib has shown promising results for the treatment of myeloma. As a frontline therapy in combination with melphalan-prednisone, the addition of bortezomib led to increased response rates and time to progression (22). As an induction therapy prior to ASCT, bortezomib therapy leads to high response rates (23). In a study that compared the use of bortezomib or dexamethasone in relapsed myeloma, patients who received bortezomib had higher response rates, OS and PFS than those who received dexamethasone (24).

Currently, many trials are underway to determine the best combinations of novel drugs with more conventional therapies for myeloma treatment. Additionally, many studies are examining how different subgroups of myeloma patients respond to different therapies. Myeloma is a complex, heterogeneous disease, and thus there is not likely to be one uniform treatment regimen for all patients. Therefore, identifying unique genetic subgroups of myeloma patients and how these subgroups respond to treatment will be an important part of improving myeloma therapy.

1.1.4 Genetic abnormalities in multiple myeloma

As is common with many cancers, multiple myeloma cells have many genetic abnormalities and complex karyotypes. Conventional cytogenetic approaches for examining chromosome abnormalities in myeloma were often hindered by the low proliferative nature of plasma cells and an inability to obtain metaphase spreads. Through the use of interphase fluorescent *in situ* hybridization (FISH), the detection of genetic abnormalities in myeloma cells – both numerical and structural – has enabled the identification of unique genetic subgroups of patients.

By using interphase FISH, it has been determined that almost 90% of myeloma patients display chromosome aneuploidy (25). Patients can be divided into hyperdiploid and non-hyperdiploid myeloma, each of which is associated with specific genetic abnormalities and differing prognoses. Hyperdiploid myeloma (47-74 chromosomes) has been observed in 31-54% of patients with abnormal karyotypes (26-28) and is commonly associated with trisomies 3, 5, 7, 9, 11, 15, 19 and 21 (29). This subgroup of patients rarely has immunoglobulin heavy chain (IgH) locus translocations or monosomy 13 (30). Conversely, patients with non-hyperdiploid (including hypodiploid, pseudodiploid and near-tetraploid) myeloma (<47 or >74 chromosomes) often have IgH translocations and deletion of chromosome 13. One study, which compared the incidence of translocations and monosomy 13 between patient ploidy subgroups, found that IgH translocations occurred in 84% of non-hyperdiploid patients and only 39% of hyperdiploid patients, and monosomy 13 was observed in 72% of non-

hyperdiploid patients compared with 37% of hyperdiploid patients (30). Partly due to the increased incidence of IgH translocations and monosomy 13 in non-hyperdiploid myeloma, this patient subgroup has been found to have significantly reduced survival compared with hyperdiploid patients (27).

Frequent chromosome gains and losses are common in myeloma. These gains and losses involve entire chromosomes, as well as partial regions of chromosomes. Recurrent gains of chromosome 1q21 have been observed in 43% of newly diagnosed patients, and in 72% of relapsed patients, as detected by interphase FISH (31). Deletions of chromosome 13, specifically 13q14, are also frequent in myeloma. Using interphase FISH, monosomy 13 has been detected in approximately half of myeloma patients (28, 32, 33). Another frequently occurring deletion in myeloma is 17p13, which contains the tumour suppressor p53. This chromosome band is deleted in 10-20% of patients (28, 33, 34).

In addition to chromosome aneuploidy and numerical abnormalities, structural chromosome abnormalities are frequent in myeloma. Specifically, chromosome translocations involving the IgH locus on chromosome 14q32 are often observed. Numerous groups have studied the incidence of IgH translocations in myeloma using interphase FISH, and have found that these translocations are present in approximately 50-75% of myeloma patients (35-37). Additionally, multiple, recurrent translocation partner loci have been documented in myeloma, including t(11;14), t(4;14), t(14;16) and t(6;14). A detailed review of the cause, incidence and consequence of these translocations will follow in section 1.2.

1.1.5 Prognostic factors and risk stratification

Analyses of clinical, laboratory and cytogenetics data have led to the identification of different prognostic factors in myeloma, and an ability to predict patient survival and response to treatment. Recently, the International Staging System (ISS) for multiple myeloma was developed, which stratifies patients into three prognostic groups based on routine, objective laboratory tests (38). In this staging system, patients with low serum β_2-microglobulin (<3.5 mg/L) and high serum albumin (≥3.5 g/dL) have a median OS of 62 months (stage I), patients that are neither stage I nor stage III have a median OS of 44 months (stage II), and patients that have high serum β_2-microglobulin (≥5.5 mg/L) have a median OS of 29 months (stage III).

Many cytogenetic abnormalities have also been discovered to be prognostic factors in myeloma. The t(4;14) translocation has been shown to be an adverse prognostic marker by many groups (28, 32, 39), whereas presence of t(11;14) does not impact survival (28). Deletion of chromosome 13 or 17p13 leads to shortened survival in patients with multiple myeloma (28, 34). Based on these cytogenetic abnormalities, three prognostic groups have been identified. Patients who have a t(11;14) translocation or an absence of cytogenetic abnormalities have the highest median OS of 51 months, compared to 41 months in the entire patient cohort. Patients with monosomy 13, and an absence of all other abnormalities, have an intermediate prognosis, with a median OS of 42 months. Those patients who possess a t(4;14) or t(14;16) translocation, or have a

deletion of 17p13, have the worst prognosis, with a median OS of only 25 months (33).

Gene expression profiling has also led to the identification of high-risk myeloma patients. In addition to the loss of 17p13, patients who have reduced p53 gene expression have a worse prognosis (34). Whole genome gene expression profiling has led to the identification of a 70-gene risk-stratification model that can accurately identify high-risk myeloma patients (40). Genes in this model are both upregulated and downregulated, and many of these genes map to chromosome 1. This 70-gene model has been proven to be predictive of survival in patients treated with bortezomib or dexamethasone (41).

The ability to identify distinct patient subgroups that have different prognoses and responses to treatment is very important. Through this, the best treatment regimen can be selected for patients based on their unique genetic profile. Additionally, identifying patient subgroups will lead to a better understanding of myeloma origin and progression. Finally, the identification of unique genetic abnormalities in myeloma will lead to the discovery of novel therapeutic targets and treatments, which are tailored to patients' unique diseases.

1.2 Chromosome translocations

One of the key features of the humoural immune response is the ability of B cells to generate a diverse repertoire of unique antibody sequences, which can potentially bind to any foreign antigen in the body. In order to do this, the immunoglobulin genes are rearranged and mutated. This process is imperative to

a functional immune system, but creates the potential for oncogenic mutations to occur. This is evidenced by the fact that translocations involving the IgH locus at chromosome 14q32 are common in B cell malignancies. For example, mantle cell lymphoma, Burkitt's lymphoma and follicular lymphoma are all associated with unique translocations – t(11;14), t(8;14) and t(14;18), respectively (42). Similarly, primary translocations at 14q32 are present in approximately 50-75% of patients with multiple myeloma (35-37). These translocations lead to juxtaposition of the IgH enhancers with oncogenes from the translocated chromosome, and subsequent overexpression of the translocated oncogene. Primary translocations occur early in the transformation process and are caused by errors in B cell development, opposed to secondary translocations that occur later in disease progression and are not associated with errors in B cell-specific processes (43). Henceforth, the term translocation will refer only to primary translocations observed in myeloma.

Chromosome translocations at 14q32 are believed to be associated with transformation in myeloma. These translocations are present in approximately 45% of patients with MGUS (44), demonstrating that these are early, and possibly transforming, events in myeloma. Also, IgH translocations are present in 50-75% of patients with multiple myeloma and 82% of patients whose myeloma has progressed to plasma cell leukemia (45). Since the incidence of IgH translocations increases as the disease progresses, these genetic aberrations likely confer a survival advantage to cells that is selected for throughout disease evolution (43).

Due to the high incidence of translocations in myeloma, as well as their association with disease transformation and progression, these genetic abnormalities represent potential therapeutic targets. In order to learn how to target these translocations therapeutically, it is important to understand the molecular basis of how they occur during B cell development, and their downstream effects within the cell.

1.2.1 B cell development

The primary role of B cells within the immune system is to generate high affinity antibodies that can bind to, and help to eliminate, antigens. To achieve this, the antibody genes of B cells are mutated through three processes that are temporally regulated throughout B cell development: V(D)J recombination, SHM and class switch recombination (CSR).

An antibody molecule is composed of two identical heavy chains (IgH) and two identical kappa or lambda light chains (IgL). The N-terminal regions of these proteins form the variable antigen-binding region, while the C-terminus of the IgH protein determines the antibody isotype. In the earliest stages of B cell development, the variable region of the IgH gene is rearranged (Figure 1.1) (process reviewed in (46)). DNA double-strand breaks (DSB) are generated beside the D_H and J_H gene segments, intervening DNA is removed, and the ends are ligated together to form a D_H-J_H joint. Following this, a V_H gene segment is joined to the D_H-J_H joint, which forms the $V_HD_HJ_H$ antigen-binding region. A similar process then occurs on the IgL gene, whereby a V_L and J_L segment are

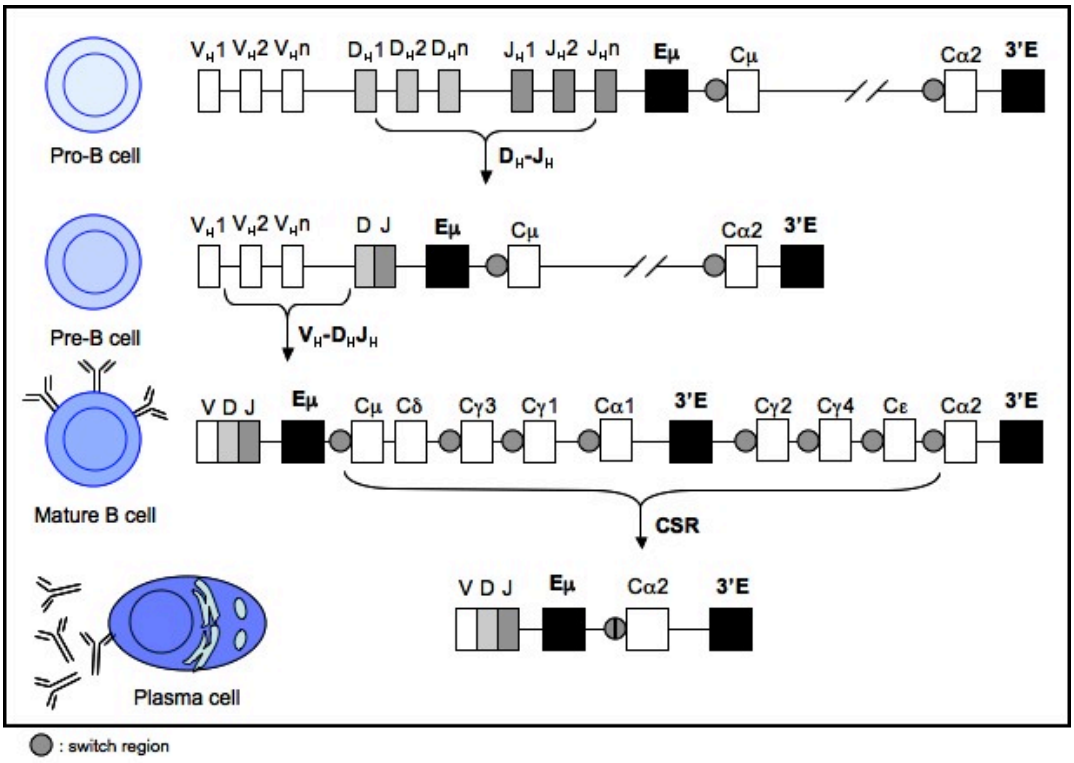

Figure 1.1. Immunoglobulin heavy chain gene rearrangement during B cell development. VDJ recombination of the heavy chain (IgH) locus occurs in pro-B cells and pre-B cells. Also in the pre-B cell, either a kappa or lambda light chain (IgL) is rearranged (not shown). Two identical IgH chains and two identical IgL chains form the IgM antibody, which is presented on the surface of a mature B cell. When a mature B cell binds specifically to an antigen, CSR occurs. This process does not affect the antigen-binding region of the antibody, but changes the constant region of the heavy chain locus. In the example shown here, the IgM isotype switches to the IgA isotype. DNA breaks are generated in the switch regions upstream of Cμ and Cα2, the intervening DNA is removed, and a hybrid switch junction is formed. The terminally differentiated plasma cells then migrate to the bone marrow and express large amounts of the high affinity, isotype-switched antibody. CSR: class switch recombination.

joined together. The rearranged IgH and IgL gene products are assembled to form IgM, which is then presented on the surface of the mature B cell. This process occurs in the bone marrow and does not require antigenic stimulation.

Mature B cells migrate to peripheral lymphoid organs, such as the spleen or lymph nodes, where they come into contact with antigen. If the surface IgM molecule binds specifically to an antigen, then affinity maturation and isotype switching will occur in the GC (process reviewed by (47)). During SHM, random mutations are introduced into the variable region, and antibodies with the highest affinity for the antigen are selected. Additionally, the constant region of the IgH gene is rearranged by CSR to generate an IgG, IgE or IgA antibody isotype. For example, to switch from IgM to IgA, DNA DSBs are generated in the switch regions upstream of the Cμ and Cα constant regions. The DNA then forms a loop so that the Sμ and Sα switch regions can be ligated together to form a hybrid switch junction, and the intervening DNA is deleted. Plasma cells, which are terminally differentiated B cells, then home to the bone marrow and secrete large amounts of high affinity, isotype-switched antibody.

1.2.2 Myeloma translocations arise due to aberrant class switch recombination

As was described previously, multiple processes, including VDJ recombination, SHM and CSR, introduce DNA DSBs into the IgH locus during B cell development. Errors in these specific processes have been linked to

translocations that occur in other hematological malignancies. The t(14;18) translocation in follicular lymphoma, the t(11;14) translocation in mantle cell lymphoma, and the t(8;14) translocation in Burkitt's lymphoma have all been shown to arise primarily due to errors in VDJ recombination (48-50). However, in multiple myeloma the translocation breakpoints on chromosome 14q32 occur most frequently in switch regions, suggesting that these translocations arise due to errors in CSR.

To determine the mechanism that leads to translocations in multiple myeloma, Bergsagel *et al*. developed a novel assay utilizing Southern blot technique (51). Briefly, pairs of probes that flanked the 5' and 3' ends of the Sμ, Sγ, Sα and Sε switch regions were generated, DNA was digested using restriction enzymes that cut outside of each probe pair, and the digested DNA was probed with the 5' and 3' switch region probes. If any of the 5' and 3' probes bound to the same restriction fragment, then a legitimate switch recombination had occurred. However, if only one probe bound to a restriction fragment, this was indicative of a candidate translocation. Using this experimental approach, it was determined that the majority of translocations in myeloma cell lines and tumour samples occurred in switch regions, due to aberrant CSR (51).

Additional studies have analyzed the chromosome breakpoints in t(4;14) and t(11;14) cell lines and patient samples. One study that analyzed the t(4;14) breakpoints of 7 myeloma patient samples found that 5/7 patients had breakpoints in Sμ switch regions, while 2/7 patients had breakpoints that were 5' of the switch region (52). The 2 patients with breakpoints upstream of Sμ had hybrid switch

junctions, indicating functional CSR had occurred. The t(11;14) breakpoints of patients and cell lines have also been studied by different groups. An analysis of 2 t(11;14) myeloma cell lines found that both breakpoints at 14q32 were in a switch region (53). A separate study of 2 tumour samples found that both breakpoints occurred adjacent to hybrid Sμ/Sγ (54). These results indicate that although aberrant CSR leads to translocations in the majority of cases, other factors that follow CSR can cause translocations.

Translocations that occur at or near the switch regions on 14q32 lead to the segregation of the Eμ and 3'IgH enhancer elements, and can potentially separate the 3'IgH enhancers downstream of both the Cα1 and Cα2 constant regions. Proto-oncogenes from the translocated chromosome become linked to these enhancers, and subsequently become overexpressed, which can be oncogenic. Additionally, since the enhancer elements are separated, this can lead to the simultaneous dysregulation of two proto-oncogenes from both derivative chromosomes. An example of aberrant CSR leading to a translocation is shown in Figure 1.2. In this case, the fibroblast growth factor receptor 3 (*FGFR3*) and *MMSET* oncogenes from 4p16 become linked to the 3'IgH enhancer and the Eμ enhancer, respectively.

1.2.3 Multiple, recurrent translocations are observed in myeloma

Unlike other hematological malignancies, which are characterized by unique translocations, four recurrent translocation partners have been identified in multiple myeloma patient samples: t(11;14)(q13;q32), t(4;14)(p16;q32),

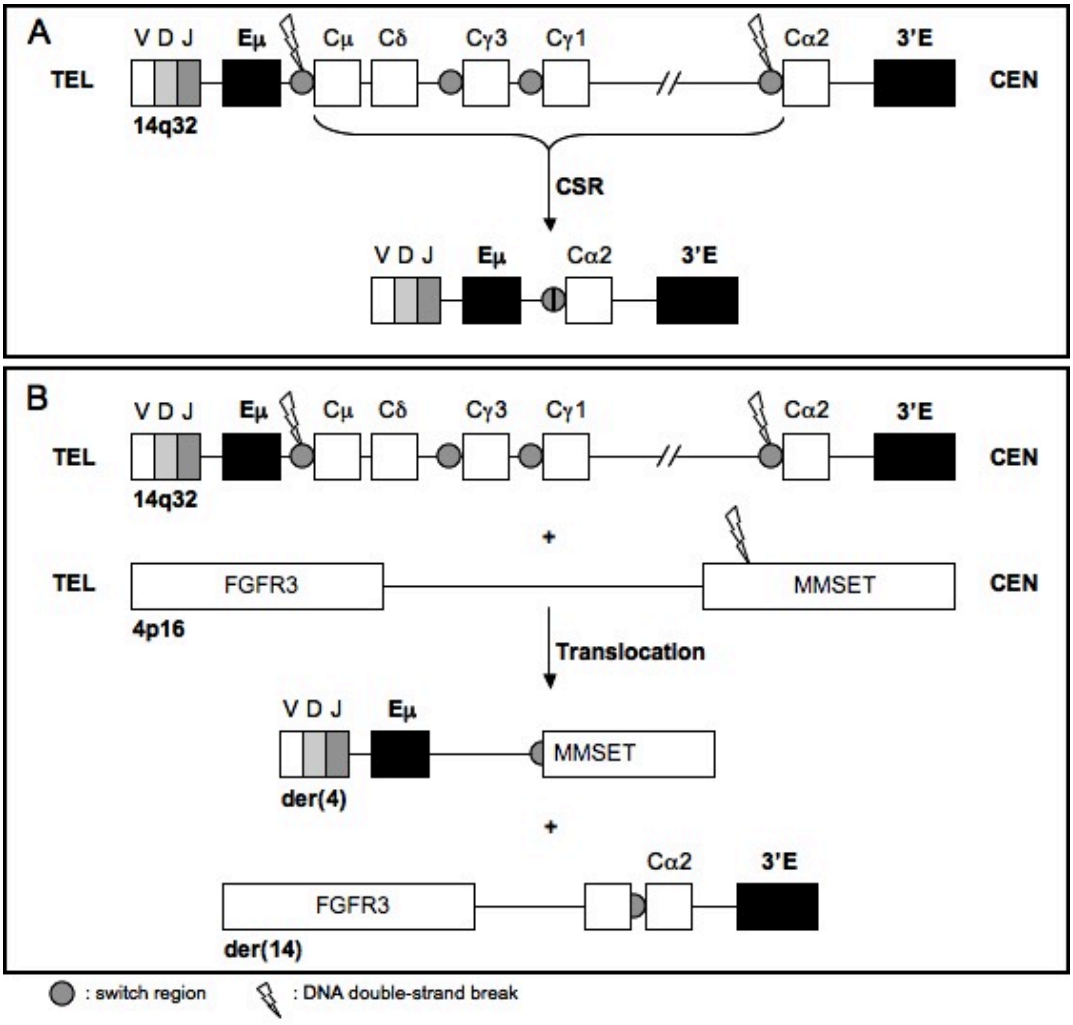

Figure 1.2. Errors during class switch recombination lead to translocations in myeloma. (A) Following antigenic stimulation, the IgH locus on 14q32 rearranges from IgM to IgA by CSR. DNA DSBs are generated in switch regions, the intervening DNA is deleted, and a hybrid switch region forms, which leads to the expression of the Cα2 constant region. (B) During CSR, a DNA DSB is also introduced in the MMSET locus on 4p16, DNA repair malfunctions, and a t(4;14) translocation occurs. This results in linkage of the IgH-MMSET fusion transcript to the Eμ enhancer on der(4) and FGFR3 with the 3'E on der(14). CSR: class switch recombination; DSB: double-strand break; Tel: telomere; Cen: centromere.

t(14;16)(q32;q23) and t(6;14)(p21;q32) (Table 1.1). The t(11;14) translocation, which occurs in approximately 16% of patients (32, 33, 55, 56), is the most frequent translocation in myeloma. The t(4;14) translocation is also frequent in myeloma, as 13% of patients have been reported to possess this abnormality (32, 33). t(14;16) and t(6;14) occur less frequently, but are recurrent, having been observed in 2-5% (32, 33) and 4% (57) of patients, respectively. The remaining translocation partners are unidentified and may or may not be recurrent, although other translocations, such as t(14;20)(q32;q12), reportedly occur in more than one myeloma cell line (58, 59).

Myeloma cells that possess the t(11;14) translocation have been shown to overexpress cyclin D1 mRNA and protein from 11q13 (53). Cyclin D1 is a positive regulator of the cell cycle and is not normally expressed in lymphoid tissue. Its overexpression can therefore lead to cell cycle progression in myeloma cells. Additionally, almost half of myeloma cell lines with t(11;14) overexpress the putative transforming gene *myeov* from 11q13. This gene was shown to be transforming in a NIH/3T3 tumourigenicity assay, and thus could also promote oncogenesis in t(11;14) myeloma (60). Many breakpoints at 11q13 have been identified in t(11;14) myeloma, which are located both telomeric and centromeric of *cyclin D1*, and are anywhere from 8-500 kb from the *cyclin D1* locus (54, 61). Depending on the location of the breakpoint on 11q13, *cyclin D1* can become linked to the Eμ or 3'IgH enhancers. Although many studies have shown a clear association between the t(11;14) translocation and expression of cyclin D1 (53, 60), the large distance between the breakpoint and the *cyclin D1* gene leads to

Table 1.1. Recurrent translocations in multiple myeloma

Translocation	Dysregulated gene(s)	Frequency (%)
t(11;14)	cyclin D1	16
t(4;14)	FGFR3 and MMSET	13
t(14;16)	c-maf	5
t(6;14)	cyclin D3	4

questions about the relationship between cyclin D1 expression and the respective translocation. Also, patients that do not have a t(11;14) translocation have been shown to express cyclin D1 (62).

The t(14;16) translocation is associated with overexpression of the c-maf proto-oncogene. c-maf belongs to the basic zipper transcription factor family, and is associated with proliferation and differentiation. In four myeloma cell lines that were shown to have this translocation by Southern blot analysis, Northern blot confirmed overexpression of c-maf mRNA in all cases (63). The breakpoints at 16q23 spanned a 500 kb region, and were all located centromeric to *c-maf*, resulting in linkage of this gene to the powerful 3'IgH enhancer (63).

A second infrequent, but nonrandom translocation in myeloma is t(6;14), which is associated with overexpression of cyclin D3 (57). Cyclin D3 expression promotes cell cycle progression. This protein is normally expressed in lymphoid tissues at low levels and varies during the cell cycle; however, myeloma tumour samples and cell lines with the t(6;14) translocation have significantly increased expression of cyclin D3 (57). The chromosome breakpoints on 6p21 are located within a 200 kb region centromeric to *cyclin D3*, which results in linkage of this proto-oncogene to the strong 3'IgH enhancer and its subsequent overexpression (57).

Myeloma cell lines and tumour samples with the t(4;14) translocation overexpress FGFR3 from 4p16. The translocation breakpoints on 4p16 are located 50-100 kb centromeric of *FGFR3*, which results in juxtaposition of this proto-oncogene to the 3'IgH enhancer on der(14) (Figure 1.2) (64, 65). FGFR3 is not

normally expressed in hematopoietic cells, and its overexpression activates cell proliferation pathways, which can be transforming in myeloma (66). In addition to FGFR3 overexpression, the t(4;14) translocation leads to upregulation of MMSET from der(4). The chromosome breakpoints on 4p16 have, in fact, been cloned to the 5' introns of the *MMSET* locus, which links *MMSET* to the Eμ enhancer (Figure 1.2). This leads to expression of both an IgH-MMSET fusion transcript and overexpression of MMSET from an endogenous promoter on 4p16 (67, 68). The role of MMSET in myeloma is unclear, but recent studies suggest it plays a role in cellular adhesion, cell cycle progression and resistance to apoptosis (69, 70).

The t(4;14) translocation has been well characterized and studied by many groups. The breakpoints on 4p16 have consistently been located in the 5' introns of *MMSET*, within 100 kb of *FGFR3*. Thus, the association between t(4;14) and overexpression of FGFR3 is well established. Overexpression of FGFR3 has been shown by many groups to be transforming in myeloma, which prompted the inhibition of FGFR3 expression and activity as a therapeutic target for myeloma.

1.2.4 FGFR3 is transforming in myeloma

FGFR3 is a receptor tyrosine kinase that is normally expressed in the lungs, kidney, developing central nervous system, and in some cartilage (71). When it is bound by its ligand, fibroblast growth factor (FGF), FGFR3 dimerizes and is transautophosphorylated. This results in downstream signaling cascades that cause proliferation and differentiation. In t(4;14) myeloma, activating

mutations of FGFR3 have been found that lead to its constitutive activation in the absence of ligand. The t(4;14) cell lines KMS11 and OPM2 were found to possess activating Y373C and K650E FGFR3 mutations, respectively (72). In an analysis of t(4;14) patients samples, only 1/11 patients had an activating FGFR3 mutation (73). A longitudinal study of t(4;14) patient samples found that one patient relapse sample had gained a FGFR3 K650E mutation that was not present in the diagnostic sample, demonstrating that activation of FGFR3 confers a growth advantage to t(4;14) cells (74).

Expression of FGFR3 in B cells can lead to oncogenesis. When the bone marrow of mice was transduced with wild-type and mutant FGFR3, this led to the formation of B cell tumours (75). Furthermore, murine B cells that were transduced with FGFR3 exhibited increased expression of bcl-x_L, an anti-apoptotic protein, and increased STAT3 phosphorylation, which promotes cell cycle progression (76). Myeloma cell lines that express FGFR3 due to a t(4;14) translocation were shown to exhibit increased phosphorylation of ERK1 and ERK2, which are effectors of the mitogen activated protein kinase (MAPK) cell proliferation pathway (66). Additionally, the activity of FGFR3 in t(4;14) myeloma cell lines leads to phosphorylation of RSK2, which is an important mediator of cell survival and proliferation (77). These results all established the ability of FGFR3 to promote growth and prevent apoptosis in t(4;14) myeloma. Therefore, inhibiting FGFR3 expression and activity has been evaluated as a potential therapeutic strategy in t(4;14) myeloma.

1.2.5 Inhibition of FGFR3 leads to growth arrest and apoptosis in t(4;14) myeloma

Using shRNA, small molecule inhibitors and neutralizing antibodies, many groups have shown the potential therapeutic effects of inhibiting FGFR3 in t(4;14) myeloma. A pool of three shRNA molecules targeting FGFR3 effectively decreased FGFR3 mRNA and protein expression in three t(4;14) myeloma cell lines. This led to increased apoptosis, and decreased expression of MAPK genes (78). Using numerous small molecule inhibitors, including CHIR-258, SU5402, PD173074 and PKC412, *in vitro* assays have shown reduced FGFR3 transautophosphorylation, decreased cell viability, increased apoptosis and decreased downstream signaling in t(4;14) myeloma cell lines, such as KMS11 (79-84). These effects were more pronounced in cell lines with constitutively active FGFR3, such as KMS11, than in cell lines with wild-type FGFR3, demonstrating the dependence of mutant FGFR3 cell lines on FGFR3 signaling. Importantly, these effects were not observed in myeloma cell lines without the t(4;14) translocation. In mouse models implanted with t(4;14) xenografts, CHIR-258 and PD173074 exhibited anti-tumour activity. The administration of these drugs led to increased tumour apoptosis, decreased tumour volume and increased survival of these mice (79, 80, 83). The anti-FGFR3 antibody PRO-001 has also shown therapeutic benefits in t(4;14) myeloma, as it caused decreased growth of a t(4;14) cell line, inhibited tumour growth in a mouse model, and inhibited FGF ligand stimulation in t(4;14) primary patient samples (85). However, this anti-FGFR3 antibody was only effective in cell lines with wild-type FGFR3 that require ligand binding for FGFR3 activation.

Furthermore, use of the FGFR3 small molecule inhibitor BIBF 1000 has shown additive and synergistic effects in combination with dexamethasone and bortezomib in t(4;14) cell lines. In OPM2 myeloma cells, which possess a t(4;14) translocation and overexpress constitutively active FGFR3, the combination of BIBF 1000 and dexamethasone worked synergistically to increase apoptosis, and the combination of BIBF 1000 and bortezomib additively increased apoptosis. In H929 cells, which are t(4;14)-positive and express wild-type FGFR3, the combination of BIBF 1000 and dexamethasone overcame single-agent drug resistance (86).

Based on these studies, inhibiting FGFR3 appears to be an effective therapeutic strategy for t(4;14) myeloma. However, there are factors that limit the application of this treatment. The t(4;14) translocation leads to simultaneous dysregulation of FGFR3 from der(14), as well as MMSET from der(4) (67, 68). Recent studies that knocked down MMSET using RNA interference (RNAi) in t(4;14) myeloma cell lines have demonstrated a role for MMSET in cell adherence, cell cycle progression, resistance to apoptosis and tumour formation in xenograft models (69, 70). In analyses of t(4;14) patient samples, FGFR3 expression was found to be lost in almost 30% of patients, due to loss of the der(14) chromosome (87, 88). Furthermore, the t(4;14) translocation was found to be an adverse prognostic marker in myeloma irrespective of FGFR3 expression (39). These data suggest that MMSET, and possibly other genes, on 4p16 contribute to oncogenesis of t(4;14) myeloma. Thus, inhibition of FGFR3 may not be beneficial to all t(4;14) patients.

Another limitation of FGFR3 inhibition is that less than 15% of myeloma patients have a t(4;14) translocation, and therefore very few would benefit from this type of therapy. Since 50-75% of myeloma patients have a 14q32 translocation, a treatment strategy that targets all translocations would have widespread clinical applications. A unifying feature of translocation-positive myeloma is the linkage of oncogenes to the Eμ and, most frequently, the 3'IgH enhancer elements. Thus, inhibiting the activity of the IgH enhancers represents a potential treatment strategy for all translocation-positive myeloma patients.

1.3 Regulation of the IgH enhancer elements

Enhancers are *cis*-acting regulatory elements that are capable of increasing transcription from promoters of nearby genes. Two enhancer regions are important for regulation of the IgH locus – the Eμ (intronic) enhancer and the 3'IgH enhancer. The tissue-specific and temporally regulated activity of these enhancers is important for regulation of IgH recombination and transcription throughout B cell development and is dependent on tissue- and cell stage-specific transcription factors that bind to the enhancers during B cell ontogenesis.

1.3.1 The Eμ enhancer

The Eμ enhancer is located between the J_H coding region and the Cμ constant region of the IgH locus (Figure 1.3). The enhancer function of this region was confirmed by reporter gene assays, whereby the enhancer was capable of

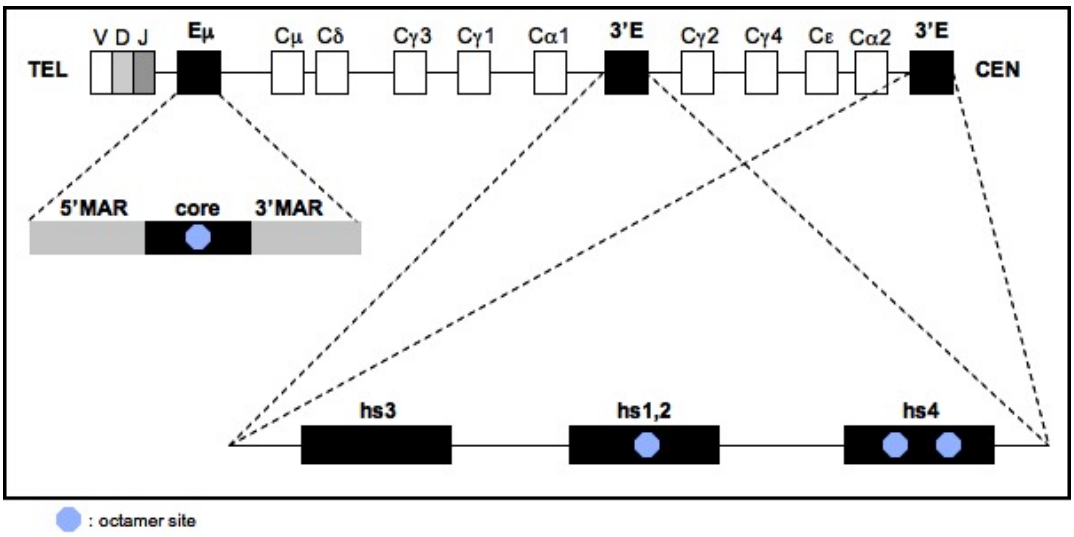

Figure 1.3. Human immunoglobulin heavy chain locus enhancers. The Eμ intronic enhancer is composed of a core region flanked by 5' and 3' matrix attachment regions (MARs). The 3'IgH enhancers are duplicated in the human IgH locus and are nearly identical. They are each composed of three DNAse I hypersensitive regions: hs3, hs1,2 and hs4. Consensus octamer binding sites ATGCAAAT present in the human IgH enhancers are shown.

increasing transcription of a linked reporter gene upon transfection into B cells (89). The Eμ enhancer region is composed of a core enhancer region, and is flanked by 5' and 3' matrix attachment regions (MAR) (90). The activity of the Eμ enhancer region has been shown to be most important for development of early stage B cells, and less important in mature B cells and plasma cells.

Deletions of either the core region or MARs of Eμ reduced μ mRNA transcription from the IgH locus by approximately 50%, while deletion of the entire Eμ element reduced transcription to only 5% of control levels (91). The Eμ enhancer is also necessary for VDJ rearrangement of the IgH locus. Numerous studies of chimeric mice, which have deletions of Eμ, have shown that these mice have impaired VDJ recombination (92, 93). The role of the Eμ enhancer in CSR and SHM has also been analyzed. B cells with deletions of Eμ have a slight, but insignificant, impairment of both CSR and SHM (94, 95). These data indicate that Eμ activity is more important in early B cell development than later stages of B cell development.

Transcription factors that bind to Eμ are important for regulating its activity. Numerous B cell-specific and ubiquitous factors, including, but not limited to, Oct1, Oct2, PU.1, Ets-1, Bright and LR1, have been identified that bind to the Eμ enhancer element. The Eμ enhancer contains the conserved octamer sequence ATGCAAAT, which is bound by the B cell-restricted Oct2 transcription factor, as well as the ubiquitous Oct1 transcription factor (96). Mutation of the octamer element leads to reduced binding of the transcription factors and decreased transcriptional activity of the enhancer (97). The ETS

family transcription factors PU.1 and Ets-1 have also been shown to bind to, and activate, the Eμ enhancer (98). These factors modify the chromatin structure at the enhancer, thus making it more accessible to transcriptional machinery (99, 100). Similarly, the B cell-restricted transcription factor Bright increases chromatin accessibility at the Eμ enhancer by binding to the 5' and 3' MARs (101). The B cell-specific DNA binding protein LR1 is also capable of binding to the core region of Eμ and activating transcription (102).

1.3.2 The 3'IgH enhancer

In addition to the intronic Eμ enhancer, enhancer elements are located downstream of the Cα constant region of the IgH locus. Homologous enhancers in the rat and mouse IgH locus were identified downstream of Cα. When linked to reporter genes and transfected into B cells, both of these enhancers increased transcription of the reporter gene (103, 104). The mouse 3'IgH enhancer is composed of four DNase I hypersensitive sites – 5'-hs3A, hs1,2, hs3B and hs4-3' (105). These hypersensitive regions are indicative of transcription factor binding sites, since exposed DNA is hypersensitive to endonuclease digestion.

In contrast to the mouse and rat IgH loci, the human IgH locus contains a partial duplication of the constant region, shown in Figure 1.3. Enhancer elements have been mapped approximately 3 kb downstream of both Cα1 and Cα2 in the human IgH locus (106-108). The 3'IgH enhancers in the human locus are nearly identical, span 15 kb and are each composed of three DNase I hypersensitive sites – 5'-hs3, hs1,2 and hs4-3' (107) (Figure 1.3). hs3 is approximately 74%

homologous to murine hs3A and hs3B, human hs1,2 is 90% homologous to murine hs1,2, and human hs4 is 76% homologous to murine hs4 (107). Due to the high sequence homology of the human and mouse 3'IgH enhancers, many functional studies done in mice have been applied to knowledge of the human 3'IgH enhancer regions.

The Eμ enhancer is necessary for VDJ recombination and μ mRNA transcription of the IgH locus. Conversely, the 3'IgH enhancer region is more important for processes occurring later in B cell development, such as CSR and possibly SHM. When the 3'IgH enhancer region was linked to a reporter gene and transfected into different B cell lines, representing different stages of development, this enhancer was inactive in pre-B cells, but was highly active in mature B cells and plasma cells (109, 110). The DNase I hypersensitive sites of the 3'IgH enhancer function synergistically in B cells and plasma cells to exert maximal enhancer activity (110).

The activity of the 3'IgH enhancer in B cell development is reflective of the role it plays in IgH gene rearrangement. Mice with deletions of the distal enhancers, hs3B and hs4, have normal levels of IgH VDJ recombination, but do not undergo normal levels of CSR in response to antigen (111). The hs3, hs1,2 and hs4 enhancers increase transcription from the γ3, γ2, ε, α1 and α2 switch region promoters, which is an important step in CSR (112, 113). Similarly, mice with a deletion of the entire 3'IgH enhancer region express reduced levels of secondary immunoglobulin isotypes when exposed to antigen. Switching to IgG3, IgG2, IgE and IgA isotypes was dramatically reduced in mice lacking the 3'IgH

enhancer region, although normal levels of IgM were present (114). Although the 3'IgH enhancer is proven to be necessary for CSR, its role in SHM remains unclear. The hs3b and hs4 enhancer regions were shown to be required for SHM in mice (115); however, a separate study found that these regions were in fact dispensable for SHM in the murine IgH locus (111).

Binding of multiple transcription factors is important for activity of the 3'IgH enhancer. Binding sites for NF-κB are located in the hs3, hs1,2, and hs4 regions of the 3'IgH enhancer (116-118). Mutating the NF-κB binding sites in hs1,2 or hs4 led to a 50% decrease of enhancer activity in the murine IgH locus (116). In the human IgH locus, mutation of the hs4 NF-κB binding site led to greater than 80% reduction in activity of this enhancer element upon transfection into mature B cells (118). Furthermore, mutation of the NF-κB binding site in murine hs1,2 was shown to impair CSR (113). YY1 transcription factor binding sites have also been identified in the murine hs3 and human hs4 enhancer regions (117, 118). Upon antigenic stimulation, YY1 was shown to bind to hs3 and increase the activity of this enhancer region (117). Binding sites for HoxC4, a lymphocyte-restricted transcription factor, were also identified in hs1,2. Binding of HoxC4 to the enhancer positively regulates its activity (119). Conversely, Pax5/BSAP binding to the 3'IgH enhancer region negatively regulates the activity of this enhancer. *Pax5* encodes the BSAP protein, which is expressed in early stages of B cell development, but not in plasma cells (120), and binding of this protein to the 3'IgH enhancer has been shown to decrease enhancer activity (120, 121).

Octamer binding sites have also been located in the mouse and human 3'IgH enhancer region, and are necessary for its activity. Consensus octamer sites are present in hs1,2 and hs4 of the human 3'IgH enhancers (Figure 1.3) (107). The ubiquitously expressed Oct1 and primarily B cell-restricted Oct2 bind to the conserved octamer sequence ATGCAAAT. Additionally, the B cell-specific coactivator Bob1 (also called OBF1 or OCA-B) interacts with Oct1 and Oct2 bound to the octamer site.

Oct1 has been shown to bind to the 3'IgH enhancer and positively regulate its activity (116); however, mice with $Oct1^{-/-}$ B cells have normal B cell development, thus demonstrating that Oct1 is not required for function of the 3'IgH enhancer (122). Binding of Oct2 to the 3'IgH enhancer has been shown to be necessary for activity of this enhancer region. Mutation of the octamer sites located in hs3, hs1,2 and hs4 of the murine IgH enhancer led to decreased enhancer activity. In cotransfection experiments with the mutated octamer 3'IgH enhancer and a mutant Oct2 isoform with affinity for the mutated octamer site, the enhancer activity was restored (123). Binding of Oct2 to the human hs4 enhancer and human hs1,2 leads to increased activity of these enhancer elements (118, 119). Binding of Bob1 to the 3'IgH enhancer, through a complex formation with Oct2, leads to greatly increased enhancer activity. In fact, concerted binding of Bob1 and Oct2 to the 3'IgH enhancer increases its activity greater than binding of either Bob1 or Oct2 alone (109, 119, 123).

In translocation-positive multiple myeloma, the Eμ and, most frequently, the 3'IgH enhancers become linked to proto-oncogenes from the translocation

partner chromosome. The juxtaposition of the strong 3'IgH enhancer and a proto-oncogene leads to overexpression of the proto-oncogene, which confers malignant properties to the plasma cell. Therefore, we proposed that inhibiting the activity of the 3'IgH enhancers would be a potential therapeutic strategy for translocation-positive myeloma. Since the activity of the 3'IgH enhancer is dependent upon binding by a variety of transcription factors, these transcription factors are potential therapeutic targets. Oct2 and Bob1 have both been shown to mediate 3'IgH enhancer activity through binding to the conserved octamer site, ATGCAAAT. Importantly, the expression of these two proteins is primarily restricted to B lineage cells. Therefore, if these proteins were targeted therapeutically in myeloma patients, few side effects would be expected.

A similar approach has been studied as a potential therapeutic strategy for follicular lymphoma (124). Follicular lymphoma is a B cell malignancy, which often has a t(14;18) translocation. This translocation juxtaposes the IgH enhancers on 14q32 with the anti-apoptotic gene *bcl-2* on 18q21, which results in overexpression of bcl-2 and resistance to apoptosis. Knockdown of Oct1, Oct2 or Bob1 proteins using RNAi led to decreased expression of bcl-2 and increased apoptosis in t(14;18) follicular lymphoma cell lines, due to decreased activity of the IgH enhancer. Decreased bcl-2 mRNA expression was most pronounced when either Oct2 or Bob1 expression was inhibited (124). Therefore, based on the results of this experiment, the primarily B cell-restricted expression of Oct2 and Bob1, and the ability of Oct2 and Bob1 to activate the 3'IgH enhancer, we

propose that inhibiting Oct2 and Bob1 is a potential therapeutic strategy for translocation-positive myeloma.

1.4 Oct2 and Bob1 transcription factors

1.4.1 Identification of Oct2 and Bob1

The conserved octamer DNA sequence ATGCAAAT is present in the IgH and IgL variable region promoters and the intronic and 3'IgH enhancers, and thus was thought to regulate tissue-specific expression of immunoglobulin genes. However, the octamer sequence is also present in the promoters of ubiquitously expressed H2B and U2 and U6 small nuclear RNA genes (125). Therefore, this sequence is not the only regulatory factor necessary for B cell-restricted immunoglobulin expression.

The octamer binding proteins Oct1 and Oct2 bind to the conserved octamer site in immunoglobulin genes to activate transcription (126, 127). Oct1 is ubiquitously expressed, whereas Oct2 expression is mainly restricted to B cells (126, 127). It was thought that since Oct2 is B cell-restricted, it restricted the expression of immunoglobulin genes to B cells; however, Oct2 alone is not sufficient for B cell-restricted expression of immunoglobulin genes. Several B cell lines that express little or no Oct2 are able to maintain high levels of immunoglobulin gene transcription (128). Additionally, Oct1 and Oct2 bind to the octamer element with equal affinity and are both able to stimulate transcription from the H2B and the immunoglobulin promoter (129). When Oct1 and Oct2 were added to octamer factor-depleted B cell extracts, they were both able to

enhance activity of an immunoglobulin promoter. However, when Oct1 and Oct2 were added to non-B cell (HeLa) extracts depleted of octamer factors, they were unable to restore transcriptional activity of the promoter. These results demonstrated the presence of a second B cell-restricted transcription factor necessary for full activation of immunoglobulin promoters (129).

Three groups independently identified the B cell-specific protein Bob1/OTF-1/OCA-B (referred to as Bob1 here), which binds to Oct1 and Oct2, and regulates immunoglobulin promoter activity (130-132). The interaction between Oct1 or Oct2 and Bob1 is necessary for Bob1 activity, as Bob1 cannot bind to the octamer motif in the absence of octamer binding factors, nor can it bind to mutant octamer sites (130). Cotransfection of an IgL variable region promoter reporter construct and Bob1 into HeLa cells significantly enhanced transcriptional activity of the promoter, through contacts with Oct1, whereas addition of Oct2 only slightly increased promoter activity (132). Thus, in addition to Oct2, Bob1 is required for immunoglobulin promoter activity.

1.4.2 Structure, expression patterns and interaction of Oct2 and Bob1

Oct2 is a member of the POU-domain family of transcription factors. These proteins share a central bipartite DNA binding domain, which is composed of a 75-80 amino acid N-terminal POU-specific domain, a short linker region, and a 60 amino acid C-terminal POU homeodomain (133). The POU homeodomains of Oct2 and Oct1 are 88% homologous, while the POU-specific domains of these two proteins are 99% homologous (133). Multiple, conserved Oct2 splice

isoforms have been identified in mouse and human B cells (134). These splice variants all retain the POU-domain important for DNA binding. Oct2.1 (Oct2A) is the dominant isoform expressed in B cells, and this transcript encodes a 464 amino acid, 57 kDa protein (134). The N-terminus of Oct2 is glutamine rich, while the C-terminus contains many serine, threonine and proline residues. The N- and C-termini of Oct2 are not homologous to Oct1 (133). Deletion experiments have demonstrated that the activity of Oct2 in B cells is dependent on its C-terminal domain (135, 136).

Oct2 is expressed primarily in B cells, and has been detected at all stages of B cell development, including pre-B cells, mature B cells and plasma cells. Oct2 expression is lowest in early stage B cells, and becomes highly expressed in response to antigenic stimulation in mature B cells (127). Additionally, Oct2 is expressed in myeloma cell lines and patient samples (137). Oct2 expression is not limited to B cells though, as it is also expressed in the developing nervous system and the adult brain (138). However, the splice variants expressed in B cells and neuronal cells differ (134). Oct2 has been detected in T lymphocytes, myeloid cells and erythroid cells, but in these lineages Oct2 expression has not been detected in all cell lines tested, and is lower than in B lineage cells (139, 140).

Bob1 is a 256 amino acid protein, which is rich in proline, serine and threonine residues (141). Two isoforms of Bob1 are generated through the use of different translation initiation sites. The 34 kDa isoform (p34) localizes to the nucleus, while the 35 kDa isoform (p35) is cytosolic (142). The C-terminal domain, specifically amino acids 65-122, is necessary for Bob1 transactivation

activity (143). Expression of Bob1 is primarily restricted to B lineage cells (130-132). During B cell development, Bob1 is expressed at low levels in pre-B cells and high levels in GC B cells and plasma cells (144-146). Bob1 is also detectable in activated T cell populations and in T cell lymphomas (146, 147).

The ability of Bob1 and Oct2 to activate immunoglobulin promoters is dependent on complex formation at the DNA octamer motif (141). Both Oct1 and Oct2 are able to recruit Bob1 to the octamer sequence in the immunoglobulin locus. Bob1 binds to Oct1 and Oct2 with high affinity, but does not bind to any other POU-domain proteins (143). Since the POU-specific domains of Oct1 and Oct2 are nearly identical, and are not shared with other POU-domain proteins, Bob1 was suspected to bind to this region. In fact, Bob1 has been shown to interact specifically with the POU-specific domain of Oct1 in purified crystals (148), and with the POU-specific region of Oct2 (149). The N-terminus of Bob1 is required for interaction with the POU-specific domain of Oct1 and Oct2 (143). This region of Bob1 also makes contacts with the POU homeodomains of Oct1 and Oct2, as well as the major groove of the octamer DNA motif. The adenine base at position 5 of ATGCAAAT is particularly important for binding (148, 149). Therefore, both protein-protein and protein-DNA interactions are important for the complex formation of Bob1, Oct2 (or Oct1) and the DNA octamer motif.

1.4.3 Oct2 and Bob1 are required for B cell development

Since Oct2 is a B cell-specific transcription factor known to bind to and activate immunoglobulin promoters and enhancers, numerous studies have aimed

to elucidate the role of Oct2 in B cell development. The Oct2 alleles in mouse embryonic stem cells (ES) have been deleted or disrupted to examine B cell development in the absence of Oct2. $Oct2^{-/-}$ mice die shortly after birth, due to unknown causes (150). Therefore, the role of Oct2 in B cell development has been examined in fetal B cells, B cells from $Oct2^{-/-}$ mice grown *in vitro*, and in chimeric mice with $Oct2^{-/-}$ reconstituted fetal liver cells.

Although Oct2 is expressed throughout B cell development, it is dispensable for early stages of B cell ontogenesis that occur in the bone marrow (150, 151). Mice that lack Oct2 have normal numbers of pro-B, pre-B and immature B cells in the bone marrow (151). Transcription and rearrangement of immunoglobulin genes in early B cells is unaffected in mice lacking Oct2 (150). However, many aberrations are apparent in late stage $Oct2^{-/-}$ B cells. Oct2-deficient mice have a complete absence of peritoneal B-1 cells (152) and Oct2 is required for activation of B cells in response to certain antigens. Although $Oct2^{-/-}$ B cells respond normally to CD40L and IL-4, they are not activated by anti-IgM and lipopolysaccharide (LPS), suggesting that Oct2 is required for signaling directly through the B cell receptor (BCR) (135, 150, 151). Furthermore, Oct2-deficient B cells express reduced levels of IgG1 and IgG3 isotypes in response to antigenic stimulation and do not form GCs (151).

The expression of Bob1 during B cell development is highest in pre-B cells and in GC B cells. Through studies of $Bob1^{-/-}$ mice, Bob1 has been found to play a role in both early and late stages of B cell development. Mice that lack Bob1 have normal numbers of pro-B and pre-B cells; however, $Bob1^{-/-}$ mice have

reduced numbers of immature B cells (153). This could be explained by the fact that Bob1, in conjunction with the zinc-finger transcription factor Aiolos, is important for downregulation of the surrogate light chain genes VpreB and λ5, which is necessary for differentiation of pre-B cells to immature B cells (154). $Bob1^{-/-}$ mice have reduced numbers of mature B cells in the bone marrow and in peripheral sites, and an absence of marginal zone B cells in the spleen (153, 155-157). It has been shown that Bob1 is upregulated in response to anti-IgM, CD40L and IL-4 signaling, which suggests that Bob1 is required for both T cell-independent (TI) and T cell-dependent (TD) stimulation (144). In line with this, mice that are deficient of Bob1 fail to form GCs upon antigenic stimulation and exhibit reduced levels of all secondary antibody isotypes (151, 155, 156, 158). $Bob1^{-/-}$ mice also have reduced numbers of fully differentiated $CD138^{+}$ plasma cells (159).

Aberrations in B cell development are observed in the absence of both Oct2 and Bob1. To explain these phenotypes, many groups sought to find target genes of Oct2 and Bob1. Mice that lack either Oct2 or Bob1 both have reduced levels of secondary antibody isotypes. Studies have shown that Oct2 and Bob1 are both required for the expression of genes that are important for the differentiation of plasma cells. IL-5 enhances terminal differentiation of plasma cells by upregulating Blimp-1, and Oct2 is required for expression of the IL-5 receptor in B cells (160). Similarly, Blimp-1 expression has been shown to be upregulated by Bob1 (159).

Mice that lack either Oct2 or Bob1 do not fully respond to signaling through the BCR. Many genes that are known to be important for BCR signaling have been shown to be direct targets of Oct2 and Bob1. Btk is a tyrosine kinase that is important for pre-B to immature B cell differentiation, formation of the B-1 compartment, and also BCR signaling (161). The promoter of Btk contains an imperfect octamer site that is activated by the binding of Oct2 and Bob1 (161), which partly explains why mice lacking Oct2 and Bob1 do not respond to BCR signaling. Also, *mb-1* and *B29*, the genes that encode Igα and Igβ, respectively, contain octamer motifs. Oct2 and Bob1 directly bind to these promoters and are necessary for transcription of these genes (162, 163). Since Igα and Igβ are components of the BCR, deficient BCR signaling in $Oct2^{-/-}$ and $Bob1^{-/-}$ mice could be caused by reduced expression of Igα and Igβ. Furthermore, Bob1 binds the promoter of the Ets family transcription factor Spi-B and enhances its expression. Spi-B has been implicated in downstream BCR signaling pathways, which also explains deficient BCR signaling in $Bob1^{-/-}$ mice (164).

The chemokine receptor *blr1* possesses an imperfect octamer site in its promoter. Both Oct2 and Bob1 bind the *blr1* promoter and activate transcription of this gene. The *blr1* gene encodes the chemokine receptor CXCR5, which is implicated in migration of B cells from the bone marrow to the periphery, and in the formation of GCs (165). Thus, the lack of peripheral B cells and GCs in $Oct2^{-/-}$ and $Bob1^{-/-}$ mice is likely mediated by deficient CXCR5 expression.

1.4.4 Regulation of Oct2 and Bob1

Oct2 expression is primarily restricted to B lineage cells, and the activity of Oct2 is important for many stages of B cell ontogenesis. Thus, it follows that the upstream regulatory mechanisms of Oct2 expression and activity are important for its function in B cell development. In response to LPS stimulation of pre-B cells, increased Oct2 transcript expression and DNA binding activity are observed (166). However, when NF-κB activity is inhibited, LPS stimulation fails to increase Oct2 expression and activity (167). Similarly, stimulation of CD86 (formerly known as B7-2) on activated B cells leads to increased expression of Oct2 mRNA and protein, and increased binding of Oct2 to the hs1,2 and hs4 3'IgH enhancer elements (168). CD86 is a co-stimulatory molecule on B cells that is upregulated in response to stimulation of the BCR, CD40, IL-4R and the LPS-receptor. Like LPS stimulation, the effect CD86 stimulation has on Oct2 expression is mediated by NF-κB. In the absence of NF-κB, CD86 stimulation does not increase Oct2 transcription or binding to the 3'IgH enhancers (168). Furthermore, inhibition of protein kinase C (PKC) abrogates Oct2 expression in response to CD86 (168).

Phosphorylation of Oct2 has been shown to be important for its DNA binding activity. The active form of Oct2 that acts as a transcriptional activator is phosphorylated (169). Specifically, T302 and S303 in the POU homeodomain of Oct2 are phosphorylated in response to LPS stimulation, and this phosphorylation is dependent on PKC (123). Phosphorylation of Oct2 at T302 and S303 is critical for binding to the 3'IgH enhancer element (123). Taken together, these results

demonstrate that mitogenic stimulation, mediated by NF-κB and PKC, can induce Oct2 expression and activation. Additionally, phosphorylation of Oct2 by PKC at specific serine and threonine residues is necessary for the DNA binding activity of Oct2.

Like Oct2, Bob1 expression can be induced by mitogenic stimulation. Stimulation with LPS and co-stimulation with CD40L and IL-4 increase Bob1 expression in B cells (144). Binding of the neurotransmitter norepinephrine to the β_2-adrenergic receptor (β_2AR) on B cells also leads to increased Bob1 protein expression and binding to the hs1,2 and hs4 3'IgH enhancer regions (168). Increased transcription and DNA binding of Bob1 in response to β_2AR stimulation is mediated through the protein kinase A (PKA) pathway (168). PKA activates CREB, which binds to the Bob1 proximal promoter and activates transcription of Bob1 (170). In addition to CREB, the lymphoid-specific transcription factor EBF1 is capable of binding the Bob1 proximal promoter and activating Bob1 transcription (171). Furthermore, distal elements in the Bob1 promoter are important for regulating B cell-restricted expression of Bob1, although specific protein binding sites in this region have not been identified (172).

The expression and activity of Bob1 are also dependent on post-translational modifications. Phosphorylation of S184 is necessary for Bob1 activity, as mutation of this residue abolishes the transactivation function of Bob1 in B cells (147). Siah-1, which is a RING finger protein capable of targeting proteins for degradation, has been shown to be a negative regulator of Bob1

(173). Siah-1 interacts with the N-terminus of Bob1, which leads to decreased Bob1 protein levels, but stable Bob1 mRNA expression. Since inhibition of the proteasome degradation pathway maintains Bob1 expression, Siah-1 likely targets Bob1 for ubiquitylation and proteasome-mediated degradation (173).

1.5 Hypothesis and experimental aims

Multiple, recurrent translocations occur in myeloma, which result in the dysregulation of a variety of oncogenes due to linkage with the Eμ and, most frequently, the 3'IgH enhancers. The B cell-restricted transcription factors Oct2 and Bob1 are necessary for the activity of these IgH enhancers. We therefore hypothesized that (1) Oct2 and Bob1 are good therapeutic targets in translocation-positive myeloma, (2) inhibition of Oct2 and/or Bob1 activity would lead to decreased expression of translocated oncogenes in myeloma, and (3) decreased expression of translocated oncogenes following Oct2 and/or Bob1 inhibition would lead to reduced cell viability and increased apoptosis in translocation-positive myeloma.

To test our hypotheses, our experimental aims were (1) to examine the expression and prognostic significance of Oct2 and Bob1 in myeloma patient samples, (2) to determine whether inhibition of Oct2 and Bob1 leads to decreased expression of FGFR3 in t(4;14) myeloma cell lines, and (3) to measure the anti-proliferative and pro-apoptotic effects of this approach in t(4;14) myeloma cell lines.

2 Materials and Methods

2.1 Primary patient sample analyses

2.1.1 Purification of patient bone marrow cells

Heparinized bone marrow aspirates from the time of diagnosis were obtained with patient consent and in accordance with the regulations of our local research ethics board and the Declaration of Helsinki. The samples were passed through a mesh, and bone marrow mononuclear cells were separated by density gradient centrifugation using Ficoll (GE Healthcare, Piscataway, NJ).

2.1.2 CD138 sorting of patient bone marrow mononuclear cells

To separate plasma cells from other bone marrow mononuclear cells, cells were sorted based on CD138 expression, which is a marker of plasma cells. Approximately 20-100 x 10^6 cells were suspended in Automated magnetic cell sorting (MACS) running buffer (Miltenyi Biotec, Auburn, CA) at 100 x 10^6 cells/mL. To this, 2 μL/10^6 cells of mouse magnetic microbead-coupled anti-CD138 (Miltenyi Biotec) was added and incubated at 4^{o}C for 15 minutes. Cells were washed and resuspended in 600 μL MACS running buffer and sorted using an autoMACS magnetic activated cell sorter (Miltenyi Biotec) based on CD138 expression. The $CD138^+$ and $CD138^-$ cell populations were resuspended in TRIZOL® reagent (Invitrogen) for RNA extraction and archived at -80^{o}C.

2.1.3 Tissue microarray patient inclusion criteria

All patients included in this retrospective study were diagnosed with multiple myeloma, as defined by the International Myeloma Working Group (IMWG) (1), and had undergone pre-treatment diagnostic bone marrow biopsies. These bone marrow biopsies were decalcified using EDTA, fixed in 10% formalin and embedded in paraffin. Patients included in this study from the Cross Cancer Institute (CCI) in Edmonton, AB were diagnosed between 2001 and 2008. Samples from the Tom Baker Cancer Centre (TBCC) in Calgary, AB were collected between 1993 and 2008. In total, 138 patient samples from Edmonton and 82 samples from Calgary were included in the tissue microarray (TMA) blocks. Of note, all patients from Calgary selected for this study received an ASCT. Patients provided written, informed consent for their biopsies and clinical data, including diagnosis, demographics, baseline features, treatment regimen, treatment response, progression, and survival, to be used for research purposes. This study complied with the regulations of our local research ethics boards and the Declaration of Helsinki. Of note, 19 patients (section 2.1.1) with mRNA data were included in the TMA.

2.1.4 Tissue microarray construction

Paraffin embedded bone marrow biopsies were retrieved from archives and compared with hematoxylin and eosin (H&E) stained sections of the retrieved specimen to identify areas of malignant plasma cells. The location of malignant plasma cells was marked and three 0.6 mm diameter cores were obtained from

each block. Triplicate cores were then placed into a TMA paraffin block along with other patient cores. Each TMA included three control spleen or tonsil samples from healthy patients. TMA blocks were cut into 0.4 μm sections, mounted on slides and stored at 4^{o}C or room temperature until further use.

2.1.5 Fluorescent immunohistochemistry

Fluorescent immunohistochemistry (IHC) allows for visualization of two proteins simultaneously in the same tissue section. It couples the use of a directly conjugated Cy3 fluorescent secondary antibody raised in mouse with a horseradish peroxidase (HRP)-labeled secondary antibody raised in rabbit. The HRP molecule can then be utilized for deposition of a Cy5 fluorophore.

Slides were baked at 60^{o}C for 45 minutes, deparaffinized in xylene, and rehydrated through an ethanol series. Antigen retrieval was carried out at 95^{o}C for 40 minutes in target retrieval solution (pH 6.0) (Dako). Endogenous peroxidase activity was quenched using peroxidase block from the EnVision TM + System (Dako) for 8 minutes. To reduce non-specific binding, the slides were blocked with cytomation protein serum-free block (Dako) for 30 minutes. TMA slides were then incubated at room temperature overnight in a humidified chamber with 1:1000 rabbit anti-Bob1 (sc-955, Santa Cruz) and 1:150 mouse anti-CD138 (Serotec, Raleigh, NC) or 1:2500 rabbit anti-Oct2 (sc-233, Santa Cruz) and 1:150 mouse anti-CD138 (Serotec). Following incubation, slides were washed 3 x 3 minutes in wash buffer (Dako), and incubated for 1 hr at room temperature in a dark, humidified chamber with 1:200 goat anti-mouse Alexa fluor 555 (Invitrogen

probes) diluted in labeled polymer-HRP anti-rabbit (Dako). With this system, the Alexa fluor 555-coupled secondary antibody binds to the CD138 antibody, and the HRP-labeled polymer coupled to anti-rabbit binds to the target protein. The slides were then washed 3 x 3 minutes in wash buffer, and incubated with 1:50 TSA-Plus Cy5 tyramide signal amplification reagent (PerkinElmer, Waltham, MA) for 10 minutes at room temperature in the dark. The TSA system deposits Cy5 fluorophore-labeled tyramide amplification reagent adjacent to the HRP molecule of the HRP-conjugated secondary antibody. The slides were washed as described previously, and a coverslip was mounted on the slide with Vectashield anti-fade mounting medium containing DAPI (Vector Laboratories, Burlingame, CA). The coverslip was sealed with nail polish and slides were stored at 4^{o}C until analysis.

2.1.6 Calculation of AQUA scores

Automated image acquisition on slides from 2.1.5 was performed using the HistoRx PM-2000 platform^{TM} and Image Grabber software (HistoRx New Haven, CT), which has previously been described (174). Briefly, an 8-bit monochromatic image (generating 256 individual intensity values per pixel) was taken for each histospot on the TMA using a DAPI filter, a Cy3 filter (CD138) and a Cy5 filter (target). Pixels were written to image files as a function of power (Power (P) = ((Pixel Intensity/256)/ exposure time)) in order to help compensate for experimental variations in staining intensity. The images were then analyzed using AQUA 1.6 software (HistoRx). To identify the CD138^{+} cell compartment

and generate a tumour mask, the PLACE (pixel-based locale assignment for compartmentalization of expression) and RESA (rapid exponential subtraction algorithm) algorithms were used, which are described in detail elsewhere (174). A threshold value of Cy3 expression was set to remove background expression, and a tumour compartment was generated that only included $CD138^+$ plasma cells. Histospots that contained <2% plasma cells were excluded from the analysis. Target protein pixels from the Cy5 channel that did not appear within the tumour compartment were excluded. Target protein pixels within the tumour mask were measured to generate an AQUA (automated quantitative analysis) score, which is equal to the intensity of target pixels within the compartment divided by the total compartment area. Average Bob1 and Oct2 AQUA scores for each patient were calculated based on 1-3 usable histospots.

2.1.7 Diaminobenzidine Immunohistochemistry

Diaminobenzidine (DAB) IHC allows for detection of one target protein on one slide. It uses a biotinylated secondary antibody, which is bound by HRP-streptavidin, and then reacted with DAB to form a brown precipitate at the site of the target protein.

TMA slides were baked for 2 hours at 60ºC, deparaffinized in xylene and rehydrated through an ethanol series. Antigen retrieval of Bob 1 was done using High pH Retrieval Solution (pH 9.9) (Dako, Mississauga, ON) in the Milestone RHS-2 histoprocessor. Antigen retrieval of Oct2 was done by heating in a pressure cooker for 20 minutes and cooling, followed by an additional 20 minutes

in 10 mM citrate buffer (pH 6.0). Antigen retrieval of CD138 was done by heating the slides in a 1.0 mM EDTA pH 8.0 solution. Peroxidase blocking and staining was performed using a Dako autostainer. Separate TMA slides were incubated with 1:900 Bob1 (sc-955, Santa Cruz), 1:2600 Oct2 (sc-233, Santa Cruz), or 1:25 CD138 (Santa Cruz) primary antibodies. Immunodetection was performed with the LSAB + Visualization system (Dako) and slides were counterstained with hematoxylin.

2.1.8 Calculation of H-scores

Bob1 and Oct2 DAB IHC staining was measured by two independent observers, who are not trained pathologists. Briefly, a slide stained for CD138 was examined and the regions of $CD138^+$ plasma cells were located. On an adjacent slide, stained for either Bob1 or Oct2, the proportion and intensity of CD138 cells that stained positively for the target protein was recorded. Negative cells received a score of 1, weak staining cells received a score of 2, and strong staining cells received a score of 3. The percentage of plasma cells receiving each score was noted, and the product of the percentage of cells multiplied by the staining intensity for each of the three intensities possible were added together to generate an H-score. For example, if 50% of plasma cells were negative for Bob1, 25% stained weakly for Bob1 and 25% stained strongly for Bob1, the H-score would be 175, calculated as follows:

$$(50x1) + (25x2) + (25x3) = 175$$

The H-scores calculated by both observers for each sample were compared, and any discrepancies larger than 20% were resolved. An average H-score for each patient was then calculated based on 1-3 replicate samples, each of which was scored twice.

2.2 Cell lines and cell culture

Multiple myeloma cell lines used in this work include KMS11 and KMS18 (gift of T. Otsuki, Kawasaki Medical School, Kurishiki, Japan) LP-1 and U266 (gift of S. Treon, Dana-Farber Cancer Institute, Boston, MA) and JIM3 (gift of L. Bergsagel, Mayo Clinic, Scottsdale, AZ). These cell lines were maintained in RPMI 1640 medium supplemented with 10% fetal bovine serum, 100 U/mL penicillin and 100 μg/mL streptomycin. Of note, KMS11, KMS18, LP-1 and JIM3 possess t(4;14) translocations. All myeloma cell lines were grown in suspension, excluding KMS11, which is adherent. HEK293T cells (gift of R. Godbout, Cross Cancer Institute, Edmonton, AB) were grown in DMEM medium supplemented with 10% fetal bovine serum, 100 U/mL penicillin and 100 μg/mL streptomycin. All cell lines were incubated at 37^{o}C with 5% CO_2.

2.3 RNA extraction and cDNA synthesis

Approximately 0.25-1.0 x 10^6 cells were collected and washed with 1x PBS. Total RNA was extracted from cells using TRIZOL® Reagent (Invitrogen) as per the manufacturer's protocol. Total RNA concentration was determined by

measuring the A_{260} of a 1 μL aliquot of the RNA solution using a NanoDrop® ND-1000 spectrophotometer (NanoDrop Technologies, Wilmington, DE). To synthesize cDNA, SuperScript™ II Reverse Transcriptase (Invitrogen) was used as per the manufacturer's instructions with 2.5 ng/μL random hexamers (Invitrogen) and 500 μM deoxynucleoside triphosphate (Invitrogen). A 20 μL reaction containing 1 μg of total RNA was reverse transcribed, yielding a final cDNA concentration of 50 ng/μL.

2.4 Quantitative real-time PCR

TaqMan® quantitative real-time polymerase chain reaction (qRT-PCR) and ΔΔCt relative quantification analysis were used to determine mRNA expression of Bob1, Oct2 and FGFR3. All reagents and equipment are from Applied Biosystems, Branchburg, NJ. For each sample, 10 μL reactions were setup, in triplicate, for the target gene and the GAPDH internal control. Each 10 μL reaction contained 10 ng diluted cDNA, 0.5 μL of the respective 20x TaqMan® gene expression primer/probe assay, 5 μL 2x universal PCR master mix, and water (Sigma, St. Louis, MO, USA). A negative control without cDNA was also included to ensure no contamination was present. TaqMan® gene expression primer/probe assays used were Bob1 (Hs00174811_m1), Oct2 (Hs00231269_m1), FGFR3 (Hs00179829_m1) and GAPDH (Hs99999905_m1). The reactions were set up in a fast optical 96-well reaction plate, covered with clear adhesive film, and centrifuged at 1000 rpm for 2 minutes. qRT-PCR was performed using the 7900 HT Fast Real-Time PCR system and SDS 2.3 software

with the following PCR conditions: 50°C for 2 minutes, 95°C for 10 minutes, and 40 cycles of 95°C for 10 seconds then 60°C for 1 minute.

Analysis was performed using SDS RQ Manager 1.2 software and ΔΔCt relative quantification. Briefly, a threshold fluorescence value above background levels was set and the cycle threshold (Ct), which is the cycle at which the fluorescence within a sample crosses the threshold value, was determined. The average Ct value of the triplicates in each sample was calculated for both the target gene and the GAPDH internal control, and the GAPDH Ct was subtracted from the target gene Ct (ΔCt). To compare relative levels of cDNA expression between samples, the difference between the ΔCt values was calculated (ΔΔCt), and to account for the doubling of PCR product each cycle, was made a negative exponent of 2 ($2^{-\Delta\Delta Ct}$).

2.5 Western blotting and antibodies

To analyze protein expression, 0.25-1.0 x 10^6 cells were collected, washed in cold 1x PBS, and whole cell extracts were obtained by adding 100 - 300 μL radio immunoprecipitation assay buffer (150 mM NaCl, 1.0% IGEPAL® CA-630/NP-40, 0.5% sodium deoxycholate, 0.1% SDS, 50 mM Tris, pH 8.0, Sigma Aldrich, St. Louis, MO) containing complete protease inhibitor cocktail (Pancreas extract, Pronase, Thermolysin, Chymotrypsin, Papain, Roche Applied Science, Indianapolis, IN) to the cells, on ice. Samples were then centrifuged at 12 000 rpm for 10 minutes at 4°C and the supernatant was collected. Protein concentrations were determined using the DC protein assay (Bio-Rad, Hercules,

CA), as per the manufacturer's instructions. A total of 15 - 30 μg of protein was separated on 10% SDS-PAGE gels and transferred to nitrocellulose membranes (Bio-rad). The membrane was stained with Ponceau S (Sigma Aldrich) to verify equal loading. Membranes were blocked in 5% milk 0.05% Tween 1x PBS for 1 hour at room temperature. Primary antibodies were diluted in 1% milk 0.05% Tween 1x PBS and incubated as follows: 1:1000 rabbit anti-Bob1 (sc-955, Santa Cruz Biotechnology, Santa Cruz, CA) for 1 hour at room temperature, 1:500 rabbit anti-Oct2 (sc-25400, Santa Cruz) for 1.5 hours at room temperature, 1:500 rabbit anti-FGFR3 (sc-9007, Santa Cruz) for 16 hours at 4^{o}C and 1:10 000 mouse anti-α-tubulin (clone B512, Sigma Aldrich) for 1 hour at room temperature. The blots were washed 3 x 5 minutes in 0.05% Tween 1x PBS and 1 x 5 minutes in 1x PBS. The membranes were then incubated with secondary antibodies diluted to 1:10 000 in 1% milk 0.05% Tween 1x PBS for 1 hour at room temperature. Odyssey® infrared imaging goat anti-rabbit IR Dye® 800 and goat anti-mouse IR Dye® 800 (Li-Cor Biosciences, Lincoln, NE) secondary antibodies were used. Membranes were then washed as following primary antibody incubation. The fluorescent signal was detected and analyzed using Odyssey® infrared imaging system and Odyssey® 2.1 software (Li-Cor Biosciences).

2.6 siRNA transient transfections and viability assays

2.6.1 Transient transfection of KMS11 and KMS18

KMS11 cells were plated at a density of 0.25 x 10^6 cells/well in a 6-well plate (1.0 x 10^4 cells/well in a 96-well plate) in antibiotic-free medium and

incubated at 37°C for 24 hr. At the time of transfection, the medium was aspirated from the cells and 2 mL antibiotic-free medium was added (80 μL to the 96-well plate). For KMS18 cells, the cells were suspended in antibiotic-free medium at 0.125 x 10^6 cells/mL and 2 mL/well of the cell suspension was plated at the time of transfection. Lipofectamine™ 2000 cationic liposome based transfection reagent (Invitrogen, Carlsbad, CA) was diluted in Opti-MEM® reduced serum medium (Invitrogen) at a 1:50 ratio and incubated for 5 minutes at room temperature. The small interfering RNA (siRNA) sequences were diluted in Opti-MEM® medium, to yield a final concentration of 1 nM-200 nM. Equal parts of the Lipofectamine™ 2000 mix and siRNA mix were combined and incubated for 20 minutes at room temperature. 500 μL of the siRNA/liposome mix was added to each respective well (20 μL to the 96-well plate) and the plates were gently mixed and incubated at 37°C until the assay time point. A non-specific siRNA control was included in each experiment. As a control for transfection efficiency, cells were transfected with 25 nM FITC-labeled BLOCK-iT™ fluorescent oligo (Invitrogen), and analyzed 24 hr after transfection by flow cytometry (Figure 2.1) using a FACSort fluorescence activated cell sorter and Cell Quest Pro 5.2 software (Becton Dickinson, Franklin Lakes, NJ).

2.6.2 siRNA sequences

Dicer-substrate pre-designed siRNA sequences (Integrated DNA Technologies, Coralville, IA) targeting Bob1 were as follows:

Duplex 1 antisense: 5'-GCGGAGCUUCUUGUCGUGACAUUGGUG-3'

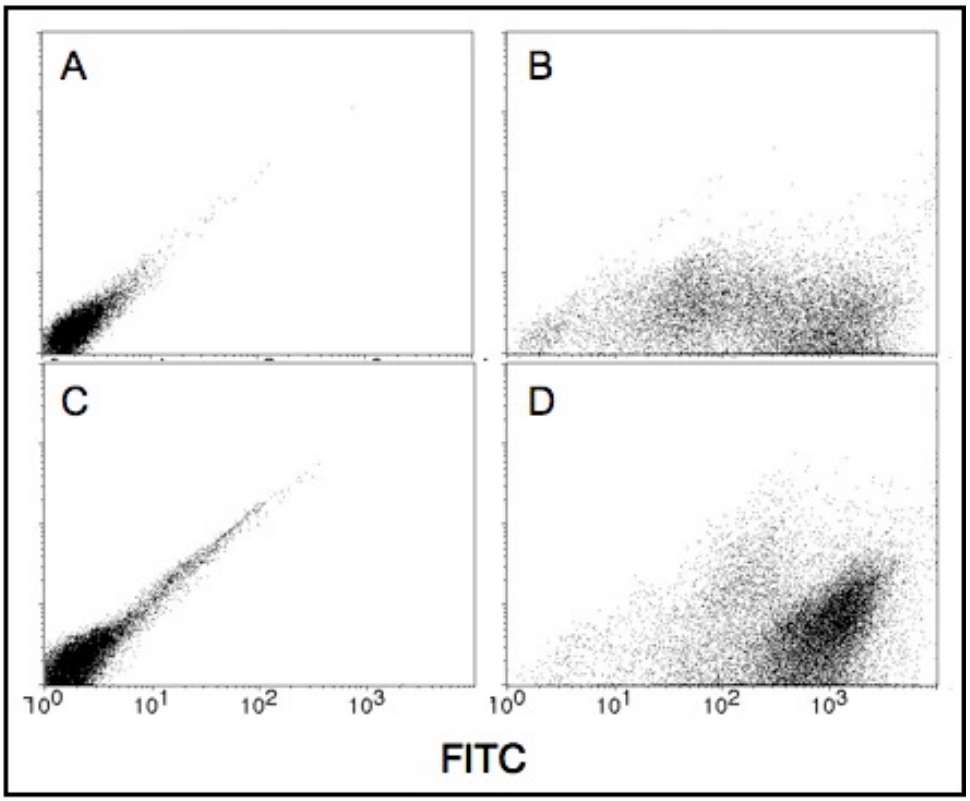

Figure 2.1. Lipid-based transfection efficiency in myeloma cell lines. The myeloma cell lines KMS11 and KMS18 were transfected with siRNA using Lipofectamine 2000, and the efficiency of this transfection was measured using a FITC-labeled siRNA control and flow cytometry. (A) KMS11 cells treated only with Lipofectamine 2000 do not fluoresce in the FITC channel. (B) 95% of KMS11 cells transfected with the FITC-siRNA are fluorescent, and thus transfected. (C) KMS18 cells treated with only Lipofectamine 2000 do not fluoresce. (D) KMS18 cells transfected with FITC-siRNA are 98% transfected.

Duplex 1 sense: 5’-CCAAUGUCACGACAAGAAGCUCCGC-3’

Duplex 2 antisense: 5’-ACAGGUCUACAAUUCUAGCUGUGCGUA-3’

Duplex 2 sense: 5’-CGCACAGCUAGAAUUGUAGACCUGT-3’

Duplex 3 antisense: 5’-AUAUGUCAAAGAAACUGUCAUUUCCCA-3’

Duplex 3 sense: 5’-GGAAAUGACAGUUUCUUUGACAUAT-3’

Dicer substrate pre-designed siRNA sequences (Integrated DNA Technologies) targeting Oct2 were as follows:

Dicer antisense: 5’-GAGGAUAAGGUAGUAACUGUUGUGCUC-3’

Dicer sense: 5’-GCACAACAGUUACUACCUUAUCCTC-3’

Pre-designed siRNA sequences (Ambion, Austin, TX) targeting Oct2 were as follows:

114257 antisense: 5’-GUAGCUGGAAUAGAUUUGGTG-3’

114257 sense: 5’-CCAAAUCUAUUCCAGCUACTT-3’

114258 antisense: 5’-AGACAUAGUCUCUGCAUCGTT-3’

114258 sense: 5’-CGAUGCAGAGACUAUGUCUTT-3’

6416 antisense: 5’-UUUGUCUCGAUGCUGGUCCTC-3’

6416 sense: 5’-GGACCAGCAUCGAGACAAATT-3’

6511 antisense: 5’-UUUCCUCCCUUGUCACUCCTG-3’

6511 sense: 5’-GGAGUGACAAGGGAGGAAATT-3’

6590 antisense: 5’-UUGUUUUUUUGGUCUUUCCTC-3’

6490 sense: 5’-GGAAAGACCAAAAAAACAATT-3’

The locations of the siRNA sequences on the respective mRNA molecules are shown schematically in Figure 2.2.

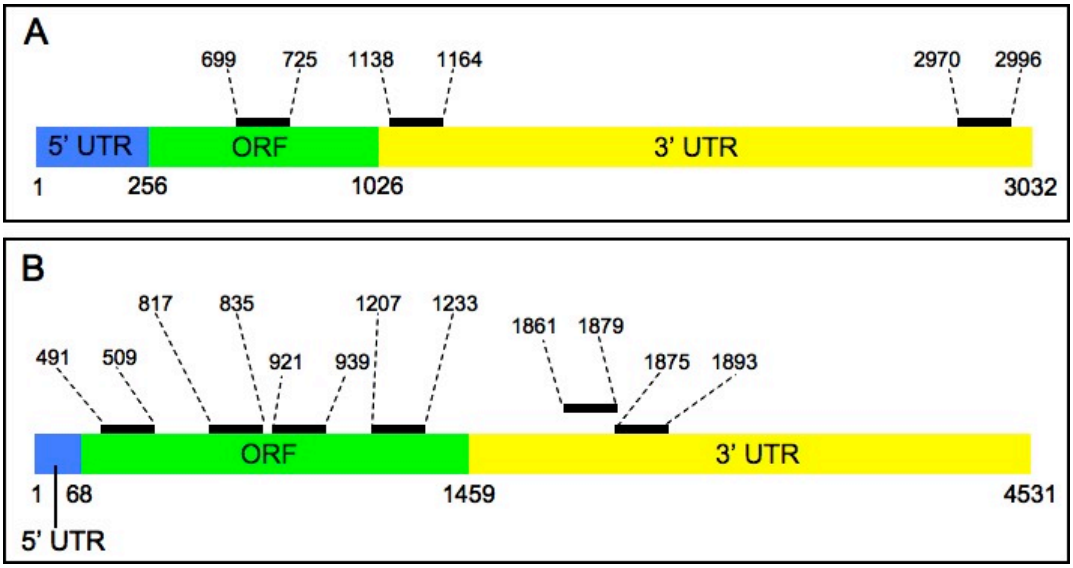

Figure 2.2. Bob1 and Oct2 mRNA schematic with siRNA locations. The mRNA sequences of Bob1 and Oct2 are shown with the 5' UTR in blue, the ORF in green and the 3' UTR in yellow. The numbers below the mRNA transcript represent the base pair of the beginning and end of the transcript, and the beginning and end of the ORF. Dotted lines and numbers correspond to the 5' and 3' ends of the siRNA molecule, which is shown as a black bar above the transcript. (A) Bob1 mRNA transcript with siRNA locations. Three dicer-substrate siRNA duplexes targeting Bob1 mRNA were tested: duplex 1 (699-725), duplex 2 (1138-1164) and duplex 3 (2970-2996). (B) Oct2 mRNA with siRNA locations. Five siRNA molecules and one dicer-substrate siRNA targeting Oct2 mRNA were tested: 114257 (491-509), 114258 (817-835), 6416 (921-939), 6511 (1861-1879), 6590 (1875-1893) and dicer (1207-1233). ORF: open reading frame; UTR: untranslated region. (mRNA sequences accessed from NCBI core nucleotide).

2.6.3 MTS assay

KMS11 cells were plated at a density of 1 x 10^4 cells/well in a 96-well tissue culture-treated plate and transfected with siRNA, as described above. Six replicates were included for each sample. At each assay time point, 20 μL of CellTiter 96® AQ_{ueous} One Solution Cell Proliferation Assay (MTS) (Promega Corporation, Madison, WI) was added to each well, and plates were incubated at 37°C for 2 hours. The A_{490} was measured using a Spectra MAX 190 microplate reader and SoftMax Pro software (Molecular Devices, Sunnyvale, CA). The average absorbance of each sample was calculated, and the relative viability was determined by dividing each average absorbance by the average absorbance of the medium-only control sample.

2.6.4 Annexin V-FITC/ Propidium iodide staining

KMS11 cells were plated at a density of 0.25 x 10^6 cells/well in a 6-well tissue culture-treated plate and transfected with siRNA, as described above. Medium, Lipofectamine™ 2000 and non-specific siRNA samples were included as controls. At assay time points, cells were trypsinized and washed twice in cold 1x PBS and resuspended at approximately 1 x 10^6 cells/mL in 1x binding buffer (10mM HEPES NaOH, pH 7.4, 140 mM NaCl, 2.5 mM $CaCl_2$). For each sample, 100 μL of cell suspension was transferred to four 5 mL polystyrene round-bottom tubes. For each sample, the following controls were included: unstained, Annexin V-FITC only and Propidium iodide only. To the test sample, 5 μL

Annexin V-FITC and 10 μL Propidium iodide (BD Pharmingen™, San Jose, CA) were added. The tubes were then incubated for 15 minutes in the dark at room temperature, 400 μL 1x binding buffer was added, and the samples were analyzed by flow cytometry with a FACSort fluorescence activated cell sorter and Cell Quest Pro 5.2 software (Becton Dickinson).

2.7 Inducible lentivirus system

2.7.1 Lentivirus vector cloning

An inducible Bob1 small hairpin RNA (shRNA) lentivirus plasmid was unavailable, so the shRNA insert was cloned from the constitutively active Bob1 pGIPZ plasmid (Open Biosystems) to the tetracycline inducible empty pTRIPZ plasmid (Open Biosystems) (Figure 2.3). Briefly, 7.5 μg of Bob1 pGIPZ DNA and 3 μg empty pTRIPZ DNA were digested with 40 U XhoI restriction enzyme (New England Biolabs, Ipswich, MA) and 40 U MluI restriction enzyme (Promega Corporation) in 100 μL reactions for 3 hr at 37°C, as per the enzyme protocols. Both restriction digest reactions were then separated on a 1% agarose gel. From the pGIPZ digest, the 345 bp shRNA insert was cut from the gel, and from the pTRIPZ digest, the 13 kb linear plasmid was cut from the gel. Both products were purified using a Qiaex II gel extraction kit (Qiagen, Mississauga, ON). Ligation reactions were set up as follows: 7.4 ng Bob1 insert, 250 ng cut pTRIPZ plasmid, 2 μL 10x ligase buffer, 0.5 μL T4 DNA ligase, and water to 20 μL, and incubated at room temperature for 2 hr. Transformations were done by adding 0.2 μL of the ligation mix to 100 μL prime plus chemically competent

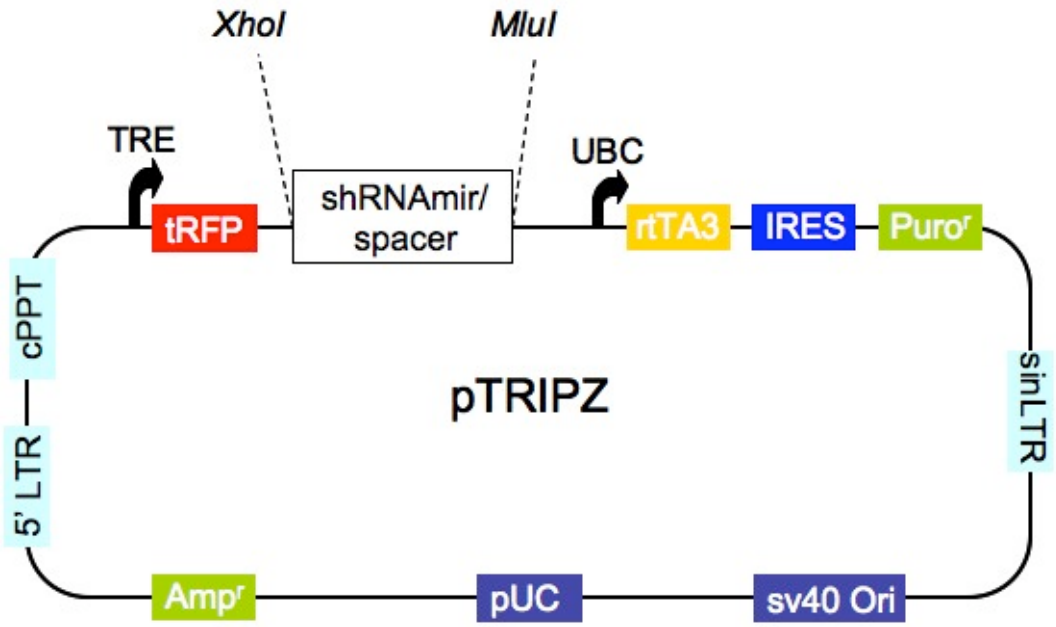

Figure 2.3. Map of the pTRIPZ lentiviral vector. The pTRIPZ lentiviral vector is a tetracycline-inducible shRNA expression system for stable transduction of mammalian cells. Different pTRIPZ plasmids are commercially available: an empty pTRIPZ plasmid for cloning has the pTRIPZ backbone, but does not contain an shRNA transcript, rather a non-specific DNA spacer sequence. The shRNAmir or spacer sequences are flanked by a unique 5' XhoI restriction site, and a unique 3' MluI restriction site, which allows cloning of an shRNA insert into the empty pTRIPZ vector. The vector is approximately 13 kb. TRE: tetracycline responsive RNA polymerase II promoter; tRFP: red fluorescent protein; UBC: UBC promoter; rtTA3: reverse tetracycline transactivator; IRES: internal ribosome entry site; Puro^r: mammalian puromycin selection marker; sinLTR: self-inactivating long terminal repeat; Amp^r: bacterial ampicillin selection marker; 5' LTR: 5' long terminal repeat; cPPT: central polypurine tract. (Figure adapted from manufacturer's protocol).

cells (Open Biosystems). The cells were incubated on ice for 30 minutes, heat shocked at 42^{o}C for 25 seconds, and incubated on ice for 2 minutes. 900 μL of SOC medium was added to the cells and incubated at 37^{o}C for 1.5 hr with shaking. 100 μL of the transformation mix was spread onto a 100 μg/mL ampicillin LB plate and incubated overnight at 37^{o}C. The following day, five colonies that grew were picked and restreaked on ampicillin LB plates and incubated overnight at 37^{o}C. From these colonies, plasmid DNA was purified and digested with either MluI and XhoI restriction enzymes or SalI (New England Biolabs) to confirm the presence of the Bob1 shRNA insert in the pTRIPZ plasmid. One clone was selected for subsequent experiments.

2.7.2 Lentivirus production

HEK293T cells were plated at a density of 3 x 10^{6} cells/ 10 cm plate and incubated until approximately 90% confluent. At the time of transfection, medium was aspirated and 10 mL of antibiotic-free medium was added to the cells. Transfection mixes containing 15 μg of psPAX2 packaging vector (Addgene, Cambridge, MA), 6 μg of pMD2.G envelope vector (Addgene) and 20 μg of the respective shRNA lentivirus vector (Open Biosystems, Huntsville, AL) were diluted in water to a final volume of 0.5 mL. Then, 0.5 mL of 2x HBS (HEPES NaOH buffered saline, pH 7.05) was added to the transfection mix, followed by 50 μL 2.5 M $CaCl_2$, and the transfection mix was incubated at room temperature for 20 minutes. The transfection mix was added, dropwise, to the cells, and the plates were incubated at 37^{o}C for 6 hr. At this point, the transfection medium was

removed and replaced with 10 mL of antibiotic-free medium, and the plates were incubated for 48 hr at 37°C. The supernatant containing the lentivirus particles was centrifuged at 2000 rpm for 10 minutes and filtered through a 0.22 μm sterile filter. The lentivirus was concentrated 100-fold by centrifugation at 26 000 rpm for 2 hr at 4°C and aliqoted and stored at -80°C until use (175).

2.7.3 Lentivirus transduction, stable selection and shRNA induction

KMS11 cells were plated at a density of 1 x 10^5 cells/well in a 24-well tissue culture treated plate in antibiotic-free medium the day prior to transduction. At the time of transduction, the medium was removed from the cells and 225 μL of RPMI 1640 with 0.05% Tet system approved FBS (Clontech, Mountain View, CA) medium was added to each well. A 25 μL aliquot of concentrated lentivirus was mixed with 2 μg polybrene (Sigma Aldrich) and incubated at room temperature for 5 minutes. The lentivirus was added to the cells and incubated at 37°C for 6 hr. Transduction medium was removed and replaced with 1 mL of RPMI 1640 with 10% Tet system approved FBS and incubated at 37°C for 48 hr. To select for stably transduced cells, 1 μg/mL puromycin medium was added. To assay for transduction efficiency following infection, or to induce shRNA expression in the stable pool, 2 μg/mL doxycycline was added to the cells. Using a fluorescence microscope, transduction efficiency was approximated by counting the proportion of cells expressing red fluorescent protein (RFP).

On the day of transduction, KMS18 cells were plated at a density of 1 x 10^5 cells/well in 225 μL of RPMI 1640 with 0.05% Tet system approved FBS in a

24-well non-treated plate. The transduction procedure followed that of KMS11, except when virus was added, the plate was centrifuged at 1800 rpm for 45 minutes at room temperature (176), and then incubated for 6 hr before the transduction medium was removed.

2.8 Statistics

Normality was assessed using the Shapiro-Wilk normality test. Paired $CD138^{+}/CD138^{-}$ patient sample means were compared using the Wilcoxan signed rank test. Viability differences were assessed using Student's t-test. Bob1 and Oct2 expression and clinical features were compared using Fisher's Exact test for two categorical variables, and Chi-square test for more than two variables. OS and PFS Kaplan-Meier curves were compared with the Log-rank test. Correlation of Bob1 and Oct2 expression was assessed with Spearman's rank correlation coefficient. All of these tests were performed using GraphPad Prism v.5 software (GraphPad Software, La Jolla, CA). To test the agreement of AQUA scores and H-scores, the kappa test was used. To adjust for known prognostic factors, a Cox regression proportional hazards model was used. Categorical variables included in this model were Bob1 or Oct2 above vs. below the median, transplant status, and ISS stage I vs. ISS stage II or III. To determine the interaction between Bob1 and Oct2, a Cox regression proportional hazards model with a Bob1 and Oct2 interaction term was used. The kappa test and multivariate Cox regression were performed with SPSS Statistics v.17.0 (SPSS, Chicago, IL). Statistical significance was set at $p<0.05$ using two-sided analysis.

3 Results

3.1 Expression of Bob1 and Oct2 in myeloma patient samples

The primary objective of this study was to analyze the potential of Bob1 and Oct2 as therapeutic targets in myeloma. To do this, the expression of Bob1 and Oct2 mRNA and protein was examined in malignant plasma cells that express CD138, which is a surface marker of plasma cells. The expression of these two putative therapeutic targets was also correlated with clinical features to determine their prognostic significance.

3.1.1 Expression of Bob1 and Oct2 mRNA in $CD138^+$ and $CD138^-$ patient samples

The relative gene expression of Bob1 and Oct2 in CD138-sorted myeloma patient samples was measured. Thirty-seven multiple myeloma patient samples had been sorted into $CD138^+$ and $CD138^-$ cell populations, and cDNA was generated for both cell populations from each patient. Using qRT-PCR, the relative gene expression of Bob1 and Oct2 in these patients was measured. As is shown in Figure 3.1, the $CD138^+$ samples express significantly higher levels of Bob1 mRNA than the $CD138^-$ cells ($p<0.0001$), and 37/37 (100%) patients assayed have higher Bob1 mRNA expression in the $CD138^+$ cells compared to the $CD138^-$ cells. Similarly, Figure 3.2 shows that the Oct2 mRNA expression in the $CD138^+$ samples of the 37 patients is significantly higher than the $CD138^-$ samples ($p<0.0001$). In this case, 32/37 (86%) patients have higher

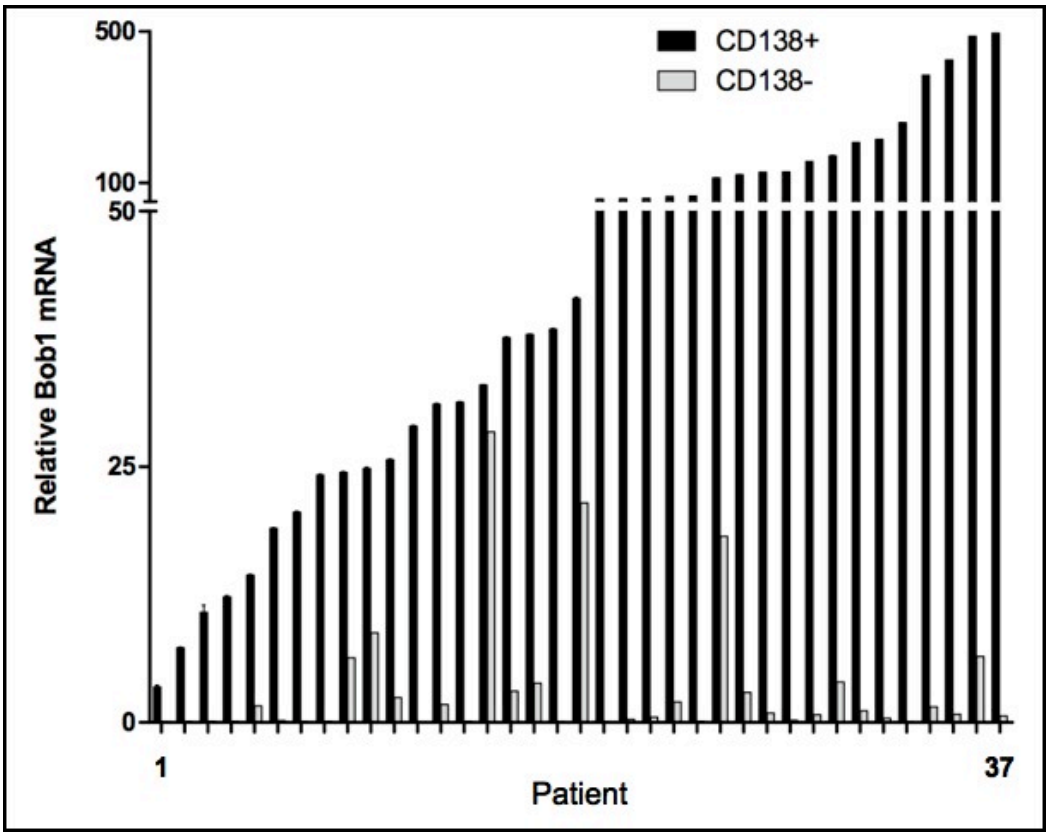

Figure 3.1. Relative Bob1 mRNA expression in CD138-sorted patient bone marrow samples. Patient bone marrow samples were MACS-sorted based on CD138 expression. Relative Bob1 mRNA expression in the $CD138^+$ and $CD138^-$ cell populations of each patient was measured by qRT-PCR. Values were normalized to KMS18, which was assigned a relative expression of 1, and plotted by ascending $CD138^+$ expression. The $CD138^+$ population has significantly higher Bob1 mRNA expression than the $CD138^-$ population ($p<0.0001$, $n=37$). Also, 37/37 patients have higher Bob1 mRNA expression in the $CD138^+$ fraction compared to the $CD138^-$ fraction. Error bars represent the standard deviation of triplicate qRT-PCR samples.

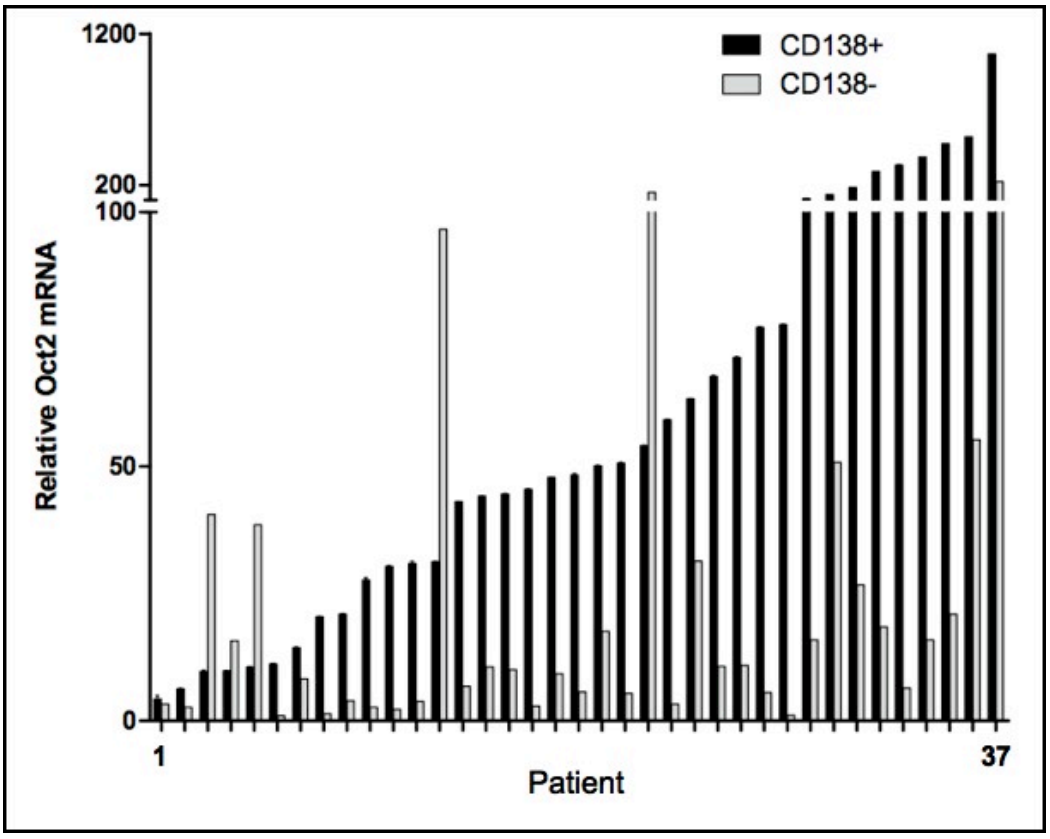

Figure 3.2. Relative Oct2 mRNA expression in CD138-sorted patient bone marrow samples. Patient bone marrow samples were MACS-sorted based on CD138 expression. Relative Oct2 mRNA expression in the $CD138^+$ and $CD138^-$ cell populations of each patient was measured by qRT-PCR. Values were normalized to KMS18, which was assigned a relative expression of 1, and plotted by increasing $CD138^+$ expression. The $CD138^+$ population has significantly higher Oct2 mRNA expression than the $CD138^-$ population ($p<0.0001$, $n=37$). Furthermore, 32/37 (86%) patients have higher Oct2 mRNA expression in the $CD138^+$ fraction as compared to the $CD138^-$ fraction. Error bars represent the standard deviation of triplicate qRT-PCR samples.

Oct2 mRNA expression in the $CD138^+$ compared to $CD138^-$ cells. To compare Bob1 and Oct2 expression in these patient samples, the correlation of Bob1 and Oct2 mRNA expression was calculated in the $CD138^+$ cells of each patient. The correlation between Bob1 and Oct2 mRNA expression was positive and large in this patient cohort (Spearman's $r = 0.8608$, $p<0.0001$).

3.1.2 Bob1 and Oct2 protein expression in myeloma tissue samples

A multiple myeloma TMA was stained using fluorescent IHC, as described in section 2.1.5. For each histospot on the TMA, three images were taken using the DAPI filter, the Cy3 filter (CD138) and the Cy5 filter (Bob1 or Oct2). Representative images of Bob1 and Oct2 fluorescent staining are shown in Figure 3.3 and 3.4, respectively. CD138 staining in the myeloma plasma cells is located at the plasma membrane and Bob1 and Oct2 proteins are located throughout the nucleus and cytoplasm of the cells. Only Bob1 and Oct2 staining that is within the $CD138^+$ cells was included in the AQUA score calculation.

An average AQUA score based on 1-3 histospots was calculated for each patient in the TMA. The Bob1 and Oct2 AQUA scores both follow a continuous distribution (Figure 3.5 and 3.6, respectively). Since no obvious patient subgroups exist based on Bob1 and Oct2 AQUA scores, subsequent statistical analyses were done by comparing patients with AQUA scores above the median to patients with AQUA scores below the median. Of note, 156 patient samples had both Bob1 and Oct2 AQUA scores available, and a positive correlation between Bob1 and Oct2 AQUA scores was present (Spearman's $r = 0.3601$, $p<0.0001$).

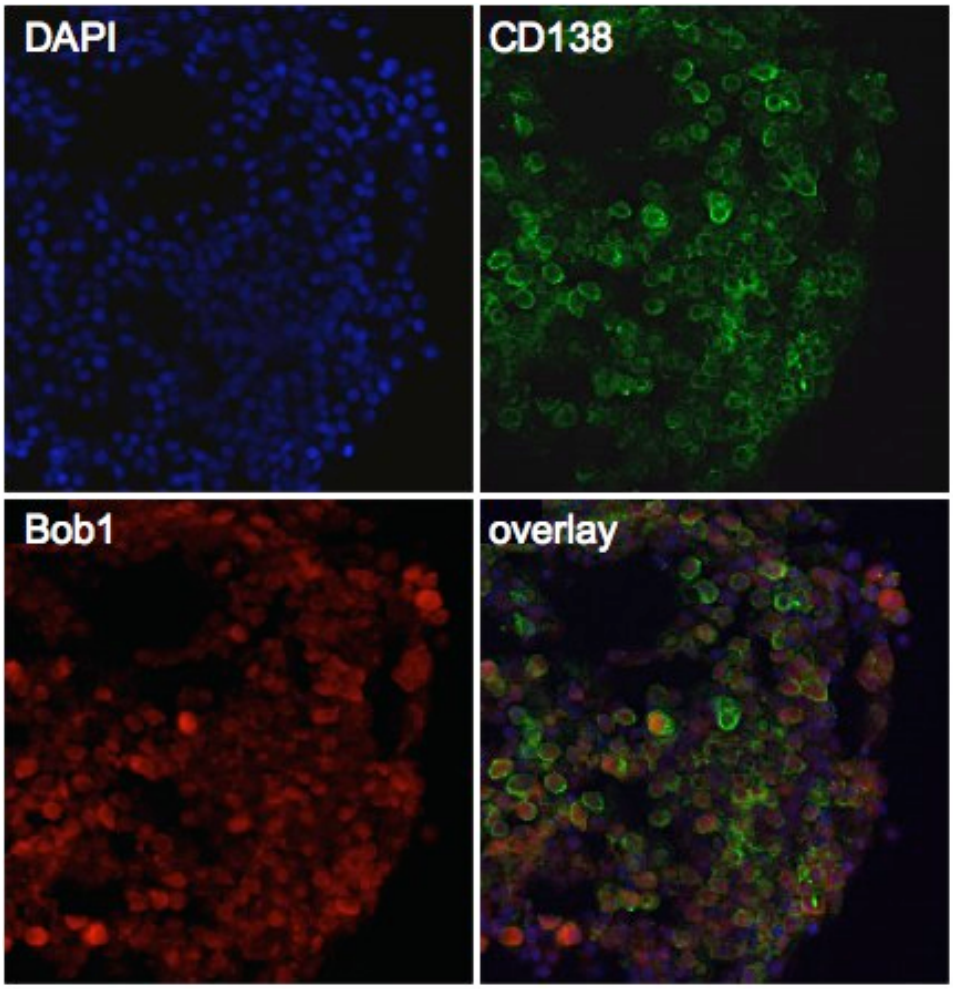

Figure 3.3. Fluorescent immunohistochemical staining of Bob1 in a myeloma TMA sample. TMA samples were stained with antibodies directed against CD138 (Cy3, green) and Bob1 (Cy5, red), as well as DAPI (blue) counterstain. The CD138 stain was used to identify the tumour mask, and an AQUA score measuring the Bob1 pixel intensity within the tumour mask was generated.

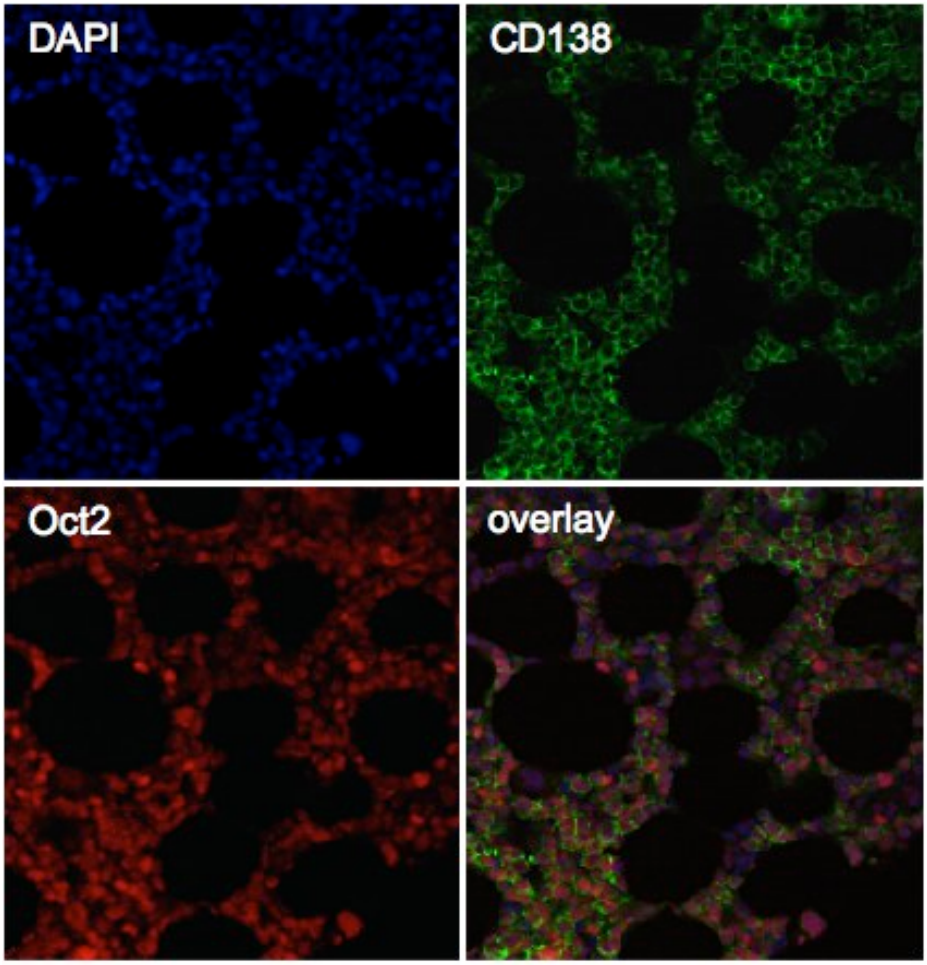

Figure 3.4. Fluorescent immunohistochemical staining of Oct2 in a myeloma TMA sample. TMA samples were stained with antibodies directed against CD138 (Cy3, green) and Oct2 (Cy5, red), as well as DAPI (blue) counterstain. The CD138 stain was used to identify the tumour mask, and an AQUA score measuring the Oct2 pixel intensity within the tumour mask was generated.

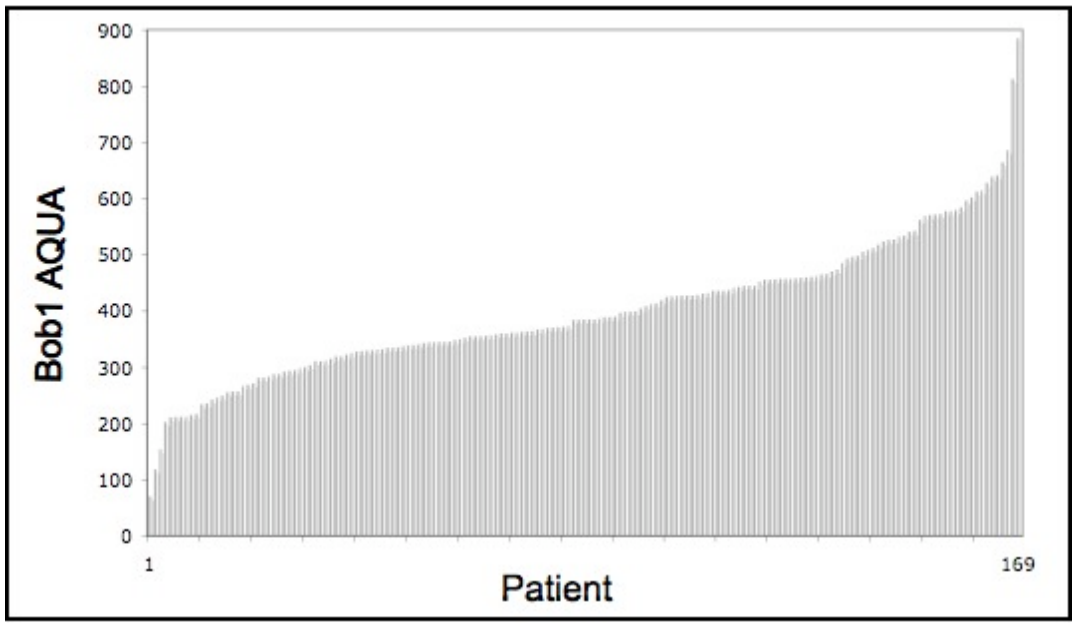

Figure 3.5. Bob1 AQUA scores in myeloma patient tissue samples. Average Bob1 AQUA scores for each myeloma patient in the TMA were calculated and plotted in a histogram. The scores follow a continuous distribution in the 169 patients assayed.

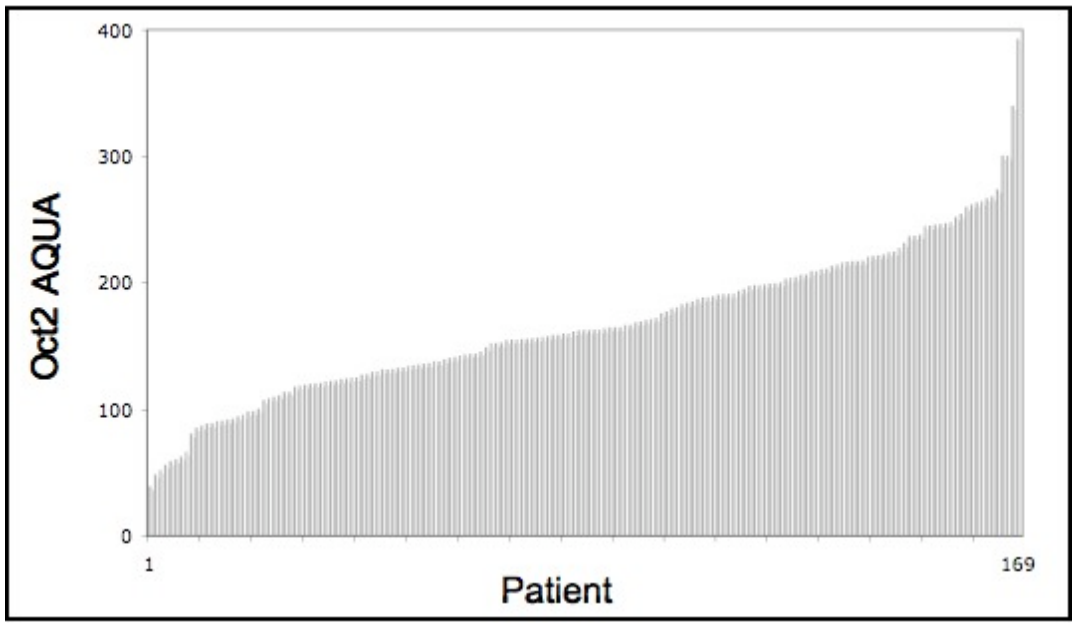

Figure 3.6. Oct2 AQUA scores in myeloma patient tissue samples. Average Oct2 AQUA scores for each myeloma patient in the TMA were calculated and plotted in a histogram. The AQUA scores of the 169 patients follow a continuous distribution.

3.1.3 Tissue microarray patient characteristics

Multiple myeloma patients included in the TMA were diagnosed at the CCI and TBCC facilities. Bone marrow biopsies in the TMA were all from the time of diagnosis. Also, clinical parameters reported in this study are from the time of diagnosis. A summary of the patient characteristics in the TMA is presented in Table 3.1. From the scorable samples, Bob1 expression data was available for 169 patients, and Oct2 data was available for 169 patients (156 patients overlap between Bob1 and Oct2 samples). AQUA scores above (high Bob1/Oct2, N=84) and below (low Bob1/Oct2, N=85) the median were compared for subsequent analyses.

For all patients with Bob1 AQUA score data, 80 patients (47%) were deceased, and the median follow-up of the survivors was 41 months, ranging from 7-96 months. For the patient group with high Bob1 AQUA scores, 33 patients (39%) were deceased, and the median follow-up of survivors was 45 months, ranging from 8-96 months. For the group with low Bob1 AQUA scores, 47 patients (55%) were deceased, and the median survivor follow-up time was 40 months, with a range of 7-90 months. For all patients with Oct2 AQUA score data, 78 patients (46%) were deceased, and the median follow-up of the survivors was 44 months, ranging from 7-139 months. For the patient group with high Oct2 AQUA scores, 44 patients (52%) were deceased, and the median follow-up of survivors was 39 months, ranging from 7-87 months. For the group with low Oct2 AQUA scores, 34 patients (40%) were deceased, and the median survivor follow-up time was 44 months, with a range of 8-139 months.

Table 3.1. Patient characteristics

	Bob1			Oct2		
	Overall	High	Low	Overall	High	Low
N	169	84	85	169	84	85
Age, y, median (range)	66 (41-90)	64 (41-83)	69 (46-90)	65 (41-87)	66 (41-87)	63 (43-85)
Gender (F/M)	68/101	36/48	32/53	70/99	36/48	34/51
Treatment centre, no. (%)						
CCI	117 (69)	40 (48)	77 (91)	110 (65)	57 (68)	53 (62)
TBCC	52 (31)	44 (52)	8 (9)	59 (35)	27 (32)	32 (38)
Primary treatment, no. (%)						
Transplant	97 (57)	*61 (73)	*36 (42)	100 (59)	*41 (49)	*59 (69)
Non-transplant	72 (43)	*23 (27)	*49 (58)	69 (41)	*43 (51)	*26 (31)
β_2-microglobulin >3.5 mg/L, no. (%)	89/133 (67)	41/66 (62)	48/67 (72)	86/129 (67)	44/66 (67)	42/63 (67)
Albumin <3.5 g/dL (%)	46/144 (32)	21/67 (31)	25/77 (32)	46/140 (33)	23/73 (32)	23/67 (34)
Serum M-protein ≥30 g/L (%)	74/147 (50)	32/73 (44)	42/74 (57)	75/145 (52)	36/71 (51)	39/74 (53)
% PC ≥50 (%)	89/161 (55)	41/79 (52)	48/82 (59)	89/157 (57)	42/78 (54)	47/79 (59)
Calcium >12 mg/dL (%)	6/115 (5)	1/39 (3)	5/76 (7)	3/108 (3)	1/56 (2)	2/52 (4)
Creatinine >2 mg/dL (%)	23/115 (20)	8/39 (21)	15/76 (20)	24/108 (22)	11/56 (20)	13/52 (25)
Hemoglobin ≤12 g/dL (%)	87/116 (75)	32/40 (80)	55/76 (72)	85/109 (80)	46/57 (81)	39/52 (75)
LDH >618 U/L (%)	18/113 (16)	*11/38 (29)	*7/75 (9)	18/106 (17)	10/55 (18)	8/51(16)
Lytic bone lesions (%)	88/108 (81)	31/36 (86)	57/72 (79)	82/102 (80)	41/52 (79)	41/50 (82)
t(4;14) (%)	5/70 (7)	3/44 (7)	2/26 (8)	6/70 (9)	3/32 (9)	3/38 (8)
Clinical isotype (%)						
IgG	93/149 (63)	42/70 (60)	51/79 (64)	90/147 (61)	46/73 (63)	44/74 (60)
IgA	32/149 (21)	18/70 (25)	14/79 (18)	35/147 (24)	13/73 (18)	22/74 (30)
Light chain	16/149 (11)	6/70 (9)	10/79 (13)	15/147 (10)	8/73 (11)	7/74 (9)
Other	8/149 (5)	4/70 (6)	4/79 (5)	7/147 (5)	6/73 (8)	1/74 (1)
Light chain (λ/κ)	48/103	19/57	29/46	48/102	22/49	26/53
Patients deceased, no. (%)	80 (47)	33 (39)	47 (55)	78 (46)	44 (52)	34 (40)
Overall survival, m, median (range)	60 (1-95)	*71 (1-95)	*38 (1-89)	62 (1-139)	*53 (1-88)	*73 (1-139)
Survivor follow-up, m, median (range)	41 (7-96)	45 (8-96)	40 (7-90)	44 (7-139)	39 (7-87)	44 (8-139)

CCI: Cross Cancer Institute; TBCC: Tom Baker Cancer Centre; PC: plasma cell; LDH: lactate dehydrogenase; y: years; m: months; * $p<0.05$ (high vs. low)

Patients included in this study had undergone different treatment regimens, which included or did not include an ASCT. Patients who had high Bob1 AQUA scores had a significantly higher proportion of ASCT recipients than patients with low Bob1 AQUA scores ($p<0.0001$). Conversely, patients who had low Oct2 AQUA scores had a significantly higher proportion of ASCT recipients than patients with high Oct2 AQUA scores ($p=0.0079$). When comparing Bob1 and Oct2 high and low AQUA score groups with respect to serum β_2-microglobulin, albumin, serum M-protein, percentage of plasma cells, calcium, creatinine, hemoglobin, lactate dehydrogenase (LDH), the presence of lytic bone lesions, the presence of t(4;14), clinical isotype, or light chain, the only significant difference observed was that patients with high Bob1 AQUA scores had higher LDH levels than those with low Bob1 AQUA scores ($p=0.0126$).

3.1.4 Bob1 overall survival and progression-free survival

Patients were separated into two groups above and below the median Bob1 AQUA score. The OS of each patient was calculated as the time to death or most recent follow-up from the time of diagnosis. Kaplan-Meier survival curves plotting OS for the low Bob1 AQUA group and high Bob1 AQUA group were generated and compared using the log-rank test. Patients who were still alive at the most recent follow-up were censored. As is shown in Figure 3.7, patients with low Bob1 AQUA scores had a significantly shorter OS of 38.3 months compared to patients with high Bob1 AQUA scores who had a median OS of 70.5 months (hazard ratio [HR]=0.46, 95% confidence interval [CI]=0.29-0.71, $p=0.0008$)

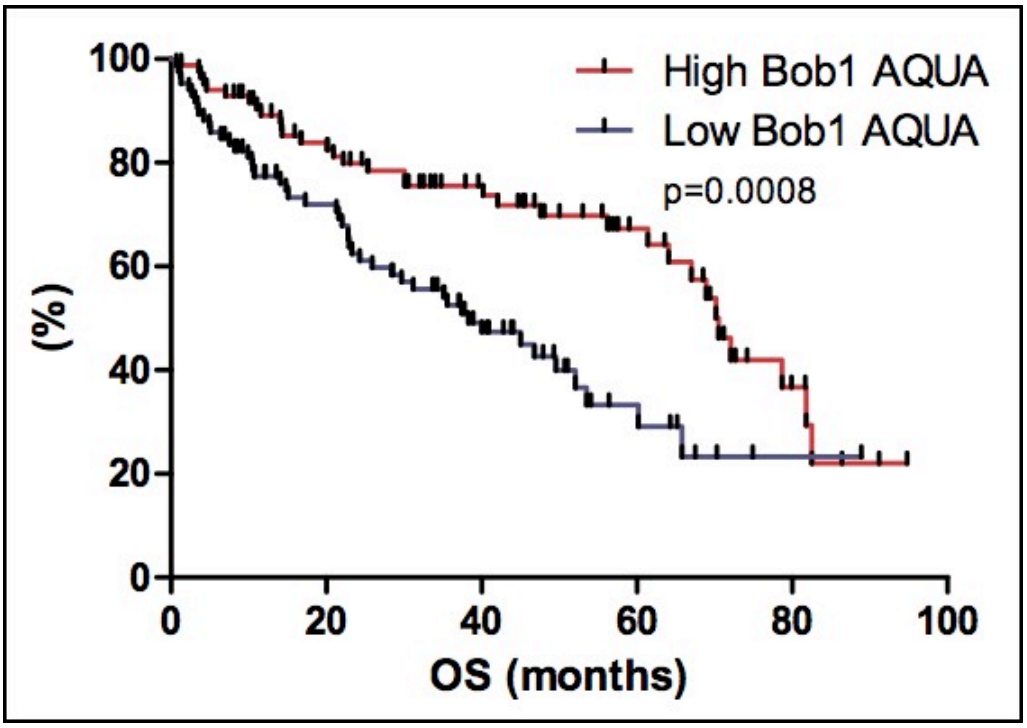

Figure 3.7. Low expression of Bob1 protein correlates with reduced overall survival in myeloma patients. Patients were divided into two groups based on Bob1 protein expression, which were defined as those with AQUA scores above the median (High Bob1) and those with AQUA scores below the median (Low Bob1). Kaplan-Meier curves for both groups were generated and compared. Patients with low Bob1 AQUA scores were found to have a significantly worse prognosis than those with high Bob1 AQUA scores (p=0.0008). OS: overall survival.

(results summary in Table 3.2). To adjust for baseline clinical features and transplant status, a Cox proportional hazards model was generated that included Bob1 expression, albumin, β2-microglobulin and transplant status. In this model, only transplant status was predictive of OS (p=0.003).

In addition to OS, the progression-free survival (PFS) for each patient was calculated. Progression is defined as death or relapse, and PFS is calculated as the time to progression or most recent follow-up from the time of diagnosis, as defined by the IMWG (177). Kaplan-Meier survival curves of PFS were plotted for the low Bob1 AQUA group and the high Bob1 AQUA group, and compared using the log-rank test. Patients who had not relapsed and were still alive were censored. As was observed with OS, Figure 3.8 shows that patients with low Bob1 AQUA scores have a shorter median PFS of 19.4 months compared to patients with high Bob1 AQUA scores whose median PFS was 25.3 months (HR=0.59, 95% CI=0.41-0.84, p=0.0037) (results summary in Table 3.2).

Since this study included patients from different treatment facilities (CCI and TBCC) and patients who had received different treatment regimens (transplant and non-transplant), the OS of these subgroups was compared using Kaplan-Meier survival curves. It is important to highlight the fact that patients selected for inclusion in the TMA from the TBCC had all undergone an ASCT, while patients from the CCI had been treated with and without transplants. Patients with Bob1 AQUA scores above and below the median of each subgroup were compared. The survival curves for all 4 subgroups are shown in Figure 3.9 and the survival data is shown in Table 3.3. Only the patient subgroup that had

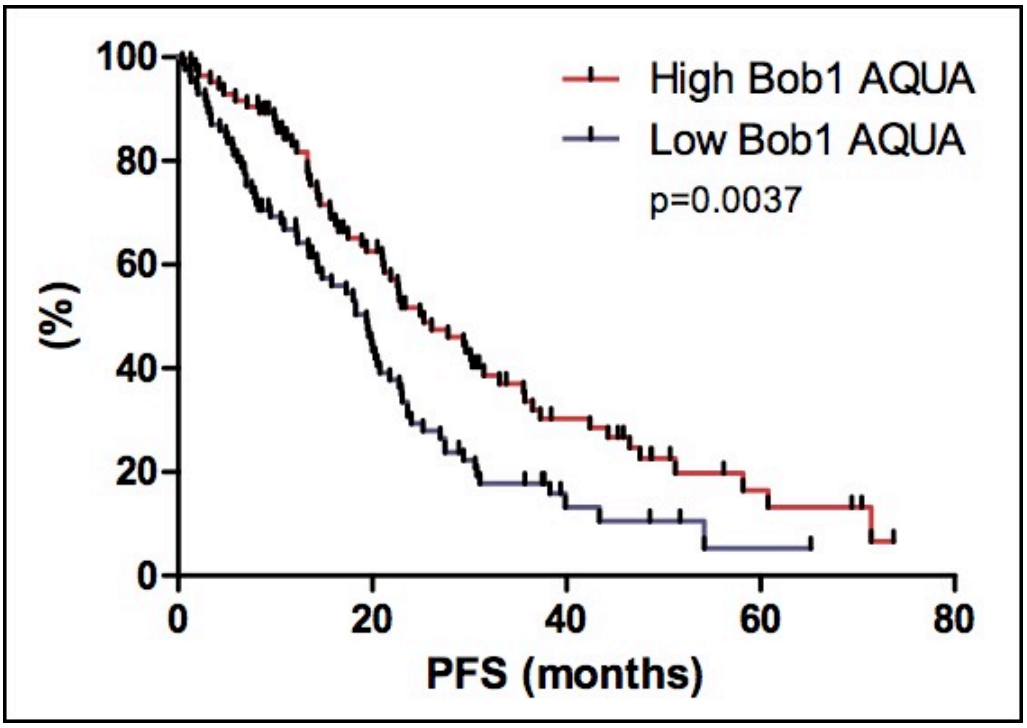

Figure 3.8. Low expression of Bob1 protein correlates with reduced progression-free survival in myeloma patients. Patients were divided into two groups based on Bob1 protein expression, which were defined as those with AQUA scores above the median (High Bob1) and those with AQUA scores below the median (Low Bob1). Kaplan-Meier curves for both groups were generated and compared using Log-rank statistics. Patients with low Bob1 AQUA scores were found to have a significantly shorter progression-free survival than those with high Bob1 AQUA scores (p=0.0037). PFS: progression-free survival.

Table 3.2. Bob1 survival analysis

End-point	HR	95% CI	High Bob1 AQUA median OS, months	Low Bob1 AQUA median OS, months	Log-rank P-value
OS*	0.46	0.29-0.71	70.5	38.3	0.0008
PFS*	0.59	0.41-0.84	25.3	19.4	0.0037

OS: Overall survival; PFS: Progression-free survival; HR: Hazard ratio; CI: Confidence interval

* A significant statistical difference exists ($p<0.05$)

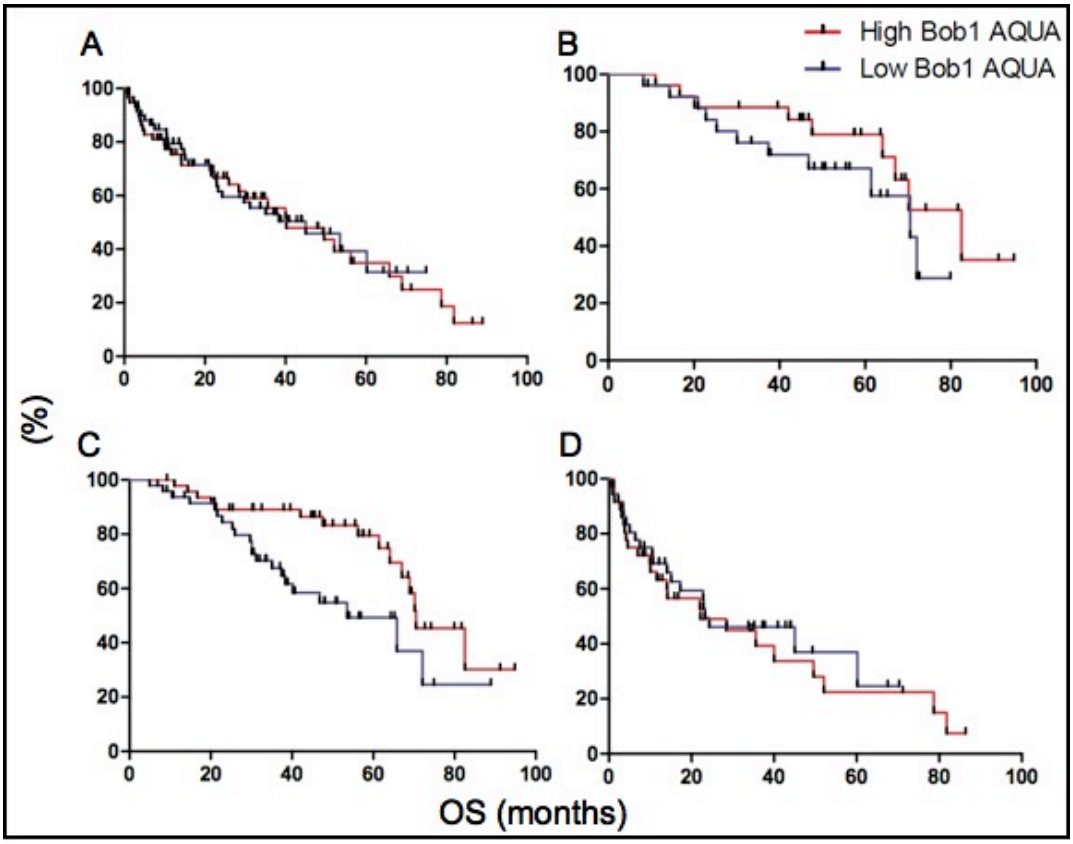

Figure 3.9. Bob1 overall survival analysis in patient subgroups. Patients were separated into subgroups based on treatment facility and treatment regimen, and further divided into two groups based on high and low Bob1 AQUA scores, above and below the median of each subgroup. (A) Patient samples collected at the Cross Cancer Institute. (B) Patients diagnosed at the Tom Baker Cancer Centre. (C) Patients who received an ASCT. (D) Patients who did not receive an ASCT. OS: overall survival.

Table 3.3. Bob1 patient subgroup overall survival analysis

Subgroup	HR	95% CI	High Bob1 AQUA median OS, months	Low Bob1 AQUA median OS, months	Log-rank P-value
CCI	1.03	0.61-1.72	40.2	45.0	0.9231
TBCC	0.57	0.23-1.43	82.5	70.5	0.2307
Transplant*	0.43	0.22-0.86	70.5	53.5	0.0160
Non-transplant	1.16	0.63-2.13	22.2	23.3	0.6311

CCI: Cross Cancer Institute; TBCC: Tom Baker Cancer Centre; OS: Overall survival; HR: Hazard ratio; CI: Confidence interval

* A significant statistical difference exists ($p<0.05$)

received ASCT had significantly different survival curves for high and low Bob1 AQUA score groups. Patients who received a transplant and had high Bob1 AQUA scores had a median OS of 70.5 months compared to patients with low Bob1 AQUA scores whose median OS was 53.5 months (HR=0.43, 95% CI=0.22-0.86, p=0.0160).

3.1.5 Oct2 overall survival and progression-free survival

Patients were separated into two groups above and below the median Oct2 AQUA score. Kaplan-Meier survival curves of OS were plotted for both groups and compared using the log-rank test. Conversely to Bob1, patients with high Oct2 AQUA scores had a shorter median OS of 52.8 months, compared to those with low Oct2 AQUA scores whose median OS was 70.5 months (HR=1.74, 95% CI=1.11-2.73, p=0.0164) (Figure 3.10 and Table 3.4). However, when a Cox proportional hazards model was used to analyze Oct2 expression and survival along with albumin, β2-microglobulin and transplant status, only transplant status was predictive of OS (p<0.0001). The PFS of these two groups was also plotted using Kaplan-Meier survival curves and compared with the log-rank test. The median PFS of patients with high Oct2 AQUA scores was 16.5 months, compared to 23.6 months in the low Oct2 AQUA score group, although this difference was not statistically significant (HR=1.21, 95% CI=0.85-1.72, p=0.2947) (Figure 3.11 and Table 3.4).

To examine the correlation between Oct2 expression and OS in patient subgroups, patients were separated based on treatment centre and treatment

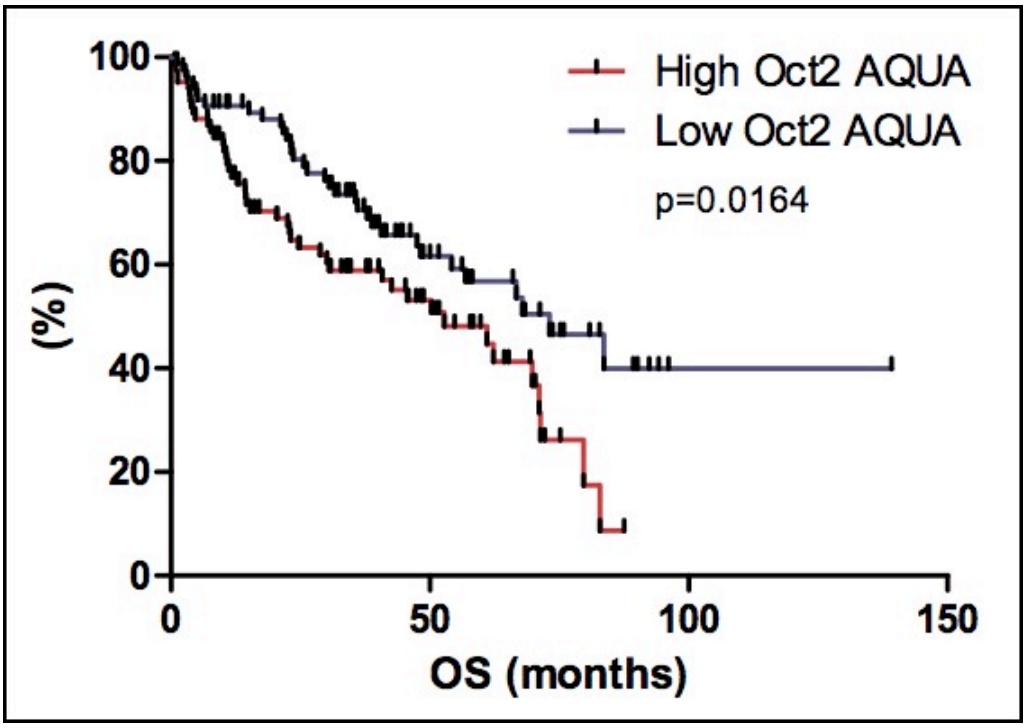

Figure 3.10. High expression of Oct2 protein correlates with reduced overall survival in myeloma patients. Patients were divided into two groups based on Oct2 protein expression, which were defined as those with AQUA scores above the median (High Oct2) and those with AQUA scores below the median (Low Oct2). Kaplan-Meier survival curves for both groups were generated and compared. Patients with high Oct2 AQUA scores were found to have a significantly worse prognosis than those with low Oct2 AQUA scores (p=0.0164). OS: overall survival.

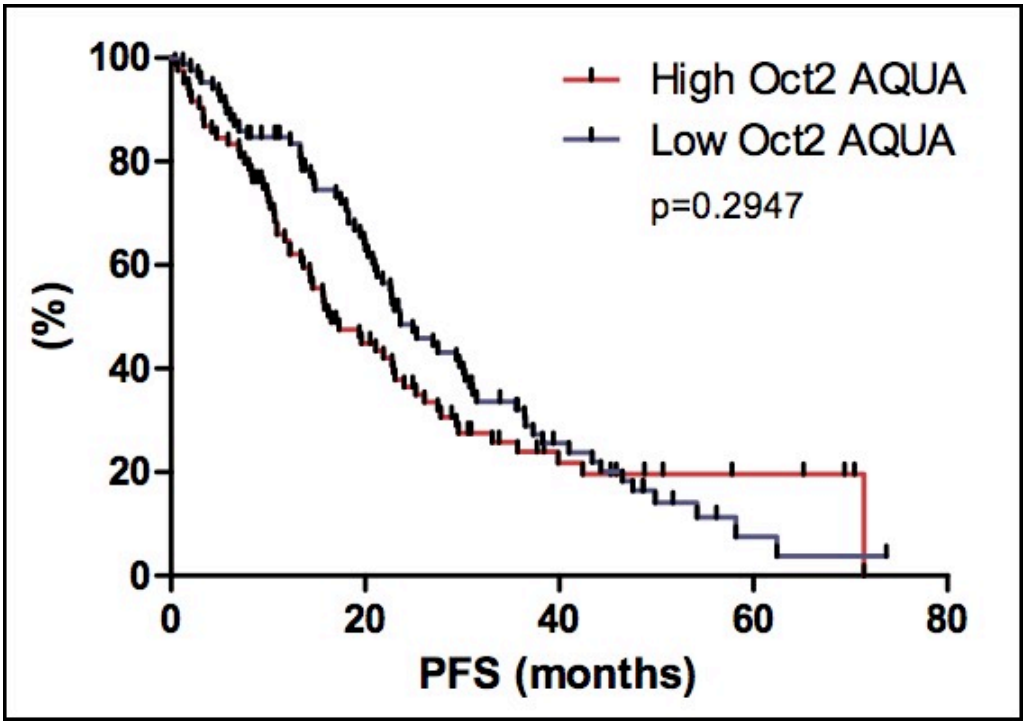

Figure 3.11. Oct2 protein expression does not significantly correlate with reduced progression-free survival in myeloma patients. Patients were divided into two groups based on Oct2 protein expression, which were defined as those with AQUA scores above the median (High Oct2) and those with AQUA scores below the median (Low Oct2). Kaplan-Meier survival curves for both groups were generated and compared. No statistical difference between the curves was observed (p=0.2947). PFS: progression-free survival.

Table 3.4. Oct2 survival analysis

End-point	HR	95% CI	High Oct2 AQUA median OS, months	Low Oct2 AQUA median OS, months	Log-rank P-value
OS*	1.74	1.11-2.73	52.8	73.1	0.0164
PFS	1.21	0.85-1.72	16.5	23.6	0.2947

OS: Overall survival; PFS: Progression-free survival; HR: Hazard ratio; CI: Confidence interval

* A significant statistical difference exists ($p<0.05$)

regimen, and further separated into two groups above and below the median Oct2 AQUA score of each group. These survival curves are shown in Figure 3.12, and the survival data is presented in Table 3.5. None of the patient subgroups had statistically different survival when comparing the high and low Oct2 AQUA score groups, although the median survival of the low Oct2 AQUA score group was consistently higher than the high Oct2 AQUA score group.

Oct2 and Bob1 are known to interact at octamer sites in the immunoglobulin locus to activate transcription. We therefore wanted to determine if there was a statistically significant interaction between Bob1 and Oct2 that is predictive of OS. A Cox regression proportional hazards model including Bob1 AQUA scores above or below the median, Oct2 AQUA scores above or below the median, and the Bob1/Oct2 interaction term was generated. In this analysis, no significant interaction was found between Bob1 and Oct2.

3.1.6 Treatment response

Since patients with high Bob1 AQUA scores have increased OS and PFS, we aimed to determine if patients with high Bob1 responded better to therapy. Patients were separated into transplant and non-transplant subgroups and divided further into two groups of Bob1 AQUA scores above the median and Bob1 AQUA scores below the median. The proportion of patients who did not respond to treatment (stable disease (SD) or worse) and the proportion of patients that responded to treatment (partial response (PR) or better) were compared. Treatment response categories were previously defined by the IMWG (177). For

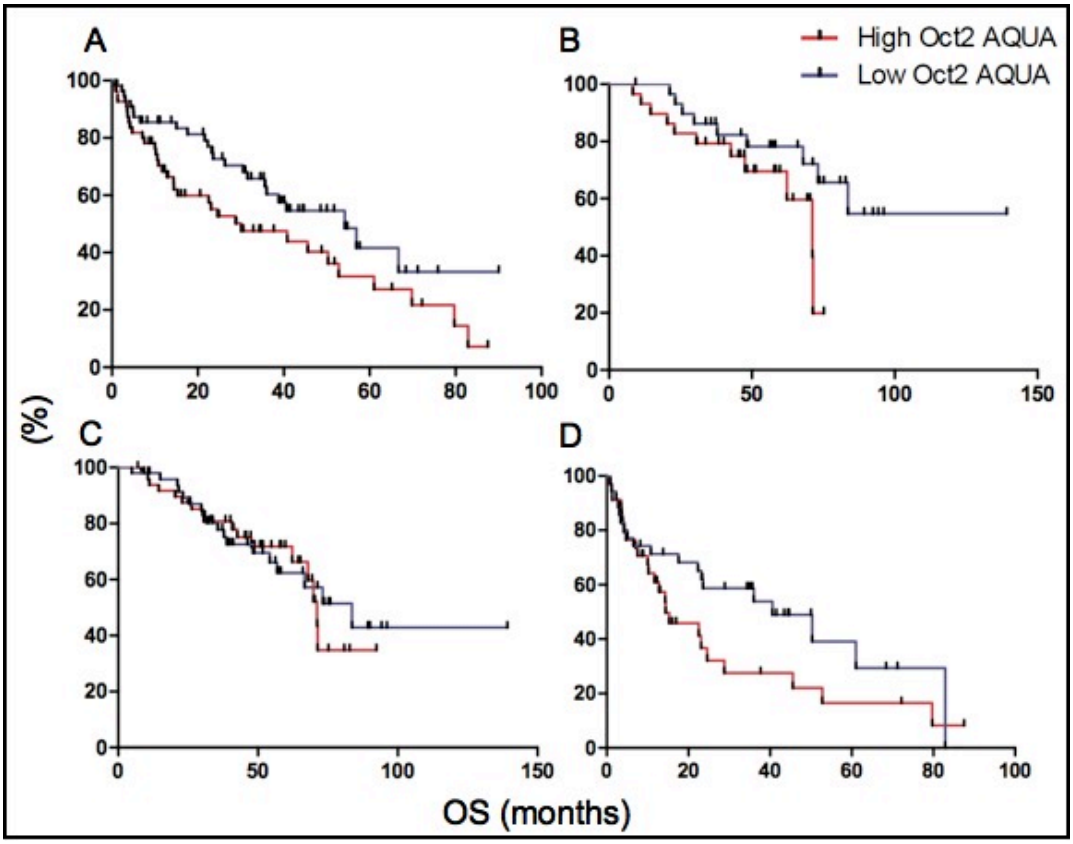

Figure 3.12. Oct2 overall survival analysis in patient subgroups. Patients were separated into subgroups based on treatment facility and treatment regimen, and further divided into two groups of Oct2 AQUA scores above and below the median of each subgroup. (A) Patient samples collected at the Cross Cancer Institute (B) Patients diagnosed at the Tom Baker Cancer Centre. (C) Patients who received an ASCT. (D) Patients who did not receive an ASCT. OS: overall survival.

Table 3.5. Oct2 patient subgroup overall survival analysis

Subgroup	HR	95% CI	High Oct2 AQUA median OS, months	Low Oct2 AQUA median OS, months	Log-rank P-value
CCI	1.67	0.99-2.80	30.1	54.2	0.0554
TBCC	2.23	0.86-5.77	71.1	§	0.0974
Transplant	1.08	0.55-2.11	71.1	83.6	0.8309
Non-transplant	1.66	0.90-3.06	14.4	40.6	0.1056

CCI: Cross Cancer Institute; TBCC: Tom Baker Cancer Centre; OS: Overall survival; HR: Hazard ratio; CI: Confidence interval
§ >50% of patient group was alive at most recent follow-up

patients who received a transplant, the proportion of patients who responded and did not respond to treatment in the high and low Bob1 groups was identical (p=1.323). In the non-transplant group, no statistical difference in treatment response between high and low Bob1 patients was present (p=0.1752).

Conversely to Bob1, patients with high Oct2 had a worse prognosis than those with low Oct2. Response to treatment was compared as it had been for the Bob1 group. Patients who received a transplant did not show any differences in response to treatment when comparing high and low Oct2 AQUA scores (p=0.6712). Similarly, no differences were observed in non-transplant patients (p=0.7799).

3.1.7 Comparison of AQUA score and H-score methods

To measure the expression of Bob1 and Oct2 proteins in the myeloma TMA, two methods were used: fluorescent IHC with AQUA scores and DAB IHC with H-scores. Opposed to AQUA scores, which are computer-generated scores, H-scores are calculated by two independent observers. Visual, qualitative examination of Bob1 and Oct2 DAB IHC staining in myeloma tissue samples showed that the expression of these proteins is highest in plasma cells. Bob1 and Oct2 protein expression was absent or very low in other cells within the bone marrow (data not shown).

To compare the AQUA score and H-score methods, the OS analysis was repeated with the H-scores. Of note, all samples for which H-scores were generated were from the CCI. To examine the OS of patients with high and low

Bob1 H-scores, patients were separated into two groups above and below the median H-score. Patients with high Bob1 H-scores had a longer median OS of 53.5 months compared with 29.7 months in the low Bob1 H-score group, although this result was not statistically different (HR=0.68, 95% CI=0.40-1.16, p=0.1572). When comparing OS differences in patients based on Oct2 H-scores, no differences were present (p=0.5600) (Figure 3.13 and Table 3.6).

To determine the agreement between the AQUA score and H-score methods, the kappa statistic was used. This method compares inter-rater agreement of categorical variables. To assess this, patients were categorized as above or below the median protein expression for each method, and the overlap of the two methods was calculated. For Bob1, the kappa measure of agreement was 0.278, p=0.002, meaning the agreement between the two methods is fair (178) (Table 3.7). For Oct2, the kappa measure of agreement was 0.320, p=0.001, again showing that the level of agreement between the two methods is fair (Table 3.8).

3.2 Expression of Bob1, Oct2 and FGFR3 in myeloma cell lines

Having established the expression and prognostic significance of Bob1 and Oct2 in clinical samples, we examined their expression in myeloma cell lines in order to select the best model system for testing the therapeutic effects of Bob1 and Oct2 knockdown.

The expression of Bob1, Oct2 and FGFR3 mRNA and protein was measured in multiple myeloma cell lines. Of the cell lines assayed, KMS11, KMS18, LP-1 and JIM3 all possess t(4;14) translocations, while U266 does not

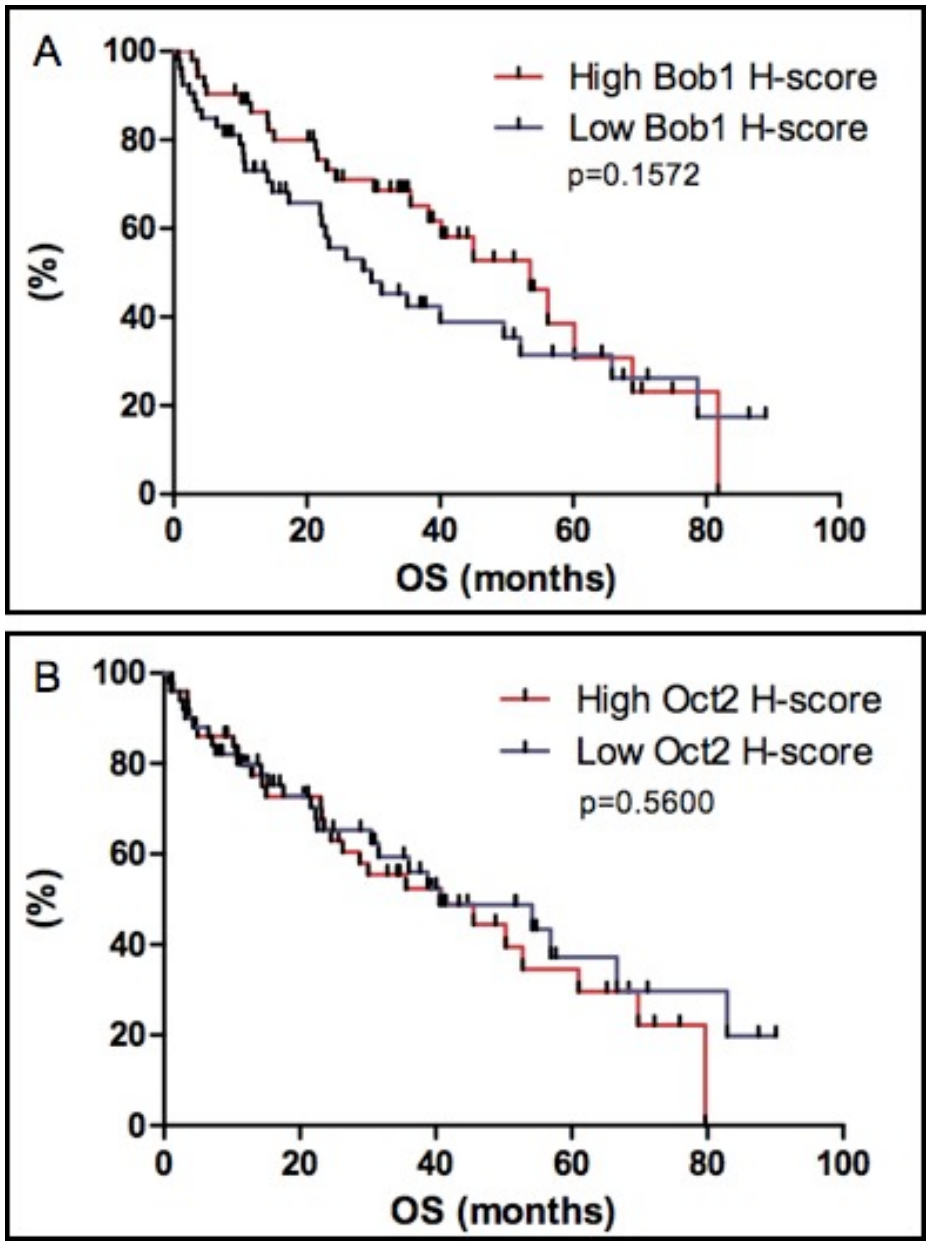

Figure 3.13. Overall survival analysis of myeloma patients stratified by H-scores. Patient samples were divided into two groups above and below the median Bob1 or Oct2 H-score, and survival curves were generated and compared. (A) Survival analysis of patients grouped by Bob1 H-scores. (B) Survival analysis of patients separated based on Oct2 H-scores. OS: overall survival.

Table 3.6. Overall survival analysis with H-scores

Protein	HR	95% CI	High H-score median OS, months	Low H-score median OS, months	Log-rank P-value
Bob1	0.68	0.40-1.16	53.5	29.7	0.1572
Oct2	1.18	0.68-2.03	40.8	40.6	0.5600

OS: Overall survival; HR: Hazard ratio; CI: Confidence interval

Table 3.7. Agreement between Bob1 AQUA and H-scores

		AQUA score		Total
		below median	above median	
H-score	below median	42	10	52
	above median	28	25	53
Total		70	35	105

Table 3.8. Agreement between Oct2 AQUA and H-scores

		AQUA score		Total
		below median	above median	
H-score	below median	32	18	50
	above median	16	34	50
Total		48	52	100

have a t(4;14) translocation. Bob1 mRNA was easily detectable in KMS11, KMS18, LP-1 and U266, but was very low in JIM3. Similarly, Bob1 protein levels were detectable in KMS11, KMS18, LP-1 and U266, but were very low in JIM3 (Figure 3.14).

Unlike Bob1, Oct2 mRNA expression in KMS11 was very low, and Oct2 protein expression was undetectable. KMS18 is the only myeloma cell line that expressed high levels of both Oct2 mRNA and protein. LP-1 expressed similar levels of Oct2 mRNA as KMS18, but did not have detectable Oct2 protein levels. JIM3 Oct2 mRNA levels were undetectable, but Oct2 protein was detectable by western blot. Finally, U266 expressed approximately 40 times the amount of Oct2 mRNA as KMS18, but had undetectable levels of Oct2 protein (Figure 3.15).

The discordance between the Oct2 mRNA and protein expression suggests that either the primer sets for qRT-PCR or the antibodies for western blots are not specific, or that the transcriptional and translational regulation of Oct2 do not directly correlate. The sequences of the primers used were checked to ensure that they would not bind to any other known mRNA sequences. Additionally, these primers are located at exon-exon junctions, so that they will not amplify genomic DNA. The fluorescent probe that binds between the primers, and is required to generate an amplification signal, adds another level of specificity. The antibody used to probe for Oct2 was also tested in HEK293T extracts, and did not produce any bands (data not shown). Since Oct2 is primarily B cell-specific, it would not be expected to be present in HEK293T, and its absence demonstrates the

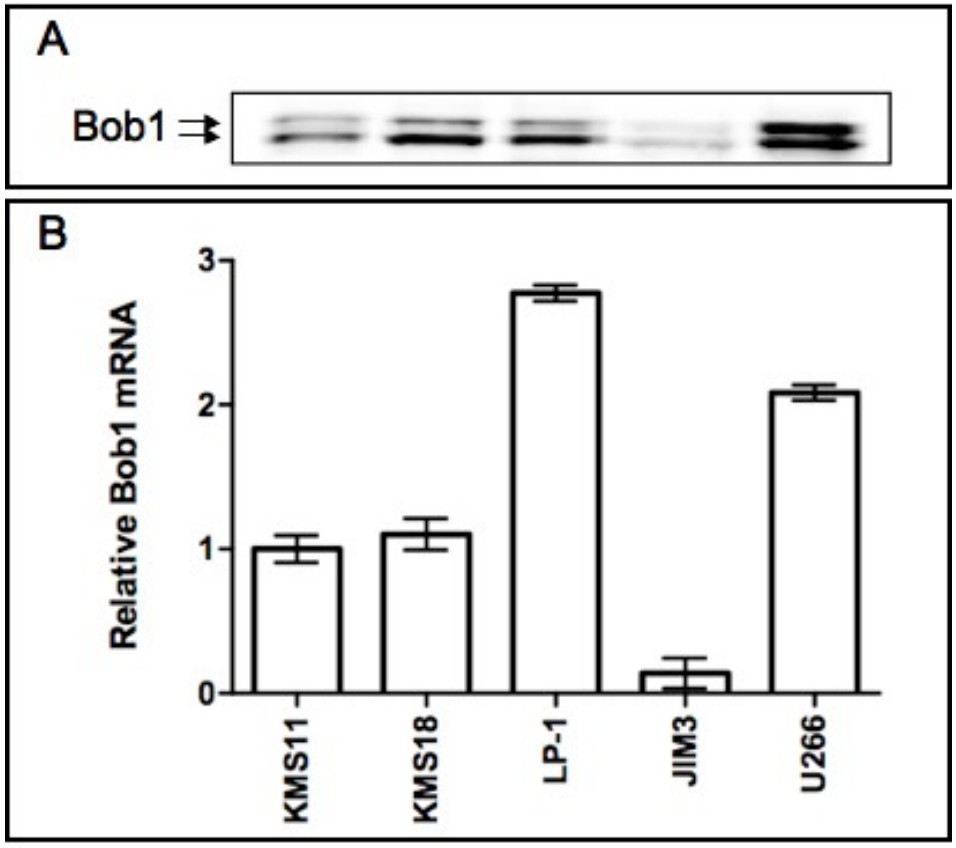

Figure 3.14. Relative Bob1 protein and mRNA expression in myeloma cell lines. The cell lines KMS11, KMS18, LP-1 and JIM3 all have t(4;14) translocations, whereas U266 does not. (A) Bob1 protein expression was assayed by western blot. Excluding the JIM3 cell line, all cell lines express high levels of Bob1 protein. Additionally, the antibody recognizes both the p35 (cytoplasmic) and p34 (nuclear) isoforms of Bob1. (B) Using qRT-PCR, the relative level of Bob1 mRNA was measured in myeloma cell lines. Similar to the protein, Bob1 mRNA is present at easily detectable levels in all cell lines assayed except JIM3. Error bars represent the standard deviation of triplicate qRT-PCR samples.

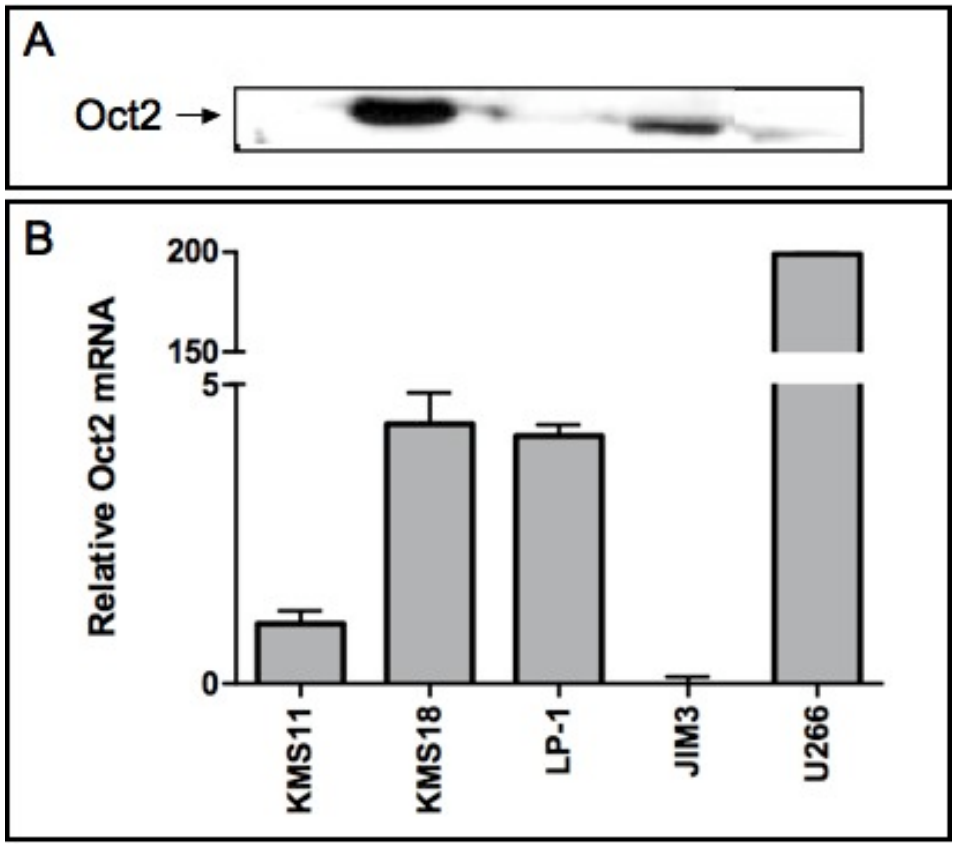

Figure 3.15. Relative Oct2 protein and mRNA expression in myeloma cell lines. The cell lines KMS11, KMS18, LP-1 and JIM3 all have t(4;14) translocations, whereas U266 does not. (A) Oct2 protein expression was assayed by western blot. Only KMS18 and JIM3 express detectable levels of Oct2 protein. (B) Using qRT-PCR, the relative level of Oct2 mRNA was measured in myeloma cell lines. Contrary to the protein levels, JIM3 does not express detectable levels of Oct2 mRNA and U266 expresses very high levels of Oct2 mRNA. KMS18 is the only cell line that expresses detectable levels of Oct2 protein and mRNA. Error bars represent the standard deviation of triplicate qRT-PCR samples.

specificity of this antibody. Thus, it is likely that the regulation and stability of Oct2 mRNA and protein is not directly correlated.

KMS11, KMS18, LP-1 and U266 were also assayed for expression of FGFR3 mRNA and protein. KMS11 and KMS18 were both found to express FGFR3 mRNA and protein, due to the presence of a t(4;14) translocation. However, LP-1, which also has a t(4;14) translocation, expressed extremely low levels of FGFR3 mRNA and protein. This is not unexpected though, as previous studies have shown that approximately one third of $t(4;14)^{+}$ myeloma patients do not express FGFR3 (87). Finally, U266 cells did not express any FGFR3 mRNA or protein, as this cell line lacks the relevant translocation (Figure 3.16).

3.3 Transient transfection of KMS11 with Bob1 siRNA

3.3.1 Selection and titration of a Bob1 siRNA duplex

Since KMS11 was shown to express both Bob1 and FGFR3 mRNA and protein, this cell line was used as a model system to test the effects of Bob1 knockdown in a t(4;14) myeloma cell line. Previously published data have shown that efficient knockdown of target mRNA and protein can be achieved using dicer-substrate siRNA duplexes (179). These duplexes are 27 nucleotides in length, as compared with synthetic siRNA molecules of 21 nucleotides. It is believed that because these molecules are longer, they require cleavage by the RNAse III-family nuclease Dicer, which leads to more efficient incorporation into the RNA-induced silencing complex (RISC). The knockdown efficiency of three separate Bob1 dicer-substrate siRNA duplexes was tested. Of the duplexes tested,

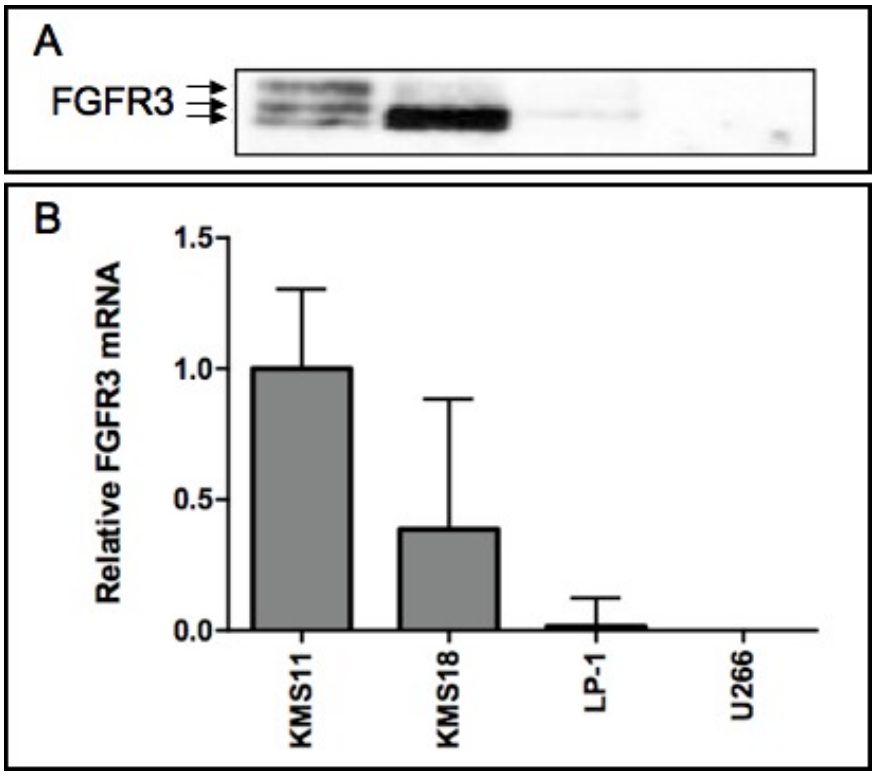

Figure 3.16. Relative FGFR3 protein and mRNA expression in myeloma cell lines. The cell lines KMS11, KMS18 and LP-1 all have t(4;14) translocations, whereas U266 does not. (A) FGFR3 protein expression was assayed by western blot. Due to the presence of a t(4;14) translocation, KMS11 and KMS18 aberrantly express FGFR3 protein, but LP-1 does not express FGFR3 protein. U266, which does not have a t(4;14) translocation, does not express FGFR3 protein. (B) Using qRT-PCR, the relative level of FGFR3 mRNA was measured in myeloma cell lines. The mRNA expression supports the FGFR3 protein expression observed. Error bars represent the standard deviation of triplicate qRT-PCR samples.

it was found that duplex 2 generated the most efficient knockdown of Bob1 protein and mRNA (Figure 3.17). When this duplex was titrated in KMS11 cells, 25 nM concentrations were found to be most effective (Figure 3.17). Thus, all subsequent knockdown experiments of Bob1 in KMS11 used 25 nM duplex 2 siRNA.

3.3.2 Knockdown of Bob1 protein leads to decreased expression of FGFR3 protein

Since KMS11 cells overexpress FGFR3 due to a t(4;14) translocation, it was hypothesized that knocking down Bob1 protein would lead to decreased FGFR3 expression, in keeping with decreased 3'IgH enhancer activity. Using siRNA, Bob1 protein levels were effectively knocked down in KMS11 48 hr, 72 hr and 96 hr after transfection. Through western blot analysis, the level of FGFR3 protein at each time point was assayed. At 48 hr post-transfection, the level of Bob1 protein was beginning to decrease, but no change in FGFR3 protein expression was apparent. However, at 72 hr when the level of Bob1 protein was very low compared to the non-specific control, the level of FGFR3 protein was also decreased compared to the control. By 96 hr the level of FGFR3 protein was dramatically lower than the control sample (Figure 3.18). These results demonstrate that knocking down Bob1 protein causes decreased FGFR3 protein expression, likely due to decreased activity of the 3'IgH enhancer.

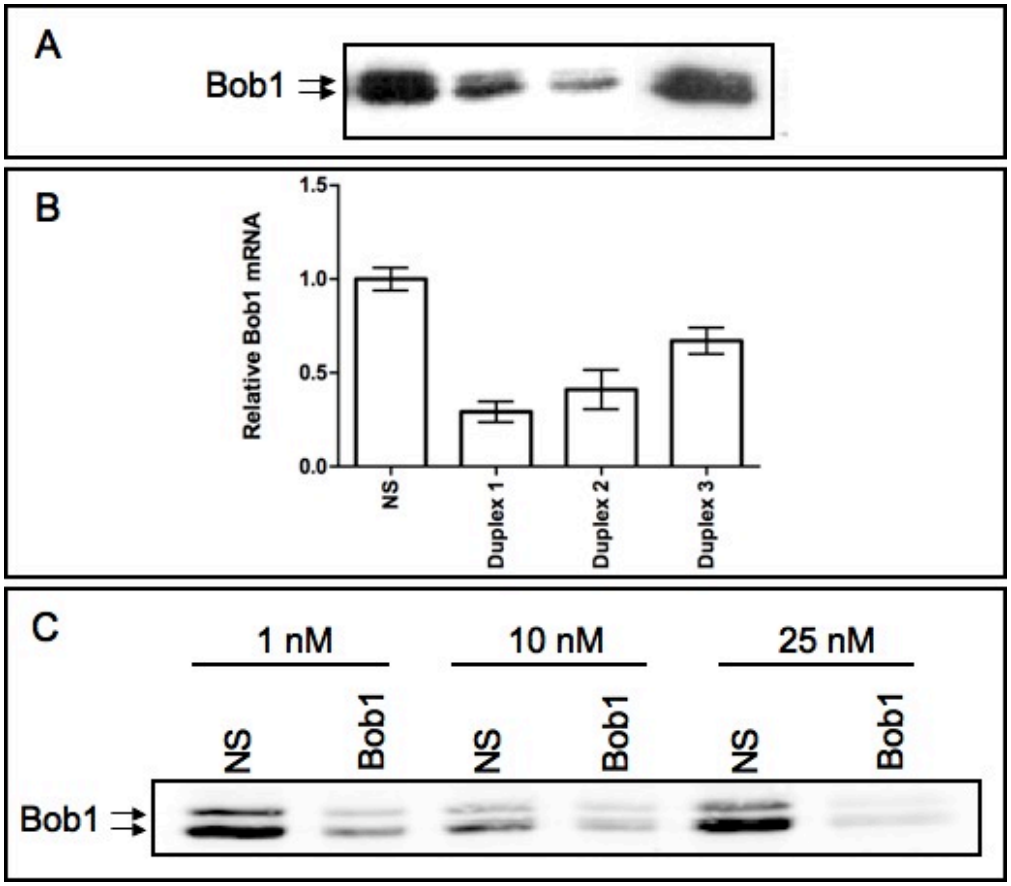

Figure 3.17. Expression of Bob1 protein and mRNA after transfection with Bob1 dicer-substrate siRNA duplexes. (A) Bob1 protein expression was assayed in KMS11 by western blot 72 hr after transfection. Compared to the NS control, duplex 2 generated the best knockdown of Bob1 protein. (B) Similarly, Bob1 mRNA levels in KMS11 were measured 24 hr post-transfection by qRT-PCR. Duplexes 1 and 2 generated approximately 70% and 60% knockdown, respectively. (C) KMS11 cells were transfected with increasing concentrations of Bob1 duplex 2 siRNA and protein expression was analyzed 72 hr post-transfection. The best knockdown results were achieved using 25 nM duplex 2 siRNA NS: Non-specific siRNA.

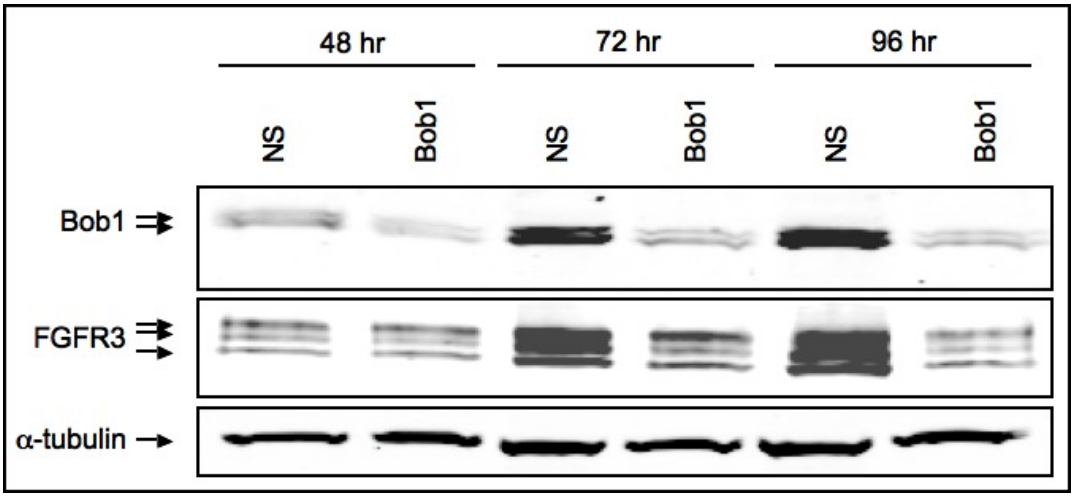

Figure 3.18. Protein expression in KMS11 after transfection with Bob1 siRNA. KMS11 cells were transfected with 25 nM Bob1 siRNA and cell lysates were collected 48 hr, 72 hr and 96 hr post-transfection. The expression of Bob1 and FGFR3 protein was analyzed by western blot. A marked reduction of Bob1 protein is observed after Bob1 siRNA transfection, as well as a decrease in FGFR3 protein expression, as compared to the 25 nM NS control. α-tubulin was included as a loading control. This blot is representative of 3 independent experiments that showed similar results. NS: Non-specific siRNA.

3.3.3 Knockdown of Bob1 protein does not affect viability or apoptosis

Since numerous studies have shown that FGFR3 expression and activity are required for survival of t(4;14) myeloma cells, it was hypothesized that decreased FGFR3 protein expression would cause reduced cell viability and increased apoptosis. Of note, assays for protein expression, viability and apoptosis were performed simultaneously to ensure that decreased levels of Bob1 and FGFR3 proteins were present. To assess relative viability, an MTS assay was used to measure the metabolic activity of the cells. Figure 3.19 shows the combined results of three independent MTS experiments. Compared to the non-specific siRNA control sample, a small, but statistically significant, decrease in relative viability was observed in KMS11 cells treated with Bob1 siRNA 72 hr post-transfection (0.84 vs. 0.91, p=0.0201). The relative viability of cells treated with Bob1 siRNA compared to the non-specific control at 48 hr and 96 hr were not significantly different (0.90 vs 0.97 at 48 hr, 0.93 vs. 0.95 at 96 hr).

To measure the percentage of cells undergoing apoptosis after transfection with Bob1 siRNA, Annexin V-FITC/ Propidium iodide staining and flow cytometry were used. Figure 3.20 shows that when KMS11 cells were transfected with Bob1 siRNA and assayed for apoptosis 48 hr, 72 hr and 96 hr post-transfection, no differences in the number of cells undergoing apoptosis were observed between the Bob1 and non-specific siRNA control samples.

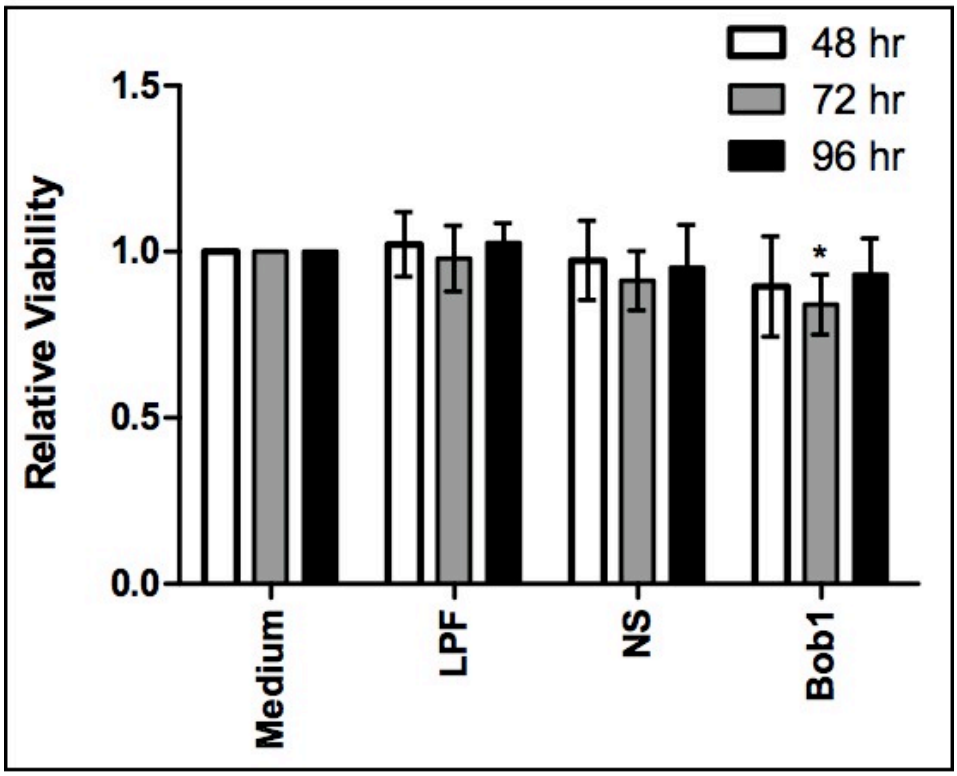

Figure 3.19. Relative viability of KMS11 after transfection with Bob1 siRNA. An MTS assay was used to measure the relative viability of KMS11 cells 48 hr, 72 hr and 96 hr after transfection with 25 nM Bob1 siRNA. Decreased Bob1 and FGFR3 protein expression was confirmed by western blot. Transfection of KMS11 cells with Bob1 siRNA led to a small, but significant decrease in viability as compared to the 25 nM NS control at 72 hr, but no significant decreases were observed at other time points. This graph shows the mean values of 3 independent experiments, of which each experiment contained 6 replicates of each sample (n=18). Error bars show the standard deviation of each sample mean. LPF: Lipofectamine 2000; NS: Non-specific siRNA; * indicates $p<0.05$.

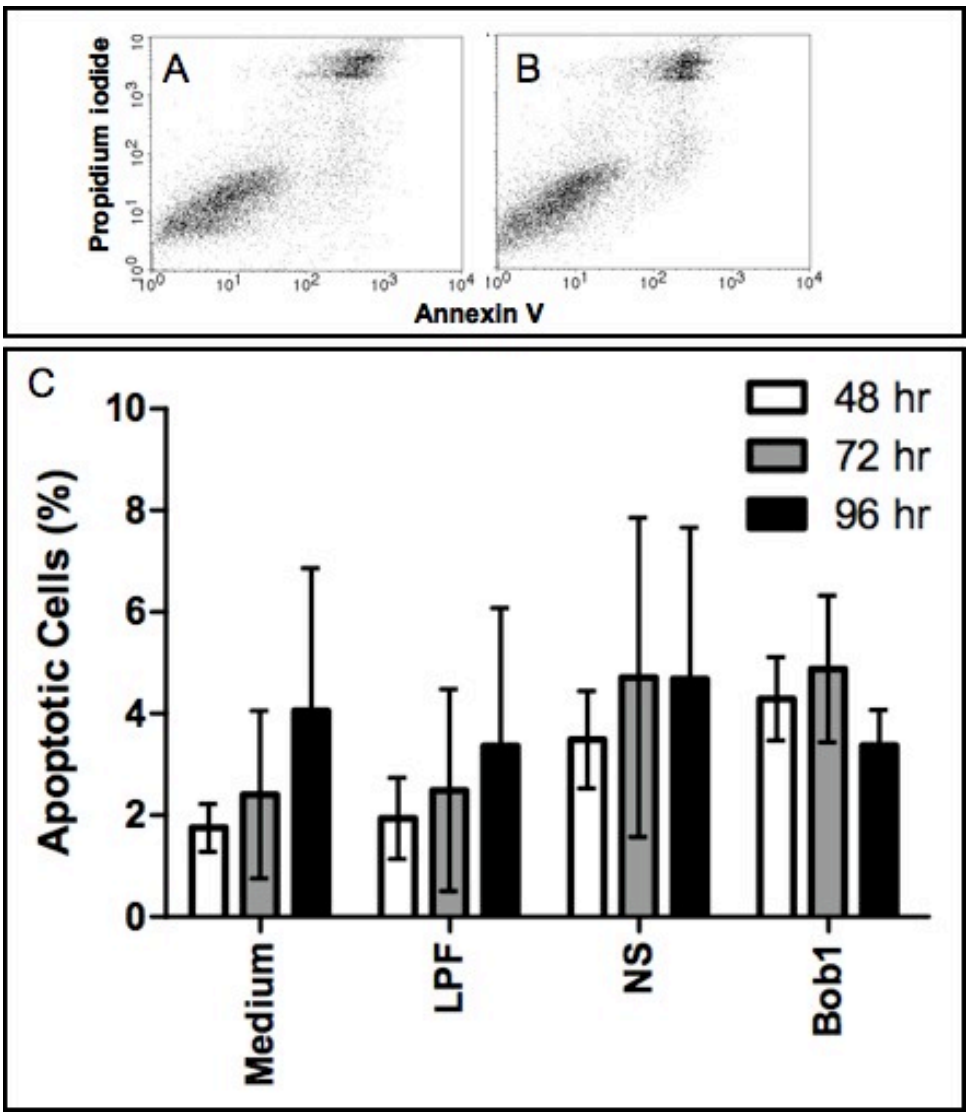

Figure 3.20. Percentage of KMS11 cells undergoing apoptosis after transfection with Bob1 siRNA. KMS11 cells were transfected with 25 nM Bob1 siRNA, and medium, LPF and 25 nM NS controls, and the percentage of cells undergoing apoptosis in each sample was measured by Annexin V/ Propidium iodide staining and flow cytometry. Decreased Bob1 and FGFR3 protein expression was confirmed by western blot. (A) In a NS control, approximately 5% of the cells are Annexin V positive and Propidium iodide negative. (B) In the Bob1 siRNA sample, similar to the NS control, about 5% of cells are Annexin V positive and Prodidium iodide negative. (C) Transfection of KMS11 cells with Bob1 siRNA did not result in any significant increase in apoptosis. This graph shows the mean values of three independent experiments and error bars represent the standard deviation. LPF: Lipofectamine 2000; NS: Non-specific siRNA.

3.4 Transient transfection of KMS18 with Bob1 and Oct2 siRNA

Unlike KMS11, which only expresses Bob1 mRNA and protein, KMS18 expresses Bob1 mRNA and protein (Figure 3.14), as well as Oct2 mRNA and protein (Figure 3.15). This cell line possesses a t(4;14) translocation that causes it to aberrantly express FGFR3 mRNA and protein (Figure 3.16). Thus, siRNA targeting Bob1 and Oct2 were employed in KMS18 to assess the combined effects of Bob1 and Oct2 knockdown.

KMS18 cells were transfected with siRNA using cationic liposome transfection, as had been used to transfect KMS11. To assess the effectiveness of this transfection method, KMS18 cells were concurrently transfected with a FITC-labeled fluorescent oligonucleotide, and analyzed with flow cytometry. As is shown in Figure 2.1, 98% of KMS18 cells were transfected using this method.
In an attempt to knockdown Bob1 protein expression, KMS18 cells were transfected with Bob1 duplex 2 siRNA. This sequence was previously shown to generate substantial knockdown of Bob1 protein in KMS11 cells at a concentration of 25 nM (Figure 3.18). However, when KMS18 cells were transfected with the same siRNA sequence at concentrations ranging from 50 nM to 200 nM, no changes in Bob1 protein expression were observed 72 hr post-transfection (Figure 3.21). Furthermore, no changes in FGFR3 protein expression were observed, as would be expected.

In a further attempt to knockdown Bob1 protein in KMS18, these cells were serially transfected with three different Bob1 dicer-substrate siRNA duplexes. Transfection of cells with siRNA is only transient, but serial

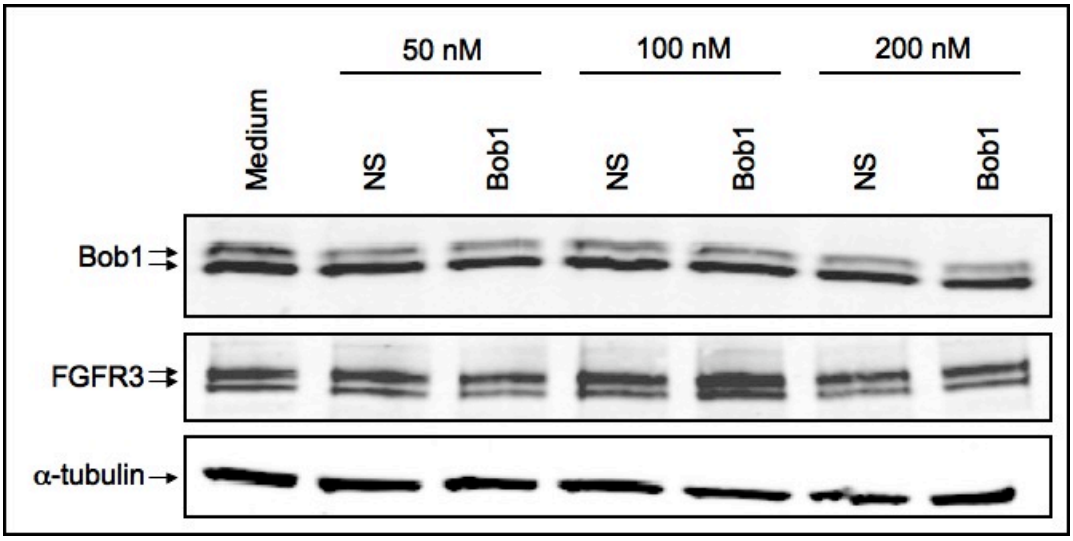

Figure 3.21. Protein expression in KMS18 after Bob1 siRNA transfection. KMS18 cells were transfected with 50 nM, 100 nM or 200 nM Bob1 duplex 2 siRNA and cell lysates were collected 72 hr post-transfection. The expression of Bob1 and FGFR3 protein was analyzed by western blot. Transfection of Bob1 siRNA does not have any effect on Bob1 protein expression, or FGFR3 protein expression. α-tubulin was included as a loading control. NS: Non-specific siRNA.

transfection maintains more "stable" levels of siRNA in the cell. Duplicate samples of KMS18 cells were transfected with 200 nM Bob1 siRNA. After 72 hr, cell lysates were collected from one of the duplicate transfections, and the second set of samples was re-transfected with 200 nM Bob1 siRNA duplexes. These cell lysates were collected 144 hr after the first transfection. A western blot analysis of these samples showed that none of the duplexes tested, including duplex 2, generated knockdown in KMS18 after serial transfection (Figure 3.22).

Since KMS18 also expresses Oct2 mRNA and protein, multiple Oct2 siRNA sequences were tested in this cell line. KMS18 cells were transfected with five different siRNA sequences (114257, 114258, 6416, 6511, 6590) or dicer-substrate siRNA, at 25 nM concentrations. Twenty-four hours and 48 hr post-transfection, total RNA was collected from the cells, reverse transcribed, and relative Oct2 mRNA expression was determined using qRT-PCR. Compared to the non-specific siRNA control, none of the sequences tested generated greater than a 50% decrease in relative Oct2 mRNA expression (Figure 3.23). After 48 hr, the 114257 siRNA sequence generated near 50% knockdown; however, further experiments with higher concentrations of this siRNA did not show any dose-dependent decrease, and even had reduced levels of effectiveness (data not shown).

3.5 Generation of lentiviruses for inducible knockdown of Bob1 and Oct2

Since siRNA-mediated knockdown was unsuccessful in KMS18, lentivirus-delivered shRNA plasmids were tested in an attempt to knockdown

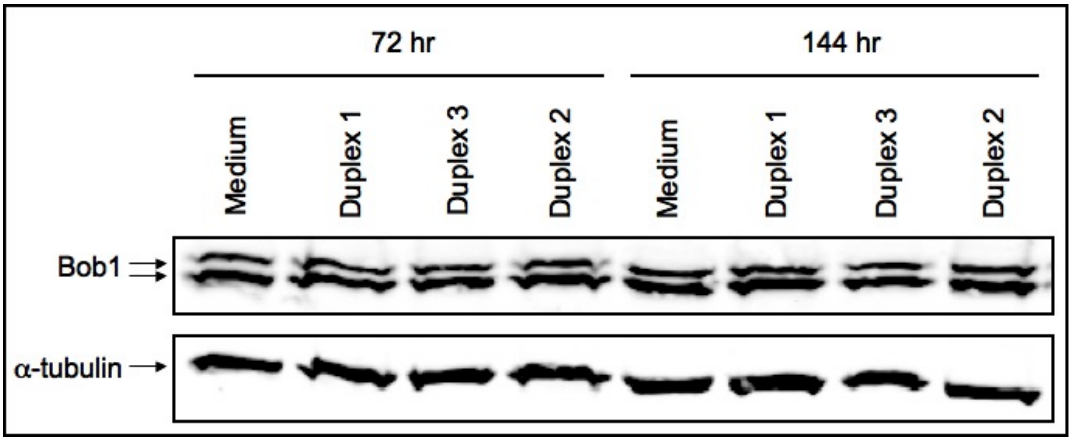

Figure 3.22. Bob1 protein expression in KMS18 after serial Bob1 siRNA transfection. Duplicate samples of KMS18 cells were transfected with three different Bob1 siRNA duplexes at 200 nM concentrations. Cell lysates were collected at 72 hr from one set of samples, while the second set of cells was re-transfected with 200 nM Bob1 siRNA. These cell lysates were collected at 144 hr after the initial transfection. Serial transfection of 200 nM Bob1 siRNA did not affect Bob1 protein expression in KMS18 compared to a medium-only control. α-tubulin was included as a loading control.

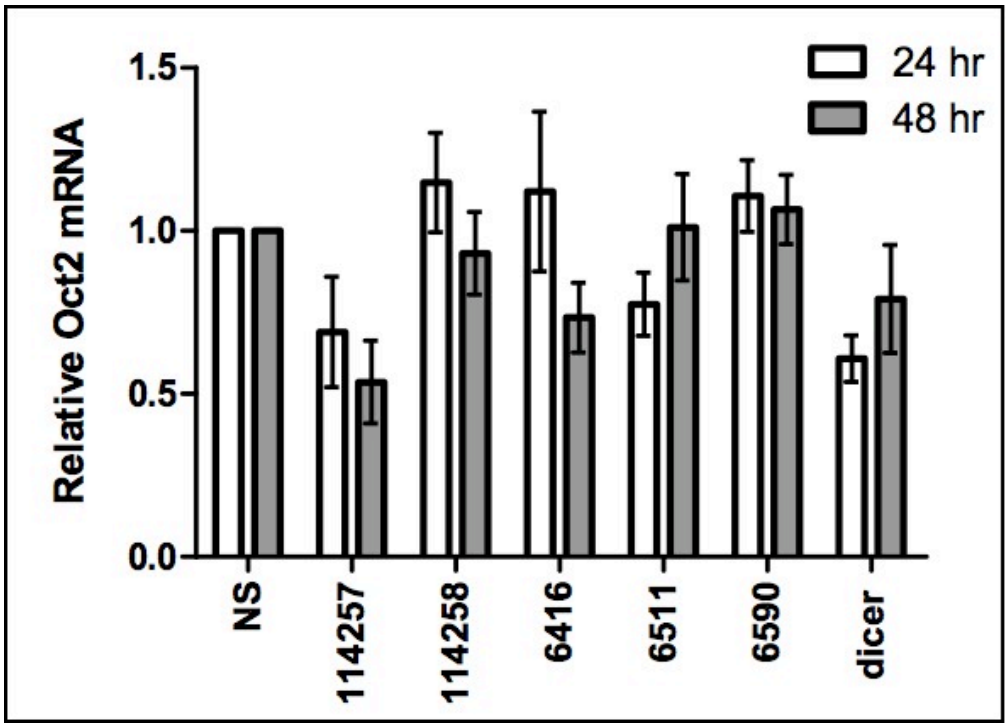

Figure 3.23. Oct2 mRNA expression in KMS18 after transfection with Oct2 siRNA. KMS18 cells were transfected with 5 different siRNA sequences and 1 dicer-substrate siRNA sequence targeting Oct2. Total RNA was extracted from cells 24 hr and 48 hr after transfection, and qRT-PCR was used to determine the relative Oct2 mRNA expression in each sample compared to the NS control. None of the sequences tested generated greater than 50% knockdown of Oct2 mRNA. The error bars represent the standard deviation of triplicate qRT-PCR samples. NS: Non-specific siRNA.

Bob1 and Oct2 in this cell line. KMS11 cells were also transduced with lentivirus shRNA plasmids to generate more stable knockdown of Bob1.

A second generation lentivirus system with a tetracycline inducible shRNA transcript was selected. This lentivirus has been pseudotyped with vesicular stomatitis virus glycoprotein (VSV-G) to increase its tropism. The lentivirus vector integrates into the host cell genome and contains a puromycin resistance marker, so that stable cell lines can be generated. The shRNA and a RFP gene are expressed from the same transcript under the control of a tetracycline inducible promoter to allow for inducible shRNA transcription and a marker for shRNA expression and transduction.

3.5.1 Subcloning Bob1 shRNA from pGIPZ to pTRIPZ

The pTRIPZ lentivirus plasmid is a tetracycline-inducible system, whereas the pGIPZ system is a constitutively expressed shRNA lentivirus plasmid. Since it was hypothesized that knocking down Bob1 and/or Oct2 expression would lead to cell death, the pTRIPZ lentivirus system was chosen to generate stable cell lines that would only express the shRNA insert in the presence of the tetracycline derivative, doxycycline. A non-specific shRNA control pTRIPZ plasmid and an Oct2 shRNA pTRIPZ plasmid were commercially available; however, only the constitutively active pGIPZ plasmid was available for Bob1 shRNA. Therefore, the Bob1 shRNA insert was subcloned from a pGIPZ plasmid to an empty pTRIPZ plasmid.

The restriction enzymes XhoI and MluI were used to cut the Bob1 shRNA insert from the pGIPZ plasmid, and this insert was subcloned into the empty pTRIPZ plasmid (pTRIPZ map Figure 2.3). The presence of the Bob1 shRNA insert in the pTRIPZ plasmid clone was confirmed by restriction digest and agarose gel electrophoresis (Figure 3.24). As a control, the Bob1 shRNA pGIPZ plasmid was digested with XhoI and MluI to show the size and presence of the Bob1 shRNA insert. The Bob1 pTRIPZ clone was also digested with XhoI and MluI and separated alongside the pGIPZ control on an agarose gel. Both plasmids contained a 345 bp fragment, which confirmed the presence of the Bob1 shRNA in the pTRIPZ plasmid. As a second diagnostic restriction digest, the Bob1 pTRIPZ clone was digested with SalI. This digest confirmed the presence of the three expected bands at 7104 bp, 4028 bp and 2188 bp. Sequencing was not used to confirm the presence of the Bob1 shRNA insert. This Bob1 shRNA pTRIPZ clone was used in subsequent lentivirus experiments.

3.5.2 Transduction of KMS11 and KMS18 with lentivirus

Lentivirus particles carrying a non-specific shRNA pTRIPZ plasmid, an Oct2 shRNA pTRIPZ plasmid, or the Bob1 shRNA pTRIPZ plasmid were produced as described in section 2.7.2. The titres of these viruses were all tested in KMS11. When 25 μL of the non-specific, Bob1 or Oct2 concentrated lentivirus was added to KMS11 and incubated for 48 hr in the presence of doxycycline, >90% of KMS11 cells expressed RFP, demonstrating that the viruses produced had high titres (data not shown).

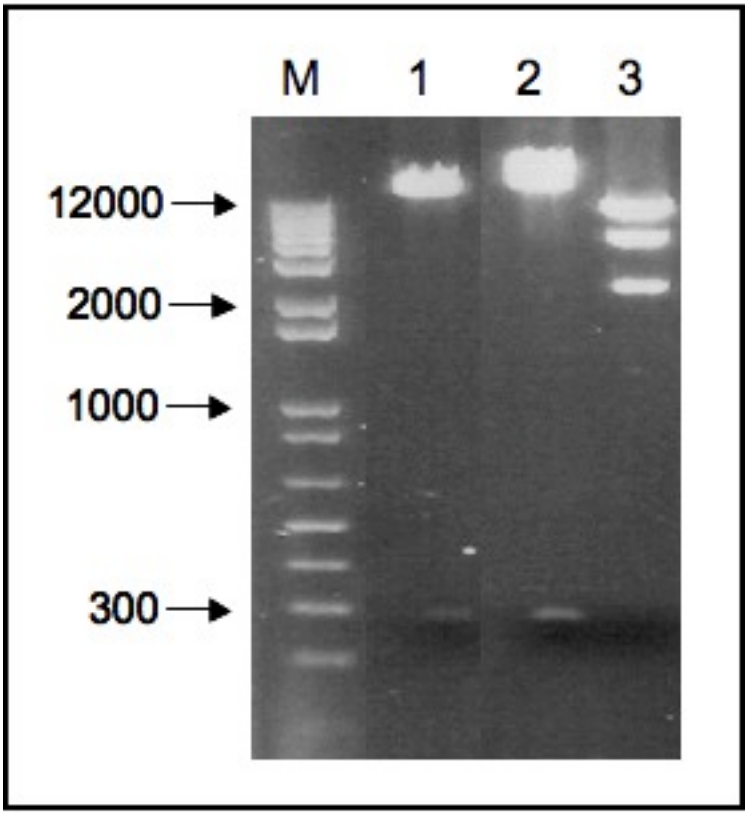

Figure 3.24. Restriction digest agarose gel confirming the presence of Bob1 shRNA in pTRIPZ. A Bob1 shRNA insert was subcloned from the constitutively active pGIPZ plasmid into the tetracycline-inducible pTRIPZ plasmid and the presence of the Bob1 shRNA insert was confirmed by restriction digest and agarose gel electrophoresis. (1) The Bob1 shRNA pGIPZ plasmid was digested with XhoI and MluI as a positive control to show the presence and size of the 345 bp shRNA insert. (2) The Bob1 shRNA pTRIPZ clone was digested with XhoI and MluI, and was shown to contain the 345 bp shRNA insert. (3) A diagnostic SalI digest was performed with the Bob1 shRNA pTRIPZ clone, which generated the expected 7104 bp, 4028 bp and 2188 bp fragments. M: marker.

Once the lentivirus titres were confirmed to be effective, KMS11 cells were transduced with either a non-specific shRNA lentivirus or a Bob1 shRNA lentivirus. Forty-eight hours after transduction, 1 μg/mL puromycin was added to the cells to select for stably transduced cells. The cells were grown in the presence of 1 μg/mL puromycin for 60 days to select for stable pools of cells that expressed the puromycin resistance gene from the pTRIPZ plasmid. From these experiments, 2 non-specific shRNA stable pools and 3 Bob1 shRNA stable pools were produced.

Duplicate samples of these cells were plated, and to induce expression of the shRNA transcript, 2 μg/mL doxycycline was added to half of the plates. As a control for "leakiness" of the tetracycline-inducible system, medium without doxycycline was added to the other half of the plates. The expression of RFP was examined in the stable pools using fluorescence microscopy. Figure 3.25 shows the expression of RFP in the non-specific pTRIPZ 2 stable pool with and without doxycycline. In the absence of doxycycline, approximately 10% of cells express the RFP transcript. When doxycycline is added to the medium, 100% of cells express the RFP transcript. This demonstrates that all of the cells in the stable pool were transduced and expressed the non-specific shRNA from the pTRIPZ plasmid. Figure 3.26 shows the expression of RFP in the Bob1 pTRIPZ 3 stable pool. In the absence of doxycycline in this stable pool of cells, approximately 50% of cells express the RFP transcript, and are therefore "leaky". In the presence of doxycycline, 100% of the cells express RFP and are thus expressing the Bob1 shRNA from the pTRIPZ plasmid.

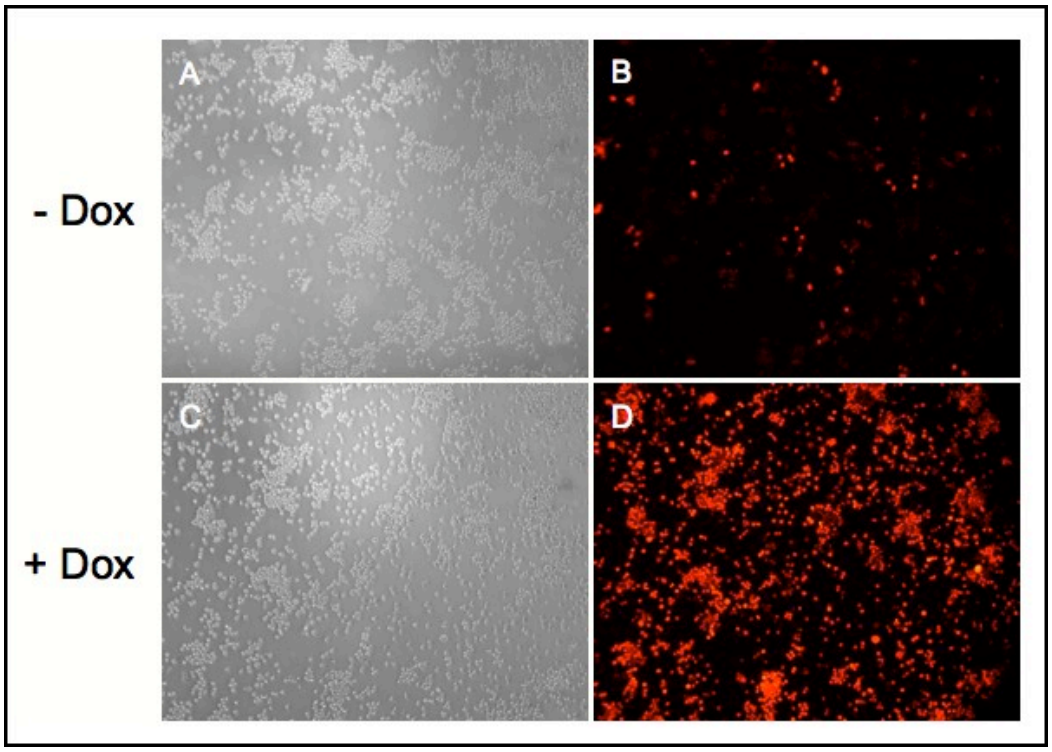

Figure 3.25. Expression of RFP in KMS11 NS pTRIPZ stable cells. KMS11 cells were transduced with NS pTRIPZ lentivirus and transduced cells were stably selected with puromycin. The NS pTRIPZ 2 stable pool is shown here. (A) Bright field image of cells without doxycycline. (B) Without the addition of doxycycline, approximately 10% of the cells express the shRNA transcript. (C) Bright field image of cells with doxycycline. (D) When doxycycline was added to stably transduced NS pTRIPZ cells, 100% of cells expressed the RFP. NS: Non-specific shRNA pTRIPZ; Dox: doxycycline; RFP: red fluorescent protein.

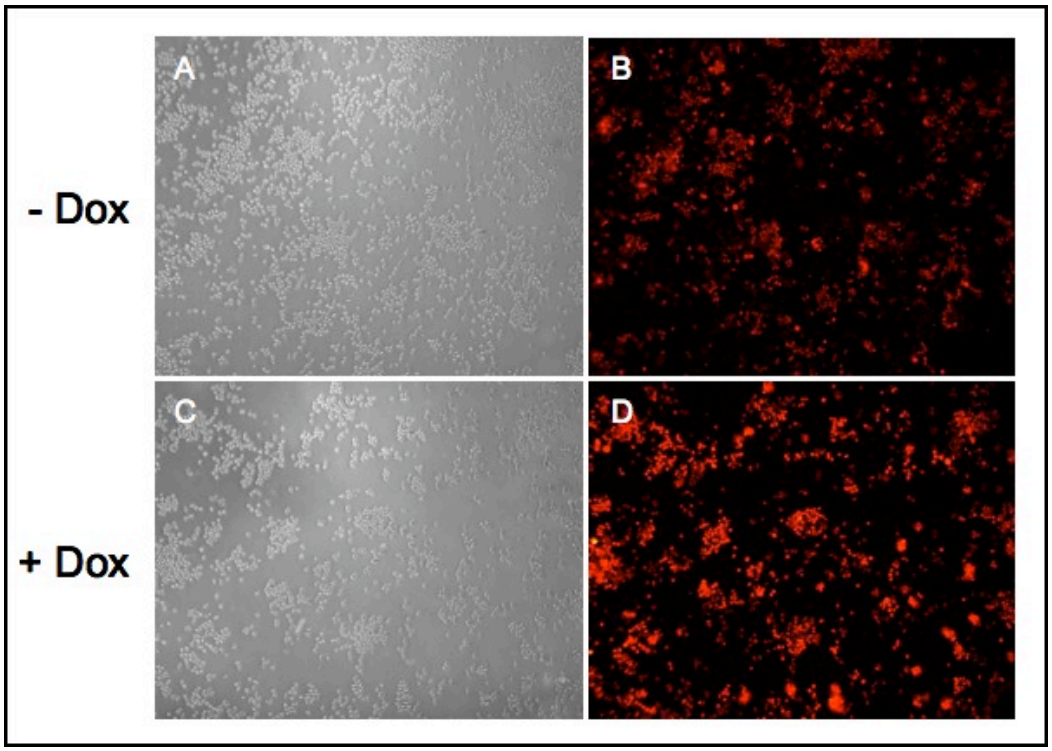

Figure 3.26. Expression of RFP in KMS11 Bob1 pTRIPZ stable cells. KMS11 cells were transduced with Bob1 pTRIPZ lentivirus and transduced cells were stably selected with puromycin. The Bob1 pTRIPZ 3 stable pool is shown here. (A) Bright field image of cells without doxycycline. (B) Without the addition of doxycycline, approximately 50% of the cells express the shRNA transcript at low levels. (C) Bright field image of cells with doxycycline. (D) When doxycycline was added to stably transduced Bob1 pTRIPZ cells, 100% of cells strongly expressed RFP. Dox: doxycycline; RFP: red fluorescent protein.

The expression of RFP in all of the stable pools was confirmed to ensure that the shRNA transcript was being expressed in the cells (data for all pools not shown). Cell lysates were collected 48 hr – 120 hr after the addition of doxycycline from the 2 non-specific pTRIPZ pools and the 3 Bob1 pTRIPZ pools. The level of Bob1 protein was measured by western blot in the stable cell lines, as well as in the KMS11 parent cell line, to assay for Bob1 knockdown. As is shown in Figure 3.27, none of the stable Bob1 shRNA pools had any knockdown of Bob1 protein.

The non-specific, Bob1 and Oct2 shRNA pTRIPZ lentiviruses were all shown to infect KMS11 cells efficiently (data not shown for Oct2 lentivirus). These viruses were then used to transduce KMS18 cells, as described in section 2.7.3. However, in KMS18, these viruses did not transduce more than 1% of cells, as determined by RFP expression (data not shown).

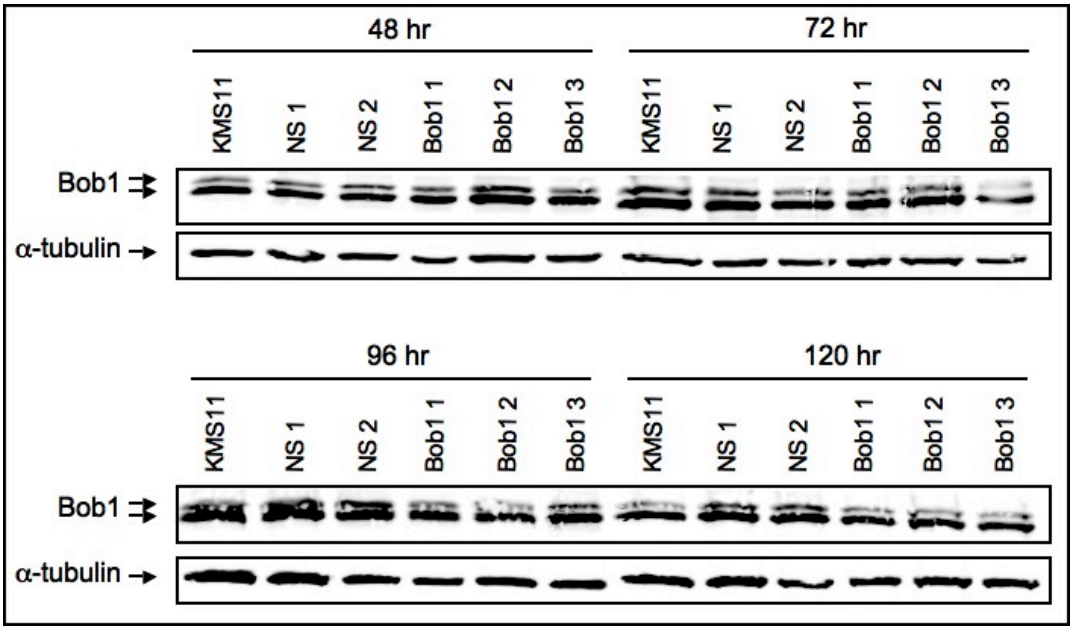

Figure 3.27. Bob1 protein expression in stably transduced KMS11 pools. KMS11 cells were infected with lentivirus particles containing either a NS shRNA pTRIPZ plasmid or a Bob1 shRNA pTRIPZ plasmid. These cells were grown under puromycin selection to select cells containing the shRNA plasmid, and doxycycline was then added to induce shRNA expression. Bob1 expression was assayed by western blot 48 hr – 120 hr after doxycycline addition in 2 NS pTRIPZ stable cell lines and 3 Bob1 pTRIPZ stable cell lines. Compared to the NS controls and the KMS11 parent cell line, Bob1 protein expression remained unchanged after the induction of a Bob1 shRNA transcript. α-tubulin was included as a loading control. NS: Non-specific shRNA pTRIPZ.

4 Discussion

4.1 Expression of Bob1 and Oct2 in myeloma patient samples

The primary objective of this study was to identify novel therapeutic targets for the treatment of multiple myeloma. Since the transcription factors Bob1 and Oct2 are required for activity of the 3'IgH enhancers, we hypothesized that they conferred a survival advantage to translocation-positive myeloma cells. Also, the primarily B cell-restricted expression of these proteins makes them desirable therapeutic targets, as their inhibition would be specific to malignant myeloma cells. To evaluate our hypothesis, we examined the expression of Bob1 and Oct2 mRNA and protein in myeloma patient samples, and correlated protein expression with clinical features. We compared the use of two methods – AQUA scores and H-scores – for measuring protein expression within myeloma patient samples.

Bob1 expression is lymphoid-restricted and is highest in pre-B cells, GC B cells and plasma cells (144-146). Similarly, Oct2 is highly expressed in mature B cells and plasma cells (127, 137). To measure Bob1 and Oct2 gene expression in malignant myeloma cells, patient bone marrow aspirates were sorted based on CD138 expression, and the relative gene expression of Bob1 and Oct2 in the $CD138^+$ and $CD138^-$ patient cell populations was measured using qRT-PCR. Bob1 and Oct2 gene expression was significantly higher in the $CD138^+$ cells compared to the $CD138^-$ cells, and 100% and 86% of patients had higher Bob1 and Oct2 gene expression, respectively, in $CD138^+$ cells. The DAB IHC staining

also qualitatively showed that Bob1 and Oct2 protein expression was highest in plasma cells, and very low or absent in other cell types.

CD138 is a marker of plasma cell differentiation and can be used to identify malignant plasma cells in myeloma patients (180). Although normal plasma cells also express CD138, non-malignant plasma cells only constitute approximately 2% of bone marrow cells (181), so in a myeloma patient, most of the $CD138^+$ cells are malignant plasma cells. By selecting for $CD138^+$ cells, Bob1 and Oct2 expression can be measured in the malignant plasma cells of a patient. The qRT-PCR and DAB IHC data demonstrate that Bob1 and Oct2 gene and protein expression is highest in the plasma cells of myeloma bone marrow samples.

Although Bob1 and Oct2 expression is highest in plasma cells, these proteins are also expressed at variable levels throughout B cell development. Inhibition of Bob1 and Oct2 would thus not be completely specific to plasma cells, but would target all B cells. Rituximab is a monoclonal antibody that specifically binds to CD20 on B cells and is used to treat B cell lymphomas (182). This drug can cause immunosuppression but is generally well tolerated by patients. This suggests that B cell-specific therapies, such as Bob1 or Oct2 inhibitors, would also be well tolerated. Many of the currently used myeloma therapeutics, such as thalidomide, lenalidomide and bortezomib, cause myelosuppression (183), which limits the dose and duration of treatment. Therefore, B cell-specific therapies that primarily target malignant plasma cells

would be well tolerated, and could likely be combined with currently used therapeutics without causing additive side effects.

Many clinical and cytogenetic features have prognostic significance in newly diagnosed myeloma. The ISS has identified serum β_2-microglobulin and serum albumin as powerful, independent predictors of survival in myeloma patients (38). The presence of t(4;14), t(14;16), monosomy 13 or deletion of 17p13 are useful prognostic factors in myeloma (33). We aimed to determine if Bob1 and Oct2 expression have prognostic significance in myeloma, as these data could help to elucidate the biological roles of Bob1 and Oct2 in malignant plasma cells and also determine the potential of these two proteins as therapeutic targets for myeloma.

In the entire patient cohort, patients with high Bob1 AQUA scores had significantly longer OS and PFS than patients with low Bob1 AQUA scores. Notably, the patient group with high Bob1 expression had a significantly higher proportion of transplant recipients than the patient group with low Bob1 AQUA scores. To adjust for known prognostic factors, a multivariate Cox proportional hazards model was used. This model demonstrated that only transplant status was an independent predictor of survival, whereas Bob1, β_2-microglobulin, and albumin were not. Since patients included in this study had been diagnosed at two treatment facilities and had undergone different treatment regimens, we wanted to determine if the same survival trend was present within patient subgroups. Patients who had received an ASCT displayed the same results – the high Bob1 group had significantly longer OS than the low Bob1 group. None of the other

subgroups displayed significant survival differences when dichotomized by Bob1 expression.

Bob1 expression was compared with numerous clinical features as well as treatment response. The only significant association was patients with high Bob1 had increased levels of lactate dehydrogenase (LDH). In myeloma elevated LDH is predictive of poor survival (184). While LDH is a known poor prognostic factor our data demonstrate that Bob1 is a good prognostic factor. Bob1 and LDH levels in our patient cohort may reflect different aspects of myeloma biology that both affect clinical outcome, but are not biologically related. Since multiple statistical analyses were done, it is also possible that this is a false positive result, which is likely to occur when testing multiple hypotheses. When comparing Bob1 expression with treatment response, no differences were observed between patients with high and low Bob1 AQUA scores.

Since Bob1 is required for activity of the 3'IgH enhancer (109, 119, 123), and because this enhancer drives oncogene expression in the 50-75% of myeloma patients who have translocations (35-37), we hypothesized that high Bob1 expression would be associated with a poor prognosis. However, in this study high Bob1 protein expression was associated with improved OS and PFS. These data suggest that the role of Bob1 in myeloma cells extends beyond its ability to activate the 3'IgH enhancer.

Bob1 is necessary for expression of Blimp-1 in terminally differentiated plasma cells (159). Blimp-1 is expressed throughout plasma cell ontogeny, with lower levels in plasmablasts and the highest levels in mature plasma cells (185).

Myeloma patients with high numbers of plasmablasts have shorter survival than patients with mature plasma cell morphology (186). Therefore, high levels of Bob1 protein may be indicative of mature plasma cell morphology in myeloma patients, which would explain why high Bob1 protein expression is associated with improved OS and PFS in this study.

ASCT leads to significantly improved OS and PFS in myeloma patients (13, 14). In this study, we found that the patient group with high Bob1 had a significantly higher proportion of transplant recipients than the patient group with low Bob1, which could explain why the patient group with high Bob1 has a better prognosis. In fact, a multivariate Cox proportional hazards model demonstrated that only transplant status was independently predictive of OS. Patients who are eligible for an ASCT must be young (<65 years) and healthy enough to undergo this aggressive treatment. High Bob1 expression is associated with less aggressive disease, so Bob1 expression is likely higher in healthy patients who subsequently receive a transplant. When comparing the OS of high and low Bob1 patient groups within the transplant subgroup, patients with high Bob1 AQUA scores in fact have a significantly higher median OS than patients with low Bob1 AQUA scores. From these data it appears that high Bob1 expression is a good prognostic factor in myeloma, as patients with high Bob1 are healthier at diagnosis and in the patient subgroup that received ASCT, high Bob1 expression is associated with increased OS.

Conversely to Bob1, patients with high Oct2 expression had significantly shorter OS than patients with low Oct2 expression, although a significant

difference in PFS was not observed. The patient group with low Oct2 had significantly more transplant recipients than the high Oct2 group. In a multivariate Cox proportional hazards model, only transplant status was independently predictive of OS, whereas Oct2, β_2-microglobulin and albumin were not. In an analysis of OS in patient subgroups, no significant differences were observed between patients with high and low Oct2, although the median OS was consistently higher in the groups with low Oct2 expression. When comparing Oct2 expression with clinical features and treatment response, no differences were observed between patients with low Oct2 and high Oct2 expression.

These results corroborate our initial hypothesis that high Oct2 expression is associated with decreased survival in myeloma, due to the ability of Oct2 to activate the 3'IgH enhancer (118, 119, 123), and contribute to overexpression of translocated oncogenes. Since translocation status was not available for all patients, no conclusions can be drawn about the role of Oct2 in translocation-positive myeloma. Oct2 has additional roles in B cells, so there are other explanations for this observation. Oct2 binds to an imperfect octamer site in the *blr1* gene promoter, which encodes the chemokine receptor CXCR5, and activates transcription of this gene (165). CXCR5 expression is upregulated on plasma cells isolated from the peripheral blood and pleural effusion of myeloma patients (187). Therefore, high Oct2 expression could induce high CXCR5 expression, and in turn confer a more aggressive phenotype to the malignant plasma cells.

As with Bob1, the disproportionately high number of patients with low Oct2 expression who received a transplant explains why this group of patients had

increased OS. Low Oct2 expression is associated with less aggressive disease and patients with low Oct2 expression are likely healthier at diagnosis. Thus, these patients are able to withstand more aggressive, but superior, treatment regimens. The patient subgroup analyses do not show any statistically significant differences in OS based on Oct2 expression, but patients with low Oct2 consistently have higher median OS compared to patients with high Oct2 expression. Also, it should be pointed out that the CCI subgroup showed a near significant survival difference ($p=0.0554$). Together, these results demonstrate that low Oct2 expression is associated with less aggressive disease and patients with low Oct2 are likely healthier at diagnosis. The high proportion of patients with low Oct2 who received an ASCT partially explains the OS data, but the subgroup analyses also suggest that low Oct2 expression is associated with a better prognosis, independently of the treatment received.

Bob1 and Oct2 are known to interact at octamer sites and act synergistically to increase promoter and enhancer activity (109, 119, 123, 130-132). However, the statistically measured interaction between Bob1 and Oct2 was not predictive of survival in our patient cohort. In this study Bob1 and Oct2 have inverse associations with OS in myeloma patients. In a continuous correlation measurement, the relationship between Bob1 and Oct2 protein expression showed a positive, medium correlation (Spearman's $r = 0.3601$). The correlation of Bob1 and Oct2 mRNA expression in plasma cells for a separate, partially overlapping, patient cohort was larger (Spearman's $r = 0.8608$). Therefore, these results indicate that the regulation and function of Bob1 and Oct2 within B cells, and

specifically in myeloma plasma cells, are likely concerted as well as independent of one another. Since the mRNA correlation is larger than the protein correlation, this suggests that the transcriptional regulation between Bob1 and Oct2 is concerted, whereas the translational regulation is more divergent. Two isoforms of Bob1 are present in B cells – p35 is located in the cytoplasm and p34 localizes to the nucleus (142). The p35 isoform binds to and stabilizes Syk protein, a tyrosine kinase that mediates BCR signaling (188). This function of Bob1 in B cells is independent of Oct2. Oct2 binds to the promoter of CD36, a receptor found on mouse B cells, and activates transcription of this gene, independently of Bob1 binding (189). Bob1 was originally identified based on its association and synergism with Oct2 (130-132), and thus many of its known functions are in concert with Oct2. As further research elucidates the role of these two proteins in B cell development, additional independent functions will likely be identified.

From this study, Bob1 and Oct2 expression has been shown to correlate directly and inversely, respectively, with OS in myeloma. High Bob1 and low Oct2 expression is associated with less aggressive disease, and these patients are healthier at diagnosis and able to withstand ASCT treatment regimens. Also, the patient subgroup analyses demonstrate that Bob1 and Oct2 have prognostic value that is independent of the treatment received, and likely reflects the biological role of these proteins in myeloma. Since Bob1 and Oct2 activate the 3'IgH enhancers, we hypothesized that these proteins would be adverse prognostic markers in myeloma. Translocation status was not available for the majority of the patients in our study, and we could not experimentally test for translocations in the samples

we had. In order to elucidate the role of Bob1 and Oct2 specifically in translocation-positive myeloma, we would like to repeat this analysis in a patient cohort for which cytogenetics data are available.

As this was an exploratory study with a limited sample size, the results of this study should be interpreted with caution. Furthermore, analyzing patients from the CCI and TBCC as one group adds experimental variation that may impact the results. As is shown in Table 3.1, the median survivor follow-up time has yet to reach the median OS in the patient cohort, and fewer than half of the patients were deceased at the most recent follow-up. Therefore, these results could change at a later follow-up time. In order to confirm the results of this study, these results must be independently verified in a larger, prospective study specifically designed to evaluate the prognostic significance of Bob1 and Oct2 expression.

4.2 Comparing the AQUA score and H-score methods

In order to measure protein expression in myeloma bone marrow biopsy samples, two methods were used – DAB IHC with H-scores and fluorescent IHC with AQUA scores. Like many experimental techniques, both of these methods have benefits and drawbacks. The H-score method is limited because the CD138 and target antigens cannot be stained on the same slide. Instead, adjacent slides are stained for each antigen, and the observers must identify malignant cells on one slide using the CD138 stain, and then measure the target protein expression in the corresponding region of the adjacent slide. H-scores are dependent on the

observers' ability to differentiate between negative, weak and strong staining cells. However, this method allows the observers to directly examine cell morphology, and easily distinguish malignant plasma cells from tissue that can stain falsely positive for CD138. Also, the H-score method requires only a light microscope for quantification.

The AQUA score method is beneficial because the CD138 and target antigens can be stained on the same slide. An automated system is used to identify the $CD138^{+}$ cells and only measure the target protein within these cells. This method does not rely on the observers' ability to differentiate between strong and weak staining cells, but rather measures the number and intensity of target pixels within the tumour mask to generate an AQUA score. However, as this system does not examine cell morphology, autofluorescent red blood cells and trabeculae may be falsely included if the user does not identify these false positive areas and exclude them from the final analysis. The equipment required for this method is also not readily available and is costly.

When comparing the inter-rater agreement between the H-score and AQUA score methods in our analysis, a fair agreement was observed for Bob1 and Oct2 (Bob1 kappa=0.278, Oct2 kappa=0.320). For both Bob1 and Oct2, approximately two thirds of the patients were identically categorized as above or below the median by both methods. The OS survival analyses were also repeated using the H-scores. H-scores were only available for patients diagnosed at the CCI, so the results of this analysis should be compared to the CCI subgroup for Bob1 and Oct2 AQUA score OS data. For the Bob1 and Oct2 OS analyses,

neither the H-score nor AQUA score methods showed statistically significant differences.

The AQUA score method correlates highly with a pathologist-based H-score method for measuring estrogen receptor expression in breast cancer tissue, and this automated analysis was shown to be more reproducible than the H-score method (190). AQUA scores obtained from one histospot are representative of the whole tissue specimen in 90% of cases (190). In our analysis, the agreement between the AQUA scores and H-scores was fair, as two thirds of the samples were identically categorized as high or low by both methods. This agreement would likely increase if H-scores were measured by experienced pathologists. The AQUA score method removes observer bias, and is thus more reproducible. However, both methods are dependent on CD138 staining to correctly identify malignant cells. In approximately 15% of myeloma cases, stromal cells stain weakly positive for CD138 (191), and could therefore be falsely identified as malignant cells. Both methods are susceptible to variations in tissue handling and IHC staining procedures. Based on the results of this study, we cannot determine which method is more accurate for quantification of protein expression in myeloma TMA samples. The reproducibility of AQUA scores and the absence of observer bias with this method are key advantages over the H-score method.

4.3 Silencing the IgH enhancer in t(4;14) myeloma

Translocations involving the IgH locus on 14q32 are common to numerous hematological malignancies, including multiple myeloma and non-

Hodgkin's lymphoma (35-37, 42). The strong enhancers in the IgH locus are responsible for dysregulation of oncogenes from the translocated chromosome, which is an important step in the transformation process (51, 105, 192). Therefore, suppressing the activity of the IgH enhancers should lead to decreased expression of the translocated oncogene. This hypothesis has been confirmed in follicular lymphoma. Inhibiting the expression of Oct2, Oct1 and Bob1, which are all required for IgH enhancer activity, led to decreased expression of the translocated oncogene, bcl-2, and increased apoptosis in these cells (124). Similarly, we hypothesized that inhibiting the expression of Bob1 and Oct2 in t(4;14) myeloma cell lines would lead to reduced expression of FGFR3.

The expression of Bob1, Oct2 and FGFR3 transcripts and proteins was measured in a panel of t(4;14) myeloma cells lines. KMS11 and KMS18 aberrantly express FGFR3, and were therefore suitable model systems for testing our hypothesis. KMS11 only expresses Bob1, whereas KMS18 expresses both Bob1 and Oct2. Therefore, we aimed to inhibit the expression of Bob1 in KMS11 and Bob1 and Oct2 in KMS18 using RNAi to test the effects of this approach on t(4;14) myeloma cells.

Bob1 mRNA and protein expression were successfully knocked down in KMS11 using dicer-substrate siRNA. Following Bob1 knockdown, the total cellular FGFR3 protein levels were significantly decreased, in following with decreased activity of the 3'IgH enhancer. Since previous groups have shown that specifically inhibiting FGFR3 in t(4;14) myeloma cells, including KMS11, leads to decreased viability and increased apoptosis (79-85), we sought to determine if

our approach would induce similar effects. However, following Bob1 knockdown and decreased FGFR3 expression, only a very small decrease in viability was observed, and no difference in the number of cells undergoing apoptosis was present.

The absence of anti-proliferative and pro-apoptotic effects was surprising, based on previous studies of FGFR3 inhibition in t(4;14) myeloma cells lines, which included KMS11. However, our study only measured the reduction of total cellular FGFR3 after Bob1 knockdown. Since FGFR3 is a receptor tyrosine kinase, the expression of FGFR3 at the plasma membrane should be measured by flow cytometry or microscopy. FGFR3 signaling activates the MAPK pathway to promote proliferation (66), so the phosphorylation of MAPK pathway mediators, such as ERK1 and ERK2, should be measured. It is possible that the remaining FGFR3 in the cell is sufficient to activate proliferative and anti-apoptotic pathways. Therefore, downstream FGFR3 signaling would need to be measured to confirm this. The results that we observed may be specific to the KMS11 cell line and need to be confirmed in additional t(4;14) myeloma cell lines. In addition to a t(4;14) translocation, KMS11 has activating ras mutations and a t(14;16) translocation (63). These mutations may confer a survival advantage to KMS11 that make this cell line resistant to FGFR3 inhibition. The differences that we observed compared to other groups working with KMS11 could also be due to mutations that have occurred in this cell line over time. Since KMS11 was isolated over twenty years ago (193), the KMS11 cells in our possession are not likely the same as KMS11 cells used by other laboratories.

The results of our study also suggest that downregulation of FGFR3 alone is not capable of inhibiting the growth of t(4;14) myeloma cells. The small molecule inhibitors used to inhibit FGFR3 activity are not specific to FGFR3, but rather target multiple receptor tyrosine kinases, such as vascular endothelial growth factor receptor 2 and platelet-derived growth factor receptor (80-84). Inhibition of receptor tyrosine kinases other than FGFR3 may contribute to decreased viability and increased apoptosis in myeloma cell lines. However, the anti-proliferative and pro-apoptotic effects that result following shRNA-mediated FGFR3 inhibition specifically demonstrate that FGFR3 is involved in growth and survival of t(4;14) myeloma cells (78).

It would be interesting to measure the expression of MMSET following Bob1 knockdown in KMS11. As MMSET is also dysregulated due to the t(4;14) translocation (67, 68), and has been shown to confer oncogenic properties to myeloma cells (69, 70), MMSET in KMS11 could contribute to cell growth. Also, since approximately one third of t(4;14) patients lose FGFR3 expression, MMSET is likely a major contributor to t(4;14) oncogenesis (87, 88). Although our approach would be expected to reduce MMSET levels, since we are inhibiting the IgH enhancers, these results would need to be confirmed experimentally. If the MMSET levels in KMS11 persisted after Bob1 knockdown, this could explain why no changes in cell viability or apoptosis were observed in KMS11.

4.4 KMS18 RNAi and lentivirus-mediated RNAi in KMS11 and KMS18

In order to further test our hypothesis, we aimed to knockdown Bob1 and Oct2 protein in the t(4;14) myeloma cell line, KMS18. Since KMS18 expresses both Bob1 and Oct2, inhibiting the expression of these two proteins required for 3'IgH enhancer activity might have a more pronounced effect on FGFR3 expression. Using a second cell line as a model system to test our hypothesis would help us to determine if the effects we observed in KMS11 were true to t(4;14) myeloma, or if they were specific to the KMS11 cell line.

To knockdown Bob1 in KMS18, the same dicer-substrate siRNA sequence that had successfully been used to knockdown Bob1 protein in KMS11 was used. Despite high transfection efficiency in KMS18, no knockdown of Bob1 protein was achieved. In KMS11, this siRNA had been used at 25 nM, but at a concentration of 200 nM in KMS18, no knockdown was observed. We tested two additional dicer-substrate siRNA sequences targeting Bob1 in KMS18. As is shown in Figure 2.2, the Bob1 siRNA sequences spanned a large region on the Bob1 transcript. Thus, if mutations were present in the Bob1 transcript in KMS18, it is likely that at least one of the siRNA sequences would still bind to the transcript to induce transcript degradation.

Similarly, we tested one dicer-substrate siRNA sequence and five siRNA sequences targeting Oct2 in KMS18. None of these sequences efficiently knocked down Oct2 transcript levels in KMS18. Figure 2.2 shows that the sequences tested span the Oct2 transcript. Therefore, sequence mutations or splice variants of the

Oct2 transcript present in KMS18 should still be recognized by several of the siRNA sequences used.

Since nine different sequences tested to knockdown Bob1 and Oct2 proteins were all inefficient in KMS18, it is likely that the defect is not sequence-specific, but rather inherent to KMS18, or to the method used. It is possible that the RNAi pathway in KMS18 is not functional, as the Bob1 sequence that was confirmed to be efficient in KMS11 failed to yield any knockdown of Bob1 in KMS18. In order to test this, more positive controls that have confirmed knockdown in other cell lines should be tested in KMS18. Another possibility is that the transfection method used in KMS18 is problematic. Using cationic lipid transfection, we were able to transfect KMS18 with greater than 95% efficiency, as determined by transfection of the cells with a fluorescent oligonucleotide and flow cytometry. However, we did not examine the localization of the fluorescent oligonucleotide within the cells using microscopy, so we cannot confirm that the oligonucleotide entered the cell. It is possible that the transfection reagent and nucleic acid bound to the plasma membrane, but did not actually enter the cell, and thus appeared to be transfected with flow cytometry, but would not generate any knockdown.

In addition to siRNA, lentivirus-delivered shRNA vectors were tested in KMS11 and KMS18 to knockdown Bob1 and Oct2. This method of shRNA delivery is beneficial because lentivirus particles stably infect cells with high titres (194). The lentivirus system that we used has a puromycin resistance gene

for stable selection in mammalian cells, as well as a tetracycline-inducible promoter for inducible expression of the shRNA transcript (Figure 2.3).

KMS11 cells were efficiently transduced with lentivirus, and three pools of KMS11 cells stably infected with Bob1 pTRIPZ lentivirus were generated. Although the shRNA transcript used in this system is under the control of a tetracycline-inducible promoter, the transcript was still expressed in the absence of tetracycline, which demonstrates that this system is "leaky". Not all cells in the pool were leaky, so it is likely that the integration site of the lentivirus is important for regulation of this promoter. When knockdown of Bob1 was assayed in the stable pools, no decrease in Bob1 protein was observed. In order to generate stable knockdowns, clones should be selected. The site of integration of the lentivirus genome can affect the expression of the shRNA transcript, and thus the knockdown efficiency. Therefore, even if certain clones generated knockdown, this effect would be lost when the entire pool was assayed.

Greater than 90% of KMS11 cells were transduced by lentivirus; however, less than 1% of KMS18 cells were transduced using the same viruses. KMS11 cells are adherent, whereas KMS18 cells grow in suspension. Thus, the lentivirus particles may not contact KMS18 as efficiently as KMS11, and are unable to transduce this cell line. Lentivirus particles are pseudotyped with VSV-G to increase their tropism (195). If these lentivirus particles do not bind to KMS18, then the virus would not be internalized by these cells.

4.5 Concluding remarks

The results of our study suggest that Bob1 is a good prognostic factor in myeloma patients, whereas Oct2 is a poor prognostic factor. A previous study found that Bob1 is part of an amplicon on 11q23 that is overexpressed in myeloma, and knockdown of Bob1 caused cell death in myeloma cell lines (196), which contradicts the results of our study. As we originally hypothesized, knocking down Bob1 in a t(4;14) cell line, which overexpresses FGFR3, led to decreased expression of FGFR3 protein, in keeping with decreased activity of the 3'IgH enhancer. However, this did not lead to decreased cell viability or increased apoptosis in KMS11. In order to conclusively determine how Bob1 knockdown affects t(4;14) myeloma, additional cell lines need to be tested, and to definitively determine how Bob1 affects patient prognosis, studies of a larger patient cohort are necessary.

Despite the fact that Bob1 knockdown did not lead to decreased cell viability, these results demonstrate that knockdown of Bob1 does, in fact, lead to decreased expression of the translocated oncogene FGFR3 in t(4;14) myeloma. Since multiple recurrent translocations are present in myeloma, and in many cases the translocation partner is unidentified (197), an approach that targets the IgH enhancers would be beneficial in many myeloma patients and should be further evaluated. The t(4;14) and t(11;14) translocations can result in overexpression of two oncogenes simultaneously (60, 67, 68), and other unidentified oncogenes may also be dysregulated due to translocations. Inhibiting the IgH enhancers through inhibition of Bob1, and possibly Oct2, is not specific to one oncogene, so could

be an effective treatment strategy in patients with these translocations. Since our approach does not specifically target the translocated oncogene, but rather the enhancers responsible for overexpression of the oncogene, myeloma cell lines with t(11;14), t(14;16) or t(6;14) should be tested to see if similar results are observed.

A major limitation of chemotherapy is the harmful side effects caused by these drugs. Identification of novel therapeutic targets and the development of targeted therapies for cancer treatment are thus very important. The benefit of targeted therapies is evidenced by the use of imatinib mesylate (Gleevec) for the treatment of chronic myeloid leukaemia (CML). This drug specifically targets the t(9;22) translocation bcr-abl fusion product, and has been very successful in the treatment of CML (198). Similarly, targeting Bob1 and Oct2 proteins in translocation-positive myeloma would be a targeted treatment strategy that should result in minimal side effects. Based on the results of Bob1 and Oct2 knockdown in follicular lymphoma, as well as our results that show inhibiting Bob1 leads to decreased FGFR3 expression in t(4;14) myeloma, these studies should be pursued to further determine the potential of Bob1 and Oct2 as therapeutic targets for the treatment of translocation-positive myeloma, as well as other hematological malignancies.

5 Bibliography

1.Criteria for the classification of monoclonal gammopathies, multiple myeloma and related disorders: a report of the International Myeloma Working Group. British journal of haematology 2003;121(5):749-757.

2.Kyle RA, Gertz MA, Witzig TE*, et al.* Review of 1027 patients with newly diagnosed multiple myeloma. Mayo Clinic proceedings 2003;78(1):21-33.

3.Kumar SK, Rajkumar SV, Dispenzieri A*, et al.* Improved survival in multiple myeloma and the impact of novel therapies. Blood 2008;111(5):2516-2520.

4.Canadian Cancer Statistics 2008 Canadian Cancer Society/ National Cancer Institute of Canada;Toronto, Canada.

5.McPhedran P, Heath CW, Jr., Garcia J. Multiple myeloma incidence in metropolitan Atlanta, Georgia: racial and seasonal variations. Blood 1972;39(6):866-873.

6.Brown LM, Linet MS, Greenberg RS*, et al.* Multiple myeloma and family history of cancer among blacks and whites in the U.S. Cancer 1999;85(11):2385-2390.

7.Lynch HT, Ferrara K, Barlogie B*, et al.* Familial myeloma. The New England journal of medicine 2008;359(2):152-157.

8.Billadeau D, Ahmann G, Greipp P, Van Ness B. The bone marrow of multiple myeloma patients contains B cell populations at different stages of differentiation that are clonally related to the malignant plasma cell. The Journal of experimental medicine 1993;178(3):1023-1031.

9.Szczepek AJ, Seeberger K, Wizniak J, Mant MJ, Belch AR, Pilarski LM. A high frequency of circulating B cells share clonotypic Ig heavy-chain VDJ rearrangements with autologous bone marrow plasma cells in multiple myeloma, as measured by single-cell and in situ reverse transcriptase-polymerase chain reaction. Blood 1998;92(8):2844-2855.

10.Bakkus MH, Heirman C, Van Riet I, Van Camp B, Thielemans K. Evidence that multiple myeloma Ig heavy chain VDJ genes contain somatic mutations but show no intraclonal variation. Blood 1992;80(9):2326-2335.

11.Kyle RA, Therneau TM, Rajkumar SV*, et al.* A long-term study of prognosis in monoclonal gammopathy of undetermined significance. The New England journal of medicine 2002;346(8):564-569.

12.Landgren O, Kyle RA, Pfeiffer RM*, et al.* Monoclonal gammopathy of undetermined significance (MGUS) precedes multiple myeloma: a prospective study. Blood 2009.

13.Attal M, Harousseau JL, Stoppa AM*, et al.* A prospective, randomized trial of autologous bone marrow transplantation and chemotherapy in multiple myeloma. Intergroupe Francais du Myelome. The New England journal of medicine 1996;335(2):91-97.

14.Child JA, Morgan GJ, Davies FE*, et al.* High-dose chemotherapy with hematopoietic stem-cell rescue for multiple myeloma. The New England journal of medicine 2003;348(19):1875-1883.

15.Attal M, Harousseau JL, Facon T*, et al.* Single versus double autologous stem-cell transplantation for multiple myeloma. The New England journal of medicine 2003;349(26):2495-2502.

16.Singhal S, Mehta J, Desikan R*, et al.* Antitumor activity of thalidomide in refractory multiple myeloma. The New England journal of medicine 1999;341(21):1565-1571.

17.Palumbo A, Bringhen S, Caravita T*, et al.* Oral melphalan and prednisone chemotherapy plus thalidomide compared with melphalan and prednisone alone in elderly patients with multiple myeloma: randomised controlled trial. Lancet 2006;367(9513):825-831.

18.Facon T, Mary JY, Hulin C*, et al.* Melphalan and prednisone plus thalidomide versus melphalan and prednisone alone or reduced-intensity autologous stem cell transplantation in elderly patients with multiple myeloma (IFM 99-06): a randomised trial. Lancet 2007;370(9594):1209-1218.

19.Rajkumar SV, Blood E, Vesole D, Fonseca R, Greipp PR. Phase III clinical trial of thalidomide plus dexamethasone compared with dexamethasone alone in newly diagnosed multiple myeloma: a clinical trial coordinated by the Eastern Cooperative Oncology Group. J Clin Oncol 2006;24(3):431-436.

20.Richardson PG, Schlossman RL, Weller E*, et al.* Immunomodulatory drug CC-5013 overcomes drug resistance and is well tolerated in patients with relapsed multiple myeloma. Blood 2002;100(9):3063-3067.

21.Wang M, Dimopoulos MA, Chen C*, et al.* Lenalidomide plus dexamethasone is more effective than dexamethasone alone in patients with relapsed or refractory multiple myeloma regardless of prior thalidomide exposure. Blood 2008;112(12):4445-4451.

22.San Miguel JF, Schlag R, Khuageva NK*, et al.* Bortezomib plus melphalan and prednisone for initial treatment of multiple myeloma. The New England journal of medicine 2008;359(9):906-917.

23.Harousseau JL, Attal M, Leleu X*, et al.* Bortezomib plus dexamethasone as induction treatment prior to autologous stem cell transplantation in patients with newly diagnosed multiple myeloma: results of an IFM phase II study. Haematologica 2006;91(11):1498-1505.

24.Richardson PG, Sonneveld P, Schuster MW*, et al.* Bortezomib or high-dose dexamethasone for relapsed multiple myeloma. The New England journal of medicine 2005;352(24):2487-2498.

25.Drach J, Schuster J, Nowotny H*, et al.* Multiple myeloma: high incidence of chromosomal aneuploidy as detected by interphase fluorescence in situ hybridization. Cancer research 1995;55(17):3854-3859.

26.Debes-Marun CS, Dewald GW, Bryant S*, et al.* Chromosome abnormalities clustering and its implications for pathogenesis and prognosis in myeloma. Leukemia 2003;17(2):427-436.

27.Smadja NV, Bastard C, Brigaudeau C, Leroux D, Fruchart C. Hypodiploidy is a major prognostic factor in multiple myeloma. Blood 2001;98(7):2229-2238.

28.Avet-Loiseau H, Attal M, Moreau P*, et al.* Genetic abnormalities and survival in multiple myeloma: the experience of the Intergroupe Francophone du Myelome. Blood 2007;109(8):3489-3495.

29.Sawyer JR, Waldron JA, Jagannath S, Barlogie B. Cytogenetic findings in 200 patients with multiple myeloma. Cancer genetics and cytogenetics 1995;82(1):41-49.

30.Fonseca R, Debes-Marun CS, Picken EB*, et al.* The recurrent IgH translocations are highly associated with nonhyperdiploid variant multiple myeloma. Blood 2003;102(7):2562-2567.

31.Hanamura I, Stewart JP, Huang Y*, et al.* Frequent gain of chromosome band 1q21 in plasma-cell dyscrasias detected by fluorescence in situ hybridization: incidence increases from MGUS to relapsed myeloma and is related to prognosis and disease progression following tandem stem-cell transplantation. Blood 2006;108(5):1724-1732.

32.Moreau P, Facon T, Leleu X*, et al.* Recurrent 14q32 translocations determine the prognosis of multiple myeloma, especially in patients receiving intensive chemotherapy. Blood 2002;100(5):1579-1583.

33.Fonseca R, Blood E, Rue M*, et al.* Clinical and biologic implications of recurrent genomic aberrations in myeloma. Blood 2003;101(11):4569-4575.

34.Xiong W, Wu X, Starnes S*, et al.* An analysis of the clinical and biologic significance of TP53 loss and the identification of potential novel transcriptional targets of TP53 in multiple myeloma. Blood 2008;112(10):4235-4246.

35.Nishida K, Tamura A, Nakazawa N*, et al.* The Ig heavy chain gene is frequently involved in chromosomal translocations in multiple myeloma and plasma cell leukemia as detected by in situ hybridization. Blood 1997;90(2):526-534.

36.Avet-Loiseau H, Brigaudeau C, Morineau N*, et al.* High incidence of cryptic translocations involving the Ig heavy chain gene in multiple myeloma, as shown by fluorescence in situ hybridization. Genes, chromosomes & cancer 1999;24(1):9-15.

37.Avet-Loiseau H, Li JY, Facon T*, et al.* High incidence of translocations t(11;14)(q13;q32) and t(4;14)(p16;q32) in patients with plasma cell malignancies. Cancer research 1998;58(24):5640-5645.

38.Greipp PR, San Miguel J, Durie BG*, et al.* International staging system for multiple myeloma. J Clin Oncol 2005;23(15):3412-3420.

39.Keats JJ, Reiman T, Maxwell CA*, et al.* In multiple myeloma, t(4;14)(p16;q32) is an adverse prognostic factor irrespective of FGFR3 expression. Blood 2003;101(4):1520-1529.

40.Shaughnessy JD, Jr., Zhan F, Burington BE*, et al.* A validated gene expression model of high-risk multiple myeloma is defined by deregulated expression of genes mapping to chromosome 1. Blood 2007;109(6):2276-2284.

41.Zhan F, Barlogie B, Mulligan G, Shaughnessy JD, Jr., Bryant B. High-risk myeloma: a gene expression based risk-stratification model for newly diagnosed multiple myeloma treated with high-dose therapy is predictive of outcome in relapsed disease treated with single-agent bortezomib or high-dose dexamethasone. Blood 2008;111(2):968-969.

42.Harris NL, Jaffe ES, Stein H*, et al.* A revised European-American classification of lymphoid neoplasms: a proposal from the International Lymphoma Study Group. Blood 1994;84(5):1361-1392.

43.Bergsagel PL, Kuehl WM. Chromosome translocations in multiple myeloma. Oncogene 2001;20(40):5611-5622.

44.Avet-Loiseau H, Facon T, Daviet A*, et al.* 14q32 translocations and monosomy 13 observed in monoclonal gammopathy of undetermined significance delineate a multistep process for the oncogenesis of multiple myeloma. Intergroupe Francophone du Myelome. Cancer research 1999;59(18):4546-4550.

45.Tiedemann RE, Gonzalez-Paz N, Kyle RA*, et al.* Genetic aberrations and survival in plasma cell leukemia. Leukemia 2008;22(5):1044-1052.

46.Jung D, Giallourakis C, Mostoslavsky R, Alt FW. Mechanism and control of V(D)J recombination at the immunoglobulin heavy chain locus. Annual review of immunology 2006;24:541-570.

47.Zhang K. Immunoglobulin class switch recombination machinery: progress and challenges. Clinical immunology (Orlando, Fla 2000;95(1 Pt 1):1-8.

48.Tsujimoto Y, Gorham J, Cossman J, Jaffe E, Croce CM. The t(14;18) chromosome translocations involved in B-cell neoplasms result from mistakes in VDJ joining. Science (New York, NY 1985;229(4720):1390-1393.

49.Stamatopoulos K, Kosmas C, Belessi C*, et al.* Molecular analysis of bcl-1/IgH junctional sequences in mantle cell lymphoma: potential mechanism of the t(11;14) chromosomal translocation. British journal of haematology 1999;105(1):190-197.

50.Joos S, Falk MH, Lichter P*, et al.* Variable breakpoints in Burkitt lymphoma cells with chromosomal t(8;14) translocation separate c-myc and the IgH locus up to several hundred kb. Human molecular genetics 1992;1(8):625-632.

51.Bergsagel PL, Chesi M, Nardini E, Brents LA, Kirby SL, Kuehl WM. Promiscuous translocations into immunoglobulin heavy chain switch regions in multiple myeloma. Proceedings of the National Academy of Sciences of the United States of America 1996;93(24):13931-13936.

52.Fenton JA, Pratt G, Rawstron AC*, et al.* Genomic characterization of the chromosomal breakpoints of t(4;14) of multiple myeloma suggests more than one possible aetiological mechanism. Oncogene 2003;22(7):1103-1113.

53.Chesi M, Bergsagel PL, Brents LA, Smith CM, Gerhard DS, Kuehl WM. Dysregulation of cyclin D1 by translocation into an IgH gamma switch region in two multiple myeloma cell lines. Blood 1996;88(2):674-681.

54.Fenton JA, Pratt G, Rothwell DG, Rawstron AC, Morgan GJ. Translocation t(11;14) in multiple myeloma: Analysis of translocation breakpoints on der(11) and der(14) chromosomes suggests complex molecular mechanisms of recombination. Genes, chromosomes & cancer 2004;39(2):151-155.

55.Fonseca R, Blood EA, Oken MM*, et al.* Myeloma and the t(11;14)(q13;q32); evidence for a biologically defined unique subset of patients. Blood 2002;99(10):3735-3741.

56.Avet-Loiseau H, Facon T, Grosbois B*, et al.* Oncogenesis of multiple myeloma: 14q32 and 13q chromosomal abnormalities are not randomly distributed, but correlate with natural history, immunological features, and clinical presentation. Blood 2002;99(6):2185-2191.

57.Shaughnessy J, Jr., Gabrea A, Qi Y*, et al.* Cyclin D3 at 6p21 is dysregulated by recurrent chromosomal translocations to immunoglobulin loci in multiple myeloma. Blood 2001;98(1):217-223.

58.Hanamura I, Iida S, Akano Y*, et al.* Ectopic expression of MAFB gene in human myeloma cells carrying (14;20)(q32;q11) chromosomal translocations. Jpn J Cancer Res 2001;92(6):638-644.

59.Boersma-Vreugdenhil GR, Kuipers J, Van Stralen E*, et al.* The recurrent translocation t(14;20)(q32;q12) in multiple myeloma results in aberrant expression of MAFB: a molecular and genetic analysis of the chromosomal breakpoint. British journal of haematology 2004;126(3):355-363.

60.Janssen JW, Vaandrager JW, Heuser T*, et al.* Concurrent activation of a novel putative transforming gene, myeov, and cyclin D1 in a subset of multiple myeloma cell lines with t(11;14)(q13;q32). Blood 2000;95(8):2691-2698.

61.Ronchetti D, Finelli P, Richelda R*, et al.* Molecular analysis of 11q13 breakpoints in multiple myeloma. Blood 1999;93(4):1330-1337.

62.Bergsagel PL, Kuehl WM, Zhan F, Sawyer J, Barlogie B, Shaughnessy J, Jr. Cyclin D dysregulation: an early and unifying pathogenic event in multiple myeloma. Blood 2005;106(1):296-303.

63.Chesi M, Bergsagel PL, Shonukan OO*, et al.* Frequent dysregulation of the c-maf proto-oncogene at 16q23 by translocation to an Ig locus in multiple myeloma. Blood 1998;91(12):4457-4463.

64.Chesi M, Nardini E, Brents LA*, et al.* Frequent translocation t(4;14)(p16.3;q32.3) in multiple myeloma is associated with increased expression and activating mutations of fibroblast growth factor receptor 3. Nature genetics 1997;16(3):260-264.

65.Richelda R, Ronchetti D, Baldini L*, et al.* A novel chromosomal translocation t(4; 14)(p16.3; q32) in multiple myeloma involves the fibroblast growth-factor receptor 3 gene. Blood 1997;90(10):4062-4070.

66.Chesi M, Brents LA, Ely SA*, et al.* Activated fibroblast growth factor receptor 3 is an oncogene that contributes to tumor progression in multiple myeloma. Blood 2001;97(3):729-736.

67.Stec I, Wright TJ, van Ommen GJ*, et al.* WHSC1, a 90 kb SET domain-containing gene, expressed in early development and homologous to a Drosophila dysmorphy gene maps in the Wolf-Hirschhorn syndrome critical region and is fused to IgH in t(4;14) multiple myeloma. Human molecular genetics 1998;7(7):1071-1082.

68.Chesi M, Nardini E, Lim RS, Smith KD, Kuehl WM, Bergsagel PL. The t(4;14) translocation in myeloma dysregulates both FGFR3 and a novel gene,

MMSET, resulting in IgH/MMSET hybrid transcripts. Blood 1998;92(9):3025-3034.

69.Lauring J, Abukhdeir AM, Konishi H*, et al.* The multiple myeloma associated MMSET gene contributes to cellular adhesion, clonogenic growth, and tumorigenicity. Blood 2008;111(2):856-864.

70.Brito JL, Walker B, Jenner M*, et al.* MMSET deregulation affects cell cycle progression and adhesion regulons in t(4;14) myeloma plasma cells. Haematologica 2009;94(1):78-86.

71.Peters K, Ornitz D, Werner S, Williams L. Unique expression pattern of the FGF receptor 3 gene during mouse organogenesis. Developmental biology 1993;155(2):423-430.

72.Ronchetti D, Greco A, Compasso S*, et al.* Deregulated FGFR3 mutants in multiple myeloma cell lines with t(4;14): comparative analysis of Y373C, K650E and the novel G384D mutations. Oncogene 2001;20(27):3553-3562.

73.Intini D, Baldini L, Fabris S*, et al.* Analysis of FGFR3 gene mutations in multiple myeloma patients with t(4;14). British journal of haematology 2001;114(2):362-364.

74.Sibley K, Fenton JA, Dring AM, Ashcroft AJ, Rawstron AC, Morgan GJ. A molecular study of the t(4;14) in multiple myeloma. British journal of haematology 2002;118(2):514-520.

75.Li Z, Zhu YX, Plowright EE*, et al.* The myeloma-associated oncogene fibroblast growth factor receptor 3 is transforming in hematopoietic cells. Blood 2001;97(8):2413-2419.

76.Plowright EE, Li Z, Bergsagel PL*, et al.* Ectopic expression of fibroblast growth factor receptor 3 promotes myeloma cell proliferation and prevents apoptosis. Blood 2000;95(3):992-998.

77.Kang S, Dong S, Gu TL*, et al.* FGFR3 activates RSK2 to mediate hematopoietic transformation through tyrosine phosphorylation of RSK2 and activation of the MEK/ERK pathway. Cancer cell 2007;12(3):201-214.

78.Zhu L, Somlo G, Zhou B*, et al.* Fibroblast growth factor receptor 3 inhibition by short hairpin RNAs leads to apoptosis in multiple myeloma. Molecular cancer therapeutics 2005;4(5):787-798.

79.Xin X, Abrams TJ, Hollenbach PW*, et al.* CHIR-258 is efficacious in a newly developed fibroblast growth factor receptor 3-expressing orthotopic multiple myeloma model in mice. Clin Cancer Res 2006;12(16):4908-4915.

80.Trudel S, Li ZH, Wei E*, et al.* CHIR-258, a novel, multitargeted tyrosine kinase inhibitor for the potential treatment of t(4;14) multiple myeloma. Blood 2005;105(7):2941-2948.

81.Paterson JL, Li Z, Wen XY*, et al.* Preclinical studies of fibroblast growth factor receptor 3 as a therapeutic target in multiple myeloma. British journal of haematology 2004;124(5):595-603.

82.Grand EK, Chase AJ, Heath C, Rahemtulla A, Cross NC. Targeting FGFR3 in multiple myeloma: inhibition of t(4;14)-positive cells by SU5402 and PD173074. Leukemia 2004;18(5):962-966.

83.Trudel S, Ely S, Farooqi Y*, et al.* Inhibition of fibroblast growth factor receptor 3 induces differentiation and apoptosis in t(4;14) myeloma. Blood 2004;103(9):3521-3528.

84.Chen J, Lee BH, Williams IR*, et al.* FGFR3 as a therapeutic target of the small molecule inhibitor PKC412 in hematopoietic malignancies. Oncogene 2005;24(56):8259-8267.

85.Trudel S, Stewart AK, Rom E*, et al.* The inhibitory anti-FGFR3 antibody, PRO-001, is cytotoxic to t(4;14) multiple myeloma cells. Blood 2006;107(10):4039-4046.

86.Bisping G, Wenning D, Kropff M*, et al.* Bortezomib, dexamethasone, and fibroblast growth factor receptor 3-specific tyrosine kinase inhibitor in t(4;14) myeloma. Clin Cancer Res 2009;15(2):520-531.

87.Keats JJ, Maxwell CA, Taylor BJ*, et al.* Overexpression of transcripts originating from the MMSET locus characterizes all t(4;14)(p16;q32)-positive multiple myeloma patients. Blood 2005;105(10):4060-4069.

88.Santra M, Zhan F, Tian E, Barlogie B, Shaughnessy J, Jr. A subset of multiple myeloma harboring the t(4;14)(p16;q32) translocation lacks FGFR3 expression but maintains an IGH/MMSET fusion transcript. Blood 2003;101(6):2374-2376.

89.Banerji J, Olson L, Schaffner W. A lymphocyte-specific cellular enhancer is located downstream of the joining region in immunoglobulin heavy chain genes. Cell 1983;33(3):729-740.

90.Cockerill PN, Yuen MH, Garrard WT. The enhancer of the immunoglobulin heavy chain locus is flanked by presumptive chromosomal loop anchorage elements. The Journal of biological chemistry 1987;262(11):5394-5397.

91.Wiersma EJ, Ronai D, Berru M, Tsui FW, Shulman MJ. Role of the intronic elements in the endogenous immunoglobulin heavy chain locus. Either the matrix attachment regions or the core enhancer is sufficient to maintain expression. The Journal of biological chemistry 1999;274(8):4858-4862.

92.Serwe M, Sablitzky F. V(D)J recombination in B cells is impaired but not blocked by targeted deletion of the immunoglobulin heavy chain intron enhancer. The EMBO journal 1993;12(6):2321-2327.

93.Chen J, Young F, Bottaro A, Stewart V, Smith RK, Alt FW. Mutations of the intronic IgH enhancer and its flanking sequences differentially affect accessibility of the JH locus. The EMBO journal 1993;12(12):4635-4645.

94.Perlot T, Alt FW, Bassing CH, Suh H, Pinaud E. Elucidation of IgH intronic enhancer functions via germ-line deletion. Proceedings of the National Academy of Sciences of the United States of America 2005;102(40):14362-14367.

95.Bottaro A, Young F, Chen J, Serwe M, Sablitzky F, Alt FW. Deletion of the IgH intronic enhancer and associated matrix-attachment regions decreases, but does not abolish, class switching at the mu locus. International immunology 1998;10(6):799-806.

96.Singh H, Sen R, Baltimore D, Sharp PA. A nuclear factor that binds to a conserved sequence motif in transcriptional control elements of immunoglobulin genes. Nature 1986;319(6049):154-158.

97.Gerster T, Matthias P, Thali M, Jiricny J, Schaffner W. Cell type-specificity elements of the immunoglobulin heavy chain gene enhancer. The EMBO journal 1987;6(5):1323-1330.

98.Nelsen B, Tian G, Erman B*, et al.* Regulation of lymphoid-specific immunoglobulin mu heavy chain gene enhancer by ETS-domain proteins. Science (New York, NY 1993;261(5117):82-86.

99.Nikolajczyk BS, Sanchez JA, Sen R. ETS protein-dependent accessibility changes at the immunoglobulin mu heavy chain enhancer. Immunity 1999;11(1):11-20.

100.Marecki S, McCarthy KM, Nikolajczyk BS. PU.1 as a chromatin accessibility factor for immunoglobulin genes. Molecular immunology 2004;40(10):723-731.

101.Lin D, Ippolito GC, Zong RT, Bryant J, Koslovsky J, Tucker P. Bright/ARID3A contributes to chromatin accessibility of the immunoglobulin heavy chain enhancer. Molecular cancer 2007;6:23.

102.Hanakahi LA, Maizels N. Transcriptional activation by LR1 at the Emu enhancer and switch region sites. Nucleic acids research 2000;28(14):2651-2657.

103.Pettersson S, Cook GP, Bruggemann M, Williams GT, Neuberger MS. A second B cell-specific enhancer 3' of the immunoglobulin heavy-chain locus. Nature 1990;344(6262):165-168.

104.Lieberson R, Giannini SL, Birshtein BK, Eckhardt LA. An enhancer at the 3' end of the mouse immunoglobulin heavy chain locus. Nucleic acids research 1991;19(4):933-937.

105.Madisen L, Groudine M. Identification of a locus control region in the immunoglobulin heavy-chain locus that deregulates c-myc expression in plasmacytoma and Burkitt's lymphoma cells. Genes & development 1994;8(18):2212-2226.

106.Chen C, Birshtein BK. A region of the 20 bp repeats lies 3' of human Ig Calpha1 and Calpha2 genes. International immunology 1996;8(1):115-122.

107.Mills FC, Harindranath N, Mitchell M, Max EE. Enhancer complexes located downstream of both human immunoglobulin Calpha genes. The Journal of experimental medicine 1997;186(6):845-858.

108.Chen C, Birshtein BK. Virtually identical enhancers containing a segment of homology to murine 3'IgH-E(hs1,2) lie downstream of human Ig C alpha 1 and C alpha 2 genes. J Immunol 1997;159(3):1310-1318.

109.Stevens S, Ong J, Kim U, Eckhardt LA, Roeder RG. Role of OCA-B in 3'-IgH enhancer function. J Immunol 2000;164(10):5306-5312.

110.Ong J, Stevens S, Roeder RG, Eckhardt LA. 3' IgH enhancer elements shift synergistic interactions during B cell development. J Immunol 1998;160(10):4896-4903.

111.Morvan CL, Pinaud E, Decourt C, Cuvillier A, Cogne M. The immunoglobulin heavy-chain locus hs3b and hs4 3' enhancers are dispensable for VDJ assembly and somatic hypermutation. Blood 2003;102(4):1421-1427.

112.Hu Y, Pan Q, Pardali E*, et al.* Regulation of germline promoters by the two human Ig heavy chain 3' alpha enhancers. J Immunol 2000;164(12):6380-6386.

113.Laurencikiene J, Deveikaite V, Severinson E. HS1,2 enhancer regulation of germline epsilon and gamma2b promoters in murine B lymphocytes: evidence for specific promoter-enhancer interactions. J Immunol 2001;167(6):3257-3265.

114.Cogne M, Lansford R, Bottaro A*, et al.* A class switch control region at the 3' end of the immunoglobulin heavy chain locus. Cell 1994;77(5):737-747.

115.Terauchi A, Hayashi K, Kitamura D, Kozono Y, Motoyama N, Azuma T. A pivotal role for DNase I-sensitive regions 3b and/or 4 in the induction of somatic hypermutation of IgH genes. J Immunol 2001;167(2):811-820.

116.Michaelson JS, Singh M, Snapper CM, Sha WC, Baltimore D, Birshtein BK. Regulation of 3' IgH enhancers by a common set of factors, including kappa B-binding proteins. J Immunol 1996;156(8):2828-2839.

117.Gordon SJ, Saleque S, Birshtein BK. Yin Yang 1 is a lipopolysaccharide-inducible activator of the murine 3' Igh enhancer, hs3. J Immunol 2003;170(11):5549-5557.

118.Sepulveda MA, Emelyanov AV, Birshtein BK. NF-kappa B and Oct-2 synergize to activate the human 3' Igh hs4 enhancer in B cells. J Immunol 2004;172(2):1054-1064.

119.Kim EC, Edmonston CR, Wu X, Schaffer A, Casali P. The HoxC4 homeodomain protein mediates activation of the immunoglobulin heavy chain 3' hs1,2 enhancer in human B cells. Relevance to class switch DNA recombination. The Journal of biological chemistry 2004;279(40):42258-42269.

120.Singh M, Birshtein BK. NF-HB (BSAP) is a repressor of the murine immunoglobulin heavy-chain 3' alpha enhancer at early stages of B-cell differentiation. Molecular and cellular biology 1993;13(6):3611-3622.

121.Singh M, Birshtein BK. Concerted repression of an immunoglobulin heavy-chain enhancer, 3' alpha E(hs1,2). Proceedings of the National Academy of Sciences of the United States of America 1996;93(9):4392-4397.

122.Wang VE, Tantin D, Chen J, Sharp PA. B cell development and immunoglobulin transcription in Oct-1-deficient mice. Proceedings of the National Academy of Sciences of the United States of America 2004;101(7):2005-2010.

123.Tang H, Sharp PA. Transcriptional regulation of the murine 3' IgH enhancer by OCT-2. Immunity 1999;11(5):517-526.

124.Heckman CA, Duan H, Garcia PB, Boxer LM. Oct transcription factors mediate t(14;18) lymphoma cell survival by directly regulating bcl-2 expression. Oncogene 2006;25(6):888-898.

125.Matthias P. Lymphoid-specific transcription mediated by the conserved octamer site: who is doing what? Seminars in immunology 1998;10(2):155-163.

126.Scheidereit C, Heguy A, Roeder RG. Identification and purification of a human lymphoid-specific octamer-binding protein (OTF-2) that activates transcription of an immunoglobulin promoter in vitro. Cell 1987;51(5):783-793.

127.Staudt LM, Singh H, Sen R, Wirth T, Sharp PA, Baltimore D. A lymphoid-specific protein binding to the octamer motif of immunoglobulin genes. Nature 1986;323(6089):640-643.

128.Johnson DG, Carayannopoulos L, Capra JD, Tucker PW, Hanke JH. The ubiquitous octamer-binding protein(s) is sufficient for transcription of immunoglobulin genes. Molecular and cellular biology 1990;10(3):982-990.

129.Pierani A, Heguy A, Fujii H, Roeder RG. Activation of octamer-containing promoters by either octamer-binding transcription factor 1 (OTF-1) or OTF-2 and requirement of an additional B-cell-specific component for optimal transcription of immunoglobulin promoters. Molecular and cellular biology 1990;10(12):6204-6215.

130.Strubin M, Newell JW, Matthias P. OBF-1, a novel B cell-specific coactivator that stimulates immunoglobulin promoter activity through association with octamer-binding proteins. Cell 1995;80(3):497-506.

131.Luo Y, Fujii H, Gerster T, Roeder RG. A novel B cell-derived coactivator potentiates the activation of immunoglobulin promoters by octamer-binding transcription factors. Cell 1992;71(2):231-241.

132.Gstaiger M, Knoepfel L, Georgiev O, Schaffner W, Hovens CM. A B-cell coactivator of octamer-binding transcription factors. Nature 1995;373(6512):360-362.

133.Sturm RA, Das G, Herr W. The ubiquitous octamer-binding protein Oct-1 contains a POU domain with a homeo box subdomain. Genes & development 1988;2(12A):1582-1599.

134.Wirth T, Priess A, Annweiler A, Zwilling S, Oeler B. Multiple Oct2 isoforms are generated by alternative splicing. Nucleic acids research 1991;19(1):43-51.

135.Corcoran LM, Koentgen F, Dietrich W, Veale M, Humbert PO. All known in vivo functions of the Oct-2 transcription factor require the C-terminal protein domain. J Immunol 2004;172(5):2962-2969.

136.Sharif MN, Radomska HS, Miller DM, Eckhardt LA. Unique function for carboxyl-terminal domain of Oct-2 in Ig-secreting cells. J Immunol 2001;167(8):4421-4429.

137.Nagy M, Chapuis B, Matthes T. Expression of transcription factors Pu.1, Spi-B, Blimp-1, BSAP and oct-2 in normal human plasma cells and in multiple myeloma cells. British journal of haematology 2002;116(2):429-435.

138.He X, Treacy MN, Simmons DM, Ingraham HA, Swanson LW, Rosenfeld MG. Expression of a large family of POU-domain regulatory genes in mammalian brain development. Nature 1989;340(6228):35-41.

139.Cockerill PN, Klinken SP. Octamer-binding proteins in diverse hemopoietic cells. Molecular and cellular biology 1990;10(3):1293-1296.

140.Kang SM, Tsang W, Doll S*, et al.* Induction of the POU domain transcription factor Oct-2 during T-cell activation by cognate antigen. Molecular and cellular biology 1992;12(7):3149-3154.

141.Luo Y, Roeder RG. Cloning, functional characterization, and mechanism of action of the B-cell-specific transcriptional coactivator OCA-B. Molecular and cellular biology 1995;15(8):4115-4124.

142.Yu X, Wang L, Luo Y, Roeder RG. Identification and characterization of a novel OCA-B isoform. implications for a role in B cell signaling pathways. Immunity 2001;14(2):157-167.

143.Gstaiger M, Georgiev O, van Leeuwen H, van der Vliet P, Schaffner W. The B cell coactivator Bob1 shows DNA sequence-dependent complex formation with Oct-1/Oct-2 factors, leading to differential promoter activation. The EMBO journal 1996;15(11):2781-2790.

144.Qin XF, Reichlin A, Luo Y, Roeder RG, Nussenzweig MC. OCA-B integrates B cell antigen receptor-, CD40L- and IL 4-mediated signals for the germinal center pathway of B cell development. The EMBO journal 1998;17(17):5066-5075.

145.Greiner A, Muller KB, Hess J, Pfeffer K, Muller-Hermelink HK, Wirth T. Up-regulation of BOB.1/OBF.1 expression in normal germinal center B cells and germinal center-derived lymphomas. The American journal of pathology 2000;156(2):501-507.

146.Marafioti T, Ascani S, Pulford K*, et al.* Expression of B-lymphocyte-associated transcription factors in human T-cell neoplasms. The American journal of pathology 2003;162(3):861-871.

147.Zwilling S, Dieckmann A, Pfisterer P, Angel P, Wirth T. Inducible expression and phosphorylation of coactivator BOB.1/OBF.1 in T cells. Science (New York, NY 1997;277(5323):221-225.

148.Chasman D, Cepek K, Sharp PA, Pabo CO. Crystal structure of an OCA-B peptide bound to an Oct-1 POU domain/octamer DNA complex: specific recognition of a protein-DNA interface. Genes & development 1999;13(20):2650-2657.

149.Sauter P, Matthias P. Coactivator OBF-1 makes selective contacts with both the POU-specific domain and the POU homeodomain and acts as a molecular clamp on DNA. Molecular and cellular biology 1998;18(12):7397-7409.

150.Corcoran LM, Karvelas M, Nossal GJ, Ye ZS, Jacks T, Baltimore D. Oct-2, although not required for early B-cell development, is critical for later B-cell maturation and for postnatal survival. Genes & development 1993;7(4):570-582.

151.Schubart K, Massa S, Schubart D, Corcoran LM, Rolink AG, Matthias P. B cell development and immunoglobulin gene transcription in the absence of Oct-2 and OBF-1. Nat Immunol 2001;2(1):69-74.

152.Humbert PO, Corcoran LM. oct-2 gene disruption eliminates the peritoneal B-1 lymphocyte lineage and attenuates B-2 cell maturation and function. J Immunol 1997;159(11):5273-5284.

153.Hess J, Nielsen PJ, Fischer KD, Bujard H, Wirth T. The B lymphocyte-specific coactivator BOB.1/OBF.1 is required at multiple stages of B-cell development. Molecular and cellular biology 2001;21(5):1531-1539.

154.Karnowski A, Cao C, Matthias G*, et al.* Silencing and nuclear repositioning of the lambda5 gene locus at the pre-B cell stage requires Aiolos and OBF-1. PLoS ONE 2008;3(10):e3568.

155.Nielsen PJ, Georgiev O, Lorenz B, Schaffner W. B lymphocytes are impaired in mice lacking the transcriptional co-activator Bob1/OCA-B/OBF1. European journal of immunology 1996;26(12):3214-3218.

156.Schubart DB, Rolink A, Kosco-Vilbois MH, Botteri F, Matthias P. B-cell-specific coactivator OBF-1/OCA-B/Bob1 required for immune response and germinal centre formation. Nature 1996;383(6600):538-542.

157.Samardzic T, Marinkovic D, Nielsen PJ, Nitschke L, Wirth T. BOB.1/OBF.1 deficiency affects marginal-zone B-cell compartment. Molecular and cellular biology 2002;22(23):8320-8331.

158.Kim U, Qin XF, Gong S*, et al.* The B-cell-specific transcription coactivator OCA-B/OBF-1/Bob-1 is essential for normal production of immunoglobulin isotypes. Nature 1996;383(6600):542-547.

159.Corcoran LM, Hasbold J, Dietrich W*, et al.* Differential requirement for OBF-1 during antibody-secreting cell differentiation. The Journal of experimental medicine 2005;201(9):1385-1396.

160.Emslie D, D'Costa K, Hasbold J*, et al.* Oct2 enhances antibody-secreting cell differentiation through regulation of IL-5 receptor alpha chain expression on activated B cells. The Journal of experimental medicine 2008;205(2):409-421.

161.Brunner C, Wirth T. Btk expression is controlled by Oct and BOB.1/OBF.1. Nucleic acids research 2006;34(6):1807-1815.

162.Malone CS, Wall R. Bob1 (OCA-B/OBF-1) differential transactivation of the B cell-specific B29 (Ig beta) and mb-1 (Ig alpha) promoters. J Immunol 2002;168(7):3369-3375.

163.Malone CS, Patrone L, Wall R. An essential octamer motif in the mb-1 (Igalpha) promoter. Molecular immunology 2000;37(6):321-328.

164.Bartholdy B, Du Roure C, Bordon A, Emslie D, Corcoran LM, Matthias P. The Ets factor Spi-B is a direct critical target of the coactivator OBF-1. Proceedings of the National Academy of Sciences of the United States of America 2006;103(31):11665-11670.

165.Wolf I, Pevzner V, Kaiser E*, et al.* Downstream activation of a TATA-less promoter by Oct-2, Bob1, and NF-kappaB directs expression of the homing

receptor BLR1 to mature B cells. The Journal of biological chemistry 1998;273(44):28831-28836.

166.Miller CL, Feldhaus AL, Rooney JW, Rhodes LD, Sibley CH, Singh H. Regulation and a possible stage-specific function of Oct-2 during pre-B-cell differentiation. Molecular and cellular biology 1991;11(10):4885-4894.

167.Bendall HH, Scherer DC, Edson CR, Ballard DW, Oltz EM. Transcription factor NF-kappaB regulates inducible Oct-2 gene expression in precursor B lymphocytes. The Journal of biological chemistry 1997;272(46):28826-28828.

168.Podojil JR, Kin NW, Sanders VM. CD86 and beta2-adrenergic receptor signaling pathways, respectively, increase Oct-2 and OCA-B Expression and binding to the 3'-IgH enhancer in B cells. The Journal of biological chemistry 2004;279(22):23394-23404.

169.Tanaka M, Herr W. Differential transcriptional activation by Oct-1 and Oct-2: interdependent activation domains induce Oct-2 phosphorylation. Cell 1990;60(3):375-386.

170.Stevens S, Wang L, Roeder RG. Functional analysis of the OCA-B promoter. J Immunol 2000;164(12):6372-6379.

171.Zandi S, Mansson R, Tsapogas P, Zetterblad J, Bryder D, Sigvardsson M. EBF1 is essential for B-lineage priming and establishment of a transcription factor network in common lymphoid progenitors. J Immunol 2008;181(5):3364-3372.

172.Massa S, Junker S, Schubart K, Matthias G, Matthias P. The OBF-1 gene locus confers B cell-specific transcription by restricting the ubiquitous activity of its promoter. European journal of immunology 2003;33(10):2864-2874.

173.Tiedt R, Bartholdy BA, Matthias G, Newell JW, Matthias P. The RING finger protein Siah-1 regulates the level of the transcriptional coactivator OBF-1. The EMBO journal 2001;20(15):4143-4152.

174.Camp RL, Chung GG, Rimm DL. Automated subcellular localization and quantification of protein expression in tissue microarrays. Nature medicine 2002;8(11):1323-1327.

175.Szulc J, Wiznerowicz M, Sauvain MO, Trono D, Aebischer P. A versatile tool for conditional gene expression and knockdown. Nature methods 2006;3(2):109-116.

176.Biagi E, Bambacioni F, Gaipa G*, et al.* Efficient lentiviral transduction of primary human acute myelogenous and lymphoblastic leukemia cells. Haematologica 2001;86(1):13-16.

177.Anderson KC, Kyle RA, Rajkumar SV, Stewart AK, Weber D, Richardson P. Clinically relevant end points and new drug approvals for myeloma. Leukemia 2008;22(2):231-239.

178.Landis JR, Koch GG. The measurement of observer agreement for categorical data. Biometrics 1977;33(1):159-174.

179.Kim DH, Behlke MA, Rose SD, Chang MS, Choi S, Rossi JJ. Synthetic dsRNA Dicer substrates enhance RNAi potency and efficacy. Nature biotechnology 2005;23(2):222-226.

180.Chilosi M, Adami F, Lestani M*, et al.* CD138/syndecan-1: a useful immunohistochemical marker of normal and neoplastic plasma cells on routine trephine bone marrow biopsies. Mod Pathol 1999;12(12):1101-1106.

181.Costes V, Magen V, Legouffe E*, et al.* The Mi15 monoclonal antibody (anti-syndecan-1) is a reliable marker for quantifying plasma cells in paraffin-embedded bone marrow biopsy specimens. Human pathology 1999;30(12):1405-1411.

182.van Oers MH, Klasa R, Marcus RE*, et al.* Rituximab maintenance improves clinical outcome of relapsed/resistant follicular non-Hodgkin lymphoma in patients both with and without rituximab during induction: results of a prospective randomized phase 3 intergroup trial. Blood 2006;108(10):3295-3301.

183.Miceli T, Colson K, Gavino M, Lilleby K. Myelosuppression associated with novel therapies in patients with multiple myeloma: consensus statement of the IMF Nurse Leadership Board. Clinical journal of oncology nursing 2008;12(3 Suppl):13-20.

184.Suguro M, Kanda Y, Yamamoto R*, et al.* High serum lactate dehydrogenase level predicts short survival after vincristine-doxorubicin-dexamethasone (VAD) salvage for refractory multiple myeloma. American journal of hematology 2000;65(2):132-135.

185.Kallies A, Hasbold J, Tarlinton DM*, et al.* Plasma cell ontogeny defined by quantitative changes in blimp-1 expression. The Journal of experimental medicine 2004;200(8):967-977.

186.Kurabayashi H, Kubota K, Tsuchiya J, Murakami H, Tamura J, Naruse T. Prognostic value of morphological classifications and clinical variables in elderly and young patients with multiple myeloma. Annals of hematology 1999;78(1):19-23.

187.Trentin L, Miorin M, Facco M*, et al.* Multiple myeloma plasma cells show different chemokine receptor profiles at sites of disease activity. British journal of haematology 2007;138(5):594-602.

188.Siegel R, Kim U, Patke A*, et al.* Nontranscriptional regulation of SYK by the coactivator OCA-B is required at multiple stages of B cell development. Cell 2006;125(4):761-774.

189.Shore P, Dietrich W, Corcoran LM. Oct-2 regulates CD36 gene expression via a consensus octamer, which excludes the co-activator OBF-1. Nucleic acids research 2002;30(8):1767-1773.

190.Camp RL, Charette LA, Rimm DL. Validation of tissue microarray technology in breast carcinoma. Laboratory investigation; a journal of technical methods and pathology 2000;80(12):1943-1949.

191.O'Connell FP, Pinkus JL, Pinkus GS. CD138 (syndecan-1), a plasma cell marker immunohistochemical profile in hematopoietic and nonhematopoietic neoplasms. American journal of clinical pathology 2004;121(2):254-263.

192.Heckman CA, Cao T, Somsouk L*, et al.* Critical elements of the immunoglobulin heavy chain gene enhancers for deregulated expression of bcl-2. Cancer research 2003;63(20):6666-6673.

193.Namba M, Ohtsuki T, Mori M*, et al.* Establishment of five human myeloma cell lines. In Vitro Cell Dev Biol 1989;25(8):723-729.

194.Naldini L, Blomer U, Gallay P*, et al.* In vivo gene delivery and stable transduction of nondividing cells by a lentiviral vector. Science (New York, NY 1996;272(5259):263-267.

195.Akkina RK, Walton RM, Chen ML, Li QX, Planelles V, Chen IS. High-efficiency gene transfer into CD34+ cells with a human immunodeficiency virus type 1-based retroviral vector pseudotyped with vesicular stomatitis virus envelope glycoprotein G. Journal of virology 1996;70(4):2581-2585.

196.Zhao C, Inoue J, Imoto I*, et al.* POU2AF1, an amplification target at 11q23, promotes growth of multiple myeloma cells by directly regulating expression of a B-cell maturation factor, TNFRSF17. Oncogene 2008;27(1):63-75.

197.Kuehl WM, Bergsagel PL. Multiple myeloma: evolving genetic events and host interactions. Nature reviews 2002;2(3):175-187.

198.Hochhaus A, O'Brien SG, Guilhot F*, et al.* Six-year follow-up of patients receiving imatinib for the first-line treatment of chronic myeloid leukemia. Leukemia 2009.